2012

Unique Features and Neuronal Properties in a Multisensory Cortex

W. Alex Foxworthy
Virginia Commonwealth University

UNIQUE FEATURES OF ORGANIZATION AND NEURONAL PROPERTIES IN A MULTISENSORY CORTEX

A dissertation submitted in partial fulfillment of the requirements for the degree of Doctor of Philosophy at Virginia Commonwealth University

by

William Alex Foxworthy
Bachelor of Science
Virginia Commonwealth University
August 2006

Advisor: M. Alex Meredith, Ph.D.
Professor, Department of Anatomy and Neurobiology

Virginia Commonwealth University
Richmond, Virginia
July, 2012

ACKNOWLEDGEMENTS

I wish to thank several people who have made this endeavor possible. I would especially like to thank my advisor, Dr. Meredith, for taking me on and providing support and guidance during the years that I have been a part of the lab. He has provided me with many opportunities to develop both as a scientist and as a teacher of scientific knowledge. I am also indebted to previous lab members Brian Allman and Les Keniston, who were instrumental in teaching me the techniques that were used in the experiments contained in this thesis. I would like to thank the other members of my graduate committee: Dr. Guido, for holding me to a high standard and giving me advice in times of need; Dr. Medina for his support, thought-provoking discussions and friendship; Dr. Churn for his help and advice when things were rough; and Dr. Sim-Selley for her continuous support and seemingly endless enthusiasm. Additional thanks go to Dr. Bigbee, the director of the VCU Neuroscience Ph.D. Program, who has always been an advocate for students and has been instrumental in helping me to navigate the path through graduate school since day 1 and has also provided me with numerous scientific outreach opportunities.

I would also like to thank my fiancé, Heather, and our child Damien who have provided me with life and laughter when I have needed it the most.

TABLE OF CONTENTS

LIST OF FIGURES

CHAPTER II

CHAPTER III

LIST OF TABLES

CHAPTER III

CHAPTER IV

ABSTRACT

UNIQUE FEAUTRES OF ORGANIZATION AND NEURONAL PROPERTIES IN A MULTISENSORY CORTEX

By William Alex Foxworthy

A dissertation submitted in partial fulfillment of the requirements for the degree of Doctor of Philosophy at Virginia Commonwealth University

Virginia Commonwealth University, 2012

Advisor: M. Alex Meredith, Ph.D.
Professor, Department of Anatomy and Neurobiology

Multisensory processing is a ubiquitous sensory effect that underlies a wide variety of behaviors, such as detection and orientation, as well as perceptual phenomena from speech comprehension to binding. Such multisensory perceptual effects are presumed to be based in cortex, especially within areas known to contain multisensory neurons. However, unlike their lower-level/primary sensory cortical counterparts, little is known about the connectional, functional and laminar organization of higher-level multisensory cortex. Therefore, to examine the fundamental features of neuronal processing and organization in the multisensory cortical area of the posterior parietal cortex (PPr) of ferrets, the present experiments utilized a combination of immunohistological, neuroanatomical and multiple single-channel electrophysiological recording techniques. These experiments produced four main results. First, convergence of extrinsic inputs from unisensory cortical areas predominantly in layers 2-3 in PPr corresponded with the high proportion of multisensory neurons in those layers. This is consistent with multisensory

responses in this higher-level multisensory region being driven by cortico-cortical, rather than thalamo-cortical connections. Second, the laminar organization of the PPr differed substantially from the pattern commonly observed in primary sensory cortices. The PPr has a reduced layer 4 compared to primary sensory cortices, which does not receive input from principal thalamic nuclei. Third, the distribution of unisensory and multisensory neurons and properties differs significantly by layer. Given the laminar-dependent input-output relationships, this suggests that unisensory and multisensory signals are processed in parallel as they pass through the circuitry of the PPr. Finally, specific functional properties of bimodal neurons differed significantly from those of their unisensory counterparts. Thus, despite their coextensive distribution within cortex, these results differentiate bimodal from unisensory neurons in ways that have never been examined before. Together these experiments represent the first combined anatomical-electrophysiological examination of the laminar organization of a multisensory cortex and the first systematic comparison of the functional properties of bimodal and unisensory neurons. These results are essential for understanding the neural bases of multisensory processing and carry significant implications for the accurate interpretation of macroscopic studies of multisensory brain regions (i.e. fMRI, EEG), because bimodal and unisensory neurons within a given neural region can no longer be assumed to respond similarly to a given external stimulus.

CHAPTER I

INTRODUCTION

BACKGROUND

Most organisms possess a variety of sensory systems through which information from the external world is processed. The benefit of having multiple sensory systems is intuitively obvious, as each sensory system allows an organism to process biologically relevant information from a physically distinct domain. The bulk of scientific research has traditionally focused on how individual sensory systems encode and decode information, but animals clearly combine signals from separate sensory modalities. The behavioral effects that have been observed from experiments utilizing simultaneously presented combinations of separate sensory signals suggest that integration of sensory signals provide survival advantage. Examples of behavioral improvements as well as perceptual effects resulting from integration of sensory signals are provided below in order to put the importance of multisensory processing in context.

Many studies of multisensory processing have focused on orientation to an environmental event. This behavior requires an animal to first detect an event, locate it in space, and finally orient itself to the source of the sensory information. Compared to unisensory stimuli, combined sensory stimuli can increase an animal's ability to perform all of the above mentioned processes (Stein, Huneycutt et al. 1988; Stein, Meredith et al. 1989; Hughes, Reuter-Lorenz et al. 1994; Nozawa, Reuter-Lorenz et al. 1994; Diederich and Colonius 2004; Bell, Meredith et al. 2005). Additionally, it has been shown that the improved ability to orient to an event when comparing multisensory versus unisensory stimuli is greatest when the component stimuli are weak (Stein,

Huneycutt et al. 1988; Stein, Meredith et al. 1989). This shows that an organism is able to combine two (or more) weak sensory signals to increase the accuracy of its perception and behavior.

The combination of sensory signals by the central nervous system is not confined to orienting behaviors. This is intuitive from subjective experience – despite the myriad sensory systems we possess that respond to distinct physical energies from the external environment, we do not perceive a world that is separated into sensory channels. Instead, our perception of the world reflects the combination of several sensory modalities. The experience of taste is an obvious example – the perception of taste depends not only on the taste buds on the tongue, but also on odorant receptors in the nose, as well as the visual appearance of a food. Combined sensory cues have also been shown to be important in speech perception. Specifically, the visual stimulus of moving lips enhances comprehension of speech, especially in noisy environments(Sumby and Polack 1954). In fact, this effect is experienced rather dramatically when one watches TV. The perception that speech is emanating from the moving mouths on TV, or in a puppet show, depends on combining visual and auditory information.

These well studied examples are but a few of the behavioral and perceptual phenomena subserved by multisensory processing and they have been well described experimentally, clearly indicating that multisensory processing plays an essential role in both behavior and perception. The obvious importance of combining sensory information has prompted researchers to search for the neural underpinnings of multisensory processing. Though firm links between multisensory interactions at the neural level and the behavioral level are lacking, a number of principles have been established by which multisensory neurons processes combined sensory information.

NEUROPHYSIOLOGY – Superior Colliculus Multisensory Neurons

The principles of multisensory integration in single neurons have been largely derived from studies of multisensory neurons of the anesthetized cat's superior colliculus. Given that behavior and perception can be affected by multiple sensory modalities, it is perhaps not surprising that individual neurons can also be affected by multisensory stimuli. A number of principles have been described that pertain to a single neuron's processing of multisensory signals. In a single neuron, multisensory integration is defined as a statistically significant difference between the number of action potentials generated by a multisensory stimulus compared that that evoked by the most effective of the unisensory stimuli individually (Meredith and Stein 1983). Depending on the physical parameters of the stimuli used (as described below), it has been found that multisensory integration can result in either an enhancement or a depression of a neuron's response, and that this response change is often nonlinear (Stein and Meredith 1993).

Since multisensory neurons can respond to more than one sensory modality, it is not surprising that they possess an excitatory receptive field for each sensory modality to which they respond. These receptive fields have been found to be in spatial register with one another, and enhanced responses have been observed when multisensory stimuli are presented in these overlapping receptive fields (for review (Stein and Meredith 1993; Stein and Stanford 2008). On the other hand, if one component of a multisensory stimuli falls within a neuron's receptive field, and another does not – it has been observed that, in general, there will be either no enhancement, or response depression (Meredith and Stein 1986; Meredith and Stein 1996; Kadunce, Vaughan et al. 1997). These collective observations are known as the *spatial principle* of multisensory integration.

Another related observation is that for sensory information to be integrated, separate sensory stimuli must occur close to one another in time (Meredith and Stein 1986; Meredith, Nemitz et al. 1987). The *temporal principle* of multisensory integration holds that the magnitude of an integrated multisensory response is related to the temporal overlap of the responses that are generated by the sensory inputs. Taken together, the spatial and temporal principles indicate that the greatest degree of multisensory integration should occur when multiple sensory stimuli emanate from the same time and place.

Another important principle of multisensory processing is that the level of multisensory enhancement is inversely related to the effectiveness of the individual cues that are driving sensory responses (Meredith and Stein 1986; Wallace, Wilkinson et al. 1996; Perrault, Vaughan et al. 2003; Perrault, Vaughan et al. 2005; Stanford, Quessy et al. 2005). This phenomenon has been termed *inverse effectiveness principle*. In addition to being more effective at driving multisensory enhancement, weak multisensory cues were often found to elicit responses that exceeded the arithmetic sum of their individual unisensory responses, a phenomena termed "superadditivity" (Meredith and Stein 1986; Wallace, Wilkinson et al. 1996; Perrault, Vaughan et al. 2005; Stanford, Quessy et al. 2005; Stanford and Stein 2007).

For multisensory integration to occur, inputs from different sensory modalities must converge onto individual neurons. In that way, post-synaptic events generated by the different senses can meet and influence one another on a given membrane. The intermediate and deep layers of the superior colliculus have been demonstrated to contain 63% multisensory neurons (Wallace and Stein 1997) composed of visual-auditory, visual-somatosensory, auditory-somatosensory, and visual-auditory-somatosensory patterns of convergence (Stein and Meredith 1993). Accordingly the superior colliculus has been shown to receive inputs from subcortical

and cortical representations of these sensory modalities. The visual, auditory and somatosensory divisions of the cortical cat anterior ectosylvian sulcus and the visual lateral suprasylvian cortex (McHaffie, Kruger et al. 1988; Meredith and Clemo 1989; Wallace, Meredith et al. 1993) have been shown to project to the superior colliculus. The superior colliculus also receives inputs from various sensory subcortical structures including: the ventral lateral geniculate nucleus (Edwards, Ginsburgh et al. 1979; Taylor, Jeffery et al. 1986; Lugo-Garcia and Kicliter 1988; Jiang, Moore et al. 1997; Baldwin, Wong et al. 2011), the inferior colliculus (Edwards, Ginsburgh et al. 1979; Jiang, Moore et al. 1997), and the sensory trigeminal complex (Edwards, Ginsburgh et al. 1979; Jiang, Moore et al. 1997). The pattern of terminal projections from input areas onto the superior colliculus is well characterized (Harting and Van Lieshout 1991; Harting, Updyke et al. 1992; Harting, Feig et al. 1997). This is of particular import because axon terminals represent the physical points of contact through which multiple senses converge on an individual neuron, and overlap of the projection domains of the different sensory modalities represents the substrate for multisensory convergence and processing. In summary, these connectional studies demonstrate that the superior colliculus receives inputs from areas of distinct sensory modalities and that the termination patterns of these projections are consistent with the multisensory properties of neurons recorded in the superior colliculus (reviewed in (Clemo, Keniston et al. 2012).

The principles of multisensory processing outlined in the above section have been described largely for neurons in a subcortical structure. However, multisensory neurons are distributed throughout the neuroaxis, and it is thus informative to examine whether multisensory neurons in other areas exhibit similar features to superior colliculus multisensory neurons. The cortex is regarded as the locus of perception and as such, is the logical place to examine the neural bases of multisensory perception. For this reason the present experiments are conducted in

a multisensory cortical area. The subsequent text will focus on multisensory neurons which have suprathreshold responses to more than one sensory modality, which are the classical and definitive form of multisensory neuron (defined as bimodal neurons) that have been found in many areas of the neocortex.

NEUROPHYSIOLOGY – Cortical Bimodal Neurons

A number of cortical regions containing bimodal neurons have been described. These include the primate superior temporal sulcus (Benevento et al., 1977; Bruce et al., 1981; Hikosaka et al., 1988) intraparietal sulcus (Avillac et al., 2007; Bremmer et al., 2002; Cohen et al., 2005; Duhamel et al., 1998; Russ et al., 2006; Schlack et al., 2005), frontal and prefrontal cortex (Fogassi et al., 1996; Graziano et al., 1999; Graziano et al., 1994; Romanski, 2007), and cat anterior ectosylvian sulcal regions (Clemo et al., 2011; Jiang et al., 1994; Wallace et al., 1992). The sources of inputs to each of the above areas have been examined and in all cases, afferents from multiple unisensory areas are described (see (Cappe, Rouiller et al. 2012; Clemo, Keniston et al. 2012) for review).

Despite the identification of inputs to multisensory cortical areas, only relatively recent studies have documented the axonal termination patterns of these inputs. These studies of multisensory cortices have demonstrated a strong preference for cortico-cortical inputs to terminate within layers 2-3 of a multisensory region (Clemo et al., 2007; Clemo et al., 2008; Dehner et al., 2004; Meredith et al., 2006; Monteiro et al., 2003; reviewed in Clemo et al., 2011). As these terminations represent a likely site of multisensory convergence, one of the aims of the present experiments is to establish the pattern of terminals within a multisensory cortical region and to use laminar recording electrodes to determine if overlapping projections from separate

sensory modalities generate multisensory neurons. It is hypothesized that the cortical layers with the greatest overlap of extrinsic inputs from separate sensory modalities will contain the greatest proportion of multisensory neurons.

As the above studies suggest that multisensory responses in cortical multisensory areas are generated by connections that terminate in layers 2 and 3, and multisensory associative regions have been observed to have a relatively small layer 4, these cortical areas appear to differ in their laminar and connectional organization as compared to primary sensory cortices, in which responses are primarily generated by thalamocortical inputs to layer 4. As such, it is somewhat surprising that the fundamental features of the laminar and connectional organization of multisensory cortical regions have not been systematically examined. As higher-level cortices, these areas receive thalamic inputs primarily from the non-specific nuclei such as the lateral posterior and pulvinar nuclei (Bucci, 2009; Matsuzaki et al., 2004; Roda and Reinoso-Suarez, 1983; Romanski et al., 1997; Takahashi, 1985; Yeterian and Pandya, 1989) that terminate within cortical layer 4 (Chomsung et al., 2010) or layers 3 and 5 (Rockland et al., 1999) or layers 1-2 (Rockland et al., 1999) depending on the area and the species (Jones, 2007a for review). Therefore, unlike primary sensory cortices, there appears to be no direct route for sensory information to pass from the periphery to the thalamus and onto the cortex. Collectively, these few observations indicate that the laminar basis for multisensory processing is unresolved and largely unexplored. Thus, one of the goals of the present experiments is to examine the laminar and connectional basis of multisensory processing.

Studies of cortical bimodal neurons have shown that they do not integrate nearly as often, or to as great a level as superior colliculus bimodal neurons (Meredith, Allman et al. 2011). Bimodal neurons in the SC show a range of response enhancement that in some cases exceeds

1200% (Meredith and Stein 1986), with an average response enhancement of 88% (Meredith and Stein 1983; Meredith and Stein 1985; Meredith and Stein 1986). Recordings from multisensory cortical areas in the anesthetized cat (anterior ectosylvian sulcus (Jiang, Lepore et al. 1994; Meredith and Allman 2009), posterolateral lateral suprasylvian cortex (Allman and Meredith 2007), rostral suprasylvian sulcal cortex (Clemo, Allman et al. 2007)) found bimodal neurons which exhibited a much lower range of integration (up to 212%) with an average enhancement of only 33% (Meredith, Allman et al. 2011). In addition, while a majority of SC bimodal neurons exhibit integration, only a minority (39%) of cortical bimodal neurons exhibited integration and only 17% of these produced superadditive response levels. This is in stark contrast to the large proportion (55%) of neurons in the SC which show superadditivity (Meredith, Allman et al. 2011).

The generality of the principles of multisensory processing determined from superior colliculus studies, namely the necessity of spatio-temporal coincidence for response interaction to occur, were confirmed by similar findings in cortical bimodal neurons (Wallace, Meredith et al. 1992; Stein and Wallace 1996; Avillac, Ben Hamed et al. 2007). Similarly the principle of inverse effectiveness (weak individual stimuli produce greater multisensory enhancement when combined) has also been observed in numerous cortical areas (Stein and Wallace 1996; Ghazanfar, Maier et al. 2005; Avillac, Ben Hamed et al. 2007; Stevenson and James 2009; Stevenson, Bushmakin et al. 2012).

Since bimodal neurons are present in many areas of the cortex, and coexist with unisensory neurons, it is logical to expect that bimodal neurons provide a function that unisensory neurons do not. The early work performed on bimodal neurons in the SC has suggested that multisensory integration represents this unique function (Meredith and Stein

1983; Alvarado, Vaughan et al. 2007 for review), especially because unisensory neurons, by definition, were presumed to be insensitive to this integrative process. However, recent studies have shown (Jiang, Lepore et al. 1994; Allman and Meredith 2007; Clemo, Allman et al. 2007; Keniston, Allman et al. 2009; Meredith and Allman 2009; Meredith, Allman et al. 2011) that only a minority of cortical bimodal cells exhibit responses that meet the criterion for multisensory integration, and have demonstrated as well that unisensory neurons can be influenced by multisensory stimulation (Dehner, Keniston et al. 2004; Meredith, Keniston et al. 2006; Allman and Meredith 2007; Avillac, Ben Hamed et al. 2007; Allman, Keniston et al. 2008; Allman, Keniston et al. 2009; Keniston, Allman et al. 2009). Therefore, multisensory integration can no longer be regarded as the unique feature that distinguishes bimodal from unisensory neurons. Thus, the question remains regarding the functional distinctions between unisensory and multisensory neurons.

The question of functional differences between bimodal and unisensory neurons, in fact, has largely been unexplored because investigations of multisensory neuronal function have largely only examined bimodal neurons, while studies of unisensory areas test with only the effective stimulus modality to the exclusion of the others. Thus, missing from much of this early work are direct comparisons of unisensory and bimodal neurons, even within a multisensory area. Therefore, another goal of the present experiments is to compare the functional differences between unisensory and bimodal neurons in a cortical multisensory region. Since not all bimodal neurons integrate, and neurons previously regarded as unisensory can also integrate sensory information, it is expected that the functional properties (spontaneous rate, response magnitude, response duration, response latency) of bimodal and unisensory neurons will differ.

OUTLINE OF THESIS

To investigate and compare the organization and function of bimodal and unisensory cortical neurons, a suitable model must be identified, with the critical feature being the demonstrated presence of both bimodal and unisensory neurons. The rostral posterior parietal cortex of the ferret (PPr) is such an area. It has been previously shown that the PPr contains both bimodal and unisensory neurons which respond to visual and/or tactile stimulation (Foxworthy, Keniston et al. 2011). Also, both the visual and somatosensory receptive fields in PPr are large (visual = 20-45° diameter; tactile = mostly face and vibrissa) (Manger, Masiello et al. 2002), such that a generic set of visual-tactile stimuli would be expected to activate all, or the majority of sensory neurons in a given penetration (with multiple recording sites). This is important because it will allow permit recording from and stimulation of bimodal and unisensory neurons under identical conditions, thus allowing for their direct functional comparison.

In order to address the hypothesis that overlapping projections from separate unisensory cortical areas overlap to generate multisensory neurons, the sources of inputs to the PPr must first be identified. Previous studies indicate that the PPr receives the majority of its visual inputs from the visual caudal posterior parietal cortex, which has been characterized extensively (Manger, Masiello et al. 2002). However, a large proportion of anatomical inputs were found in an area that had not been previously characterized in the ferret. For this reason, the experiments of Chapter II are designed to characterize the anatomical and sensory response characteristics of this 'new' area. It was found that this area is homologous to the cat somatosensory area III, and has receptive field properties that are very similar to those found in the PPr, and these results have been published (Foxworthy and Meredith 2011).

Having identified the relevant areas of the ferret brain which provide inputs into the ferret PPr allowed for investigation of the connectional and laminar features which underlie cortical multisensory processing. These experiments are presented in Chapter III. Significantly, these experiments demonstrate that the laminar organization of the multisensory PPr differs from the well-described laminar organization of primary sensory cortices. The data indicate that overlapping projections from SIII and PPc in layers 2/3 of the PPr correlate with a high proportion of multisensory neurons in these layers. Additionally, these experiments provide evidence that multisensory and unisensory information is processed in parallel as it traverses a local circuit within the PPr. These results are submitted and are in review (Foxworthy, Clemo, and Meredith 2012).

The subsequent chapter (IV), directly compares the functional properties of bimodal and unisensory neurons. Surprisingly, these experiments uncover a completely novel set of features which distinguish bimodal from unisensory neurons. Additionally, the results of these experiments support the notion of parallel processing of multisensory and unisensory information as put forth in Chapter III. These observations have been submitted for review and publication (Foxworthy, Allman, Keniston, and Meredith 2012)

Finally, Chapter V discusses the significance of this work as a whole and suggests future directions for this research.

CHAPTER II

AN EXAMINATION OF SOMATOSENSORY AREA SIII IN FERRET CORTEX

INTRODUCTION:

The existence of multiple representations of a given sensory system in the neocortex is well-established, and has been found in all mammals investigated (Krubitzer 2007). For the somatosensory modality, at least six (areas 3a, 3b, 1, 2, parietal ventral area, SII) distinct regions have been mapped in the cortex of various primates (Kaas, Nelson et al. 1979; Nelson, Sur et al. 1980; Kaas 1983; Krubitzer, Clarey et al. 1995), and five (SI, SII, SIII, SIV, SV) have been identified in cats (Adrian 1940; Woolsey 1943; Haight 1972; Clemo and Stein 1983; Mori, Fuwa et al. 1996). The cortices of flying foxes and California ground squirrels have also been examined to reveal multiple somatosensory representations (Krubitzer and Calford 1992; Slutsky, Manger et al. 2000). Rats and mice, with their characteristic barrel-field modification of the SI region, have been described as exhibiting at least two somatosensory cortical representations (Carvell and Simons 1986; Koralek, Olavarria et al. 1990). Even marsupials, whose phylogeny diverged from the Eutherian line around 135 million years ago (Kirsch 1977), reveal evidence of multiple cortical somatosensory representations (Karlen and Krubitzer 2007). However, comparatively little has been done to explore the different somatosensory representations in ferrets, a species of carnivore whose neurobiology is being examined with increasing frequency.

Previous work (Hunt, Slutsky et al. 2000) suggested that the somatosensory organization of ferret cortex is similar to that of cats, but no firm homologies between cat and ferret

somatosensory cortex were described. Electrophysiological studies in the ferret cortex identified the SI region on the ansate and lateral suprasylvian gyrus (Leclerc, Rice et al. 1993; Rice, Gomez et al. 1993; McLaughlin, Sonty et al. 1998). Two to four distinct representations of the face were identified on the suprasylvian gyrus (Leclerc, Rice et al. 1993; Rice, Gomez et al. 1993). However, the most posterior representation was characterized by comparatively larger receptive fields that repeated aspects of the more rostral vibrissa pad representation. The cytoarchitectonic examination of ferret somatosensory cortex by Rice et. al. (1993) found four distinct divisions along the suprasylvian gyrus and hypothesized that the most caudal region could be part of SIII, as also suggested by Hunt et al. (2000). Given the similarities in the receptive field properties and location of this region in ferrets and those of the third somatosensory area (SIII) in the cat (Garraghty et al., 1987), the present investigation sought to determine whether other homologies exist that would justify the designation of the region as SIII in ferret cortex

MATERIALS AND METHODS

All procedures were performed in compliance with the Guide for Care and Use of Laboratory Animals (NIH publication 86-23) and the National Research Council's Guidelines for Care and Use of Mammals in Neuroscience and Behavioral Research (2003) and approved by the Institutional Animal Care and Use Committee at Virginia at Virginia Commonwealth University.

Physiological Studies

Surgical Procedures

For electrophysiological recordings, ferrets (n=3) were anesthetized with sodium pentobarbital (45 mg/kg i.p.) and their heads were secured in a stereotaxic frame. Using aseptic

surgical procedures, a craniotomy was made to expose the left suprasylvian gyrus. Over this opening a recording well/head supporting device was implanted using stainless steel screws and dental acrylic. The scalp was sutured closed around the implant and standard postoperative care was provided. Approximately 3-5 days elapsed before recordings were performed.

Electrophysiological Recording

A ferret was initially anesthetized with ketamine/dexmedetomidine (8mg/kg ketamine; .03mg/kg dexmedetomidine intramuscularly) then secured to a supporting bar via the implanted device. Supplemental anesthetics (8mg/kg ketamine; .03mg/kg dexmedetomidine intramuscularly) were administered approximately hourly, as needed. Animal temperature was maintained near 38°C with a circulating-water heating pad, and body temperature and heart rate were monitored continuously.

For recording, the well was opened to expose the cortical surface. Recordings were performed by inserting a glass-insulated tungsten electrode (tip exposure ~20µm, impedance<1MΩ) into the cortex then advancing the electrode to a depth (generally 750-850µm deep to the pial surface) that yielded vigorous neuronal activity. Neuronal discharges were amplified, displayed on an oscilloscope and played on an audio monitor. Once the electrode was in place, neuronal activity usually resembled 1-3 well-isolated units.

The location of each recording penetration was plotted onto a photograph of the cortical surface using vasculature and cortical landmarks. Somatosensory receptive fields were mapped using minimally effective stimuli (force thresholds determined using calibrated Semmes-Weinstein monofilaments) and graphically recorded on a scaled drawing of the ferret's body surface. The surface of the head was divided into 11 areas (figure 1) (after (Leclerc, Rice et al.

1993). Responsiveness to auditory stimulation was assessed using manually presented clicks, claps and whistles. Responsiveness to visual stimulation was tested using manually presented moving bars of light and dark. These were moving spots or bars of light from a hand-held ophthalmoscope, or dark stimuli from a rectangular piece of black cardboard. The activity evoked by sensory stimulation was classified as somatosensory, visual, (auditory was not observed), bimodal (somatosensory-visual), or unresponsive.

Data Analysis

To enable visualization of the somatosensory representation in the cortex, the surface of the head was divided into 11 areas (figure 1) (after (Leclerc, Rice et al. 1993) and receptive fields were designated according to those criteria. If a receptive field contained more than one of the defined subdivisions, it was assigned to the category that represented >50% of the receptive field. This receptive field was then plotted at the corresponding location of the recording penetration not as a point, but as a Voronoi plot constructed from the digital image of the penetrations using *MapViewer 2.3*(http://mapviewer.skynet.ie).

Anatomical Studies

Surgical Procedures

Ferrets (n=3) were anesthetized with sodium pentobarbital (45 mg/kg i.p.), their heads secured in a stereotaxic frame and, under aseptic conditions, a craniotomy was performed to expose the desired cortical area. Prior to tracer injections, recordings were made (same recording procedure as described above) to locate cortical sites which corresponded to the areas mapped in electrophysiological procedures. In one animal, an injection was made in a cortical

site responsive to superior vibrissa stimulation. In two other animals, the sites were responsive to anterior vibrissa stimulation. Tracer injections consisted of a 10% mixture (in phosphate buffered saline) of 10,000 and 3,000 molecular weight biotinylated dextran amine (BDA; Invitrogen, Carlsbad CA) delivered iontophoretically through glass micropipettes with tip diameters between 20 and 40µm. The pipette was lowered to the desired depth (via hydraulic microdrive) under a continuous current of -2.75 µA to retain the BDA during pipette travel. Once a depth of 800µm was reached, positive current pulses (7s on, 7s off) of 6µA were delivered for 20 minutes. Following this, the current was switched off for ten minutes. During withdrawal of the pipette, continuous current of -2.75 µA was again used to prevent tracer leakage. The cortex was then covered with bone wax, the wound sutured closed, and standard postoperative care was provided. In three additional adult male ferrets, similar procedures were used to inject BDA tracer into SI cortex on the suprasylvian gyrus. SI cortex was identified using anatomical landmarks based on the work of Leclerc (1993) and Rice (1993). To ensure that injections did not produce label in the area we hypothesized to be SIII, they were made in a region of the suprasylvian gyrus that was in the coronal plane of the postcruciate sulcus which, by any of the cited maps, is clearly within S1.

Histological Procedures

Following a 10-14 day post-injection survival period, animals were given a sodium pentobarbital overdose and perfused intracardially with saline followed by 4.0% paraformaldehyde. The brains were blocked stereotaxically, removed and cryoprotected. Coronal sections (75µm thick) were cut serially using a freezing microtome. One series of sections from each animal (at 150 µm intervals) was processed for BDA visualization using the

avidin-biotin peroxidase method, according to the protocol of Veenman (1992) and heavy-metal intensified. Reacted sections were mounted on standard chrome-alum gelatin pre-treated slides, dehydrated and coverslipped. An alternate series of sections was processed to visualize cytoarchitectonic features using the antibody SMI-32 to non-phosphorylated neurofilaments (van der Gucht, Vandesande et al. 2001). Tissue from animals used in electrophysiological experiments was also reacted for SMI-32, an antibody that labels neurofilaments in dendrites, axons and cell bodies to aid in visualizing cytoarchitecture. In immunohistochemically processed cases, during the recording session, an electrolytic, locating lesion was made in the posterior penetrations (in a series) in which exclusive somatosensory responsiveness was no longer observed (corresponding to rostral parietal area PPr; (Manger, Masiello et al. 2002). This process provided an indicator of the tissue in which somatosensory responsiveness had been observed (e.g., anterior to the lesions) and, thereby, allowed the cytoarchitectonic (using SMI-32 staining) examination of the somatosensory region.

Data Analysis

Tissue processed for BDA was examined using a light microscope and the locations of labeled neurons were plotted using a PC-driven digitizing stage controlled by Neurolucida software (Microbrightfield Biosciences, Inc., Williston, VT). Each tissue section was traced showing its tissue outline, gray matter/white matter border, and the locations of labeled neurons. The injection site was defined as the region of densest label, usually at the end of the pipette track. BDA-labeled neurons generally were sharply black throughout their soma and dendrites. Plotted tissue sections from each case were digitally transferred to a graphics program and serially superimposed for final visualization and graphic display. Cytoarchitectonic features

visualized using SMI-32 immunohistochemistry were plotted using a camera lucida and photographed.

RESULTS

Sensory Responses of Suprasylvian Gyrus

To explore the sensory features represented on the suprasylvian gyrus, extracellular recordings were performed in three adult male ferrets at 106 sites. Approximately 30 recording penetrations were performed per animal, as in the example shown in figure 2. Each penetration series began on the suprasylvian gyrus in a plane rostral to the ansate sulcus, and continued caudally until somatosensory responsiveness was lost. Most recording sites (78%) gave somatosensory responses, a few (5%) were unresponsive, and the remainder (17%) were visually responsive (figure 3). Visual responses were consistently encountered at the posterior-most recording sites, corresponding to the location of the rostral posterior parietal area (PPr, Manger et al., 2002) where bisensory responses (visual-somatosensory; n=4) were also encountered. For somatosensory-responsive neurons, receptive fields were almost exclusively found on aspects of the face, as illustrated in figure 2. Most somatosensory receptive fields (52%) included some aspect of the vibrissa, usually involving two or more whiskers but sometimes including the entire vibrissa pad. For the most part, the minimal effective somatosensory stimulus was very low intensity (figure 4), with 96% of somatosensory responses being driven by stimuli of less than 0.1 grams of force. All somatosensory responses were rapidly adapting. Although tested, none of the penetrations showed responses to auditory stimulation.

Somatotopic Organization

Somatotopy was difficult to discern in individual animals since receptive fields mostly included the vibrissa (see figure 2 for example RFs). However, when penetrations from all 3 animals were overlapped (figure 5D), a general somatotopic trend became apparent. Areas closest to the dorsal midline were defined as "upper face," which included the nose, bridge of nose and supraorbital areas; the "lower face" consisted of anything inferior to the vibrissa (the upper lip, lower lip and lower jaw). As presented in the bottom panel of figure 5, there was a general progression from the top to the bottom of the face as the recording locus moved from lateral to medial across the suprasylvian gyrus. Also consistent with a general somatotopy, five medial recording penetrations which travelled into the sulcus (into the lateral bank of the lateral sulcus; not depicted) continued the somatotopic pattern by exhibiting receptive fields on the neck and chest. Additionally, eight penetrations made into the lateral gyrus (unpublished data from another project) continued the general somatotopic pattern with receptive fields located on the hindlimb and forepaw. The face/head representation on the suprasylvian gyrus and body/limb representation on the lateral gyrus is consistent with the general somatotopic plan observed in ferret S1 (LeClerc et al., 1993; Rice et al., 1993). In the rostral-caudal dimension, however, a precise somatotopic pattern was not observed (see also figure 5).

Cytoarchitectonic Features

Electrolytic lesions were made in penetrations where responses transitioned from somatosensory to visual. Tissue anterior to the lesion sites, therefore, represented the somatosensory region explored and described above, and the corresponding cytoarchitectonic features were examined using SMI-32 immunostaining. The cytoarchitectonic and laminar

features of this portion of the suprasylvian gyrus are shown in figure 6. In general, the infragranular layers were larger than the supragranular layers. Layer I was compact and mostly devoid of label. Upper layer II/III contained mostly vertically oriented fibers (perpendicular to the pial surface) and fewer horizontal fibers (parallel to the pial surface). Lower layer II/III contained small, darkly stained pyramidal cells as well as both vertically and horizontally oriented fibers. Layer IV exhibited sparse vertically oriented fibers which appeared to arise from other layers, but was otherwise mostly devoid of label. Upper layer V was easily distinguished, having many darkly stained pyramidal cells and short labeled fibers of varying orientations. Lower aspects of layer V displayed only light staining, but could be distinguished from laver VI by the presence of a few lightly stained cells and fibers. Layer VI was mostly unlabelled.

Anatomical Connections

Under electrophysiological guidance, tracer (BDA) was injected (n=3 ferrets) into sites on the suprasylvian gyrus that exhibited the characteristic, vibrissa receptive fields. Injection sites (see figure 7) were confined to the gyral grey matter with a diameter of ~700μm. Retrogradely labeled neurons were typically layer 2-3 pyramidal neurons, as depicted in the micrograph in figure 7. As summarized for one case by the serial coronal sections in figure 7, retrogradely labeled neurons were found anteriorly on the coronal gyrus and medial bank of the suprasylvian sulcus corresponding to MI, SI and MRSS and posteriorly, on the suprasylvian gyrus, largely corresponding to parietal area PPr. These same tracer injections also labeled distinct regions of thalamus, as shown in figure 8A-B. Darkly stained, retrogradely filled neurons, as well as axon terminals, were found in the posterior thalamic nuclei (PO), but not in

the ventrobasal nucleus (VB). In contrast, in separate animals (n=3), injection of BDA tracer into S1 (figure 8C-D) labeled neurons and axon terminals in the ventrobasal nucleus (VB), but not PO.

Discussion

The data presented herein documents the somatotopic representation of the face on the suprasylvian gyrus between S1, anteriorly, and area PPr, posteriorly. Tracer injections into this region demonstrated afferent connections from cortical areas SI, MRSS, M1and PPr, as well as from the posterior nucleus of the thalamus. Collectively, these observations provide further evidence that the examined somatosensory region is distinct from SI (see below) and, given its homologies with that of cat SIII (see below), should be designated as SIII in the ferret.

Distinctions from SI

Previous work by Rice et al. (1993) in ferret found four cytoarchitectonic divisions of somatosensory cortex along the suprasylvian gyrus and hypothesized that the most caudal region (dubbed P14) could be part of SIII, based on its similar location in cat cortex. Leclerc et. al. (1993) found that this region (dubbed C2 in electrophysiological mapping experiments) had larger receptive fields than those observed at more rostral recording sites in SI. The present study is consonant with these earlier works. Furthermore, tracer injection into SI revealed strong and nearly exclusive connectivity with the ventrobasal complex of the thalamus, whereas injections into SIII labeled neurons in the posterior nucleus of the thalamus.

Cat SIII and ferret SIII homology

The somatosensory region designated SIII has been described in cat cortex (Darian-Smith, Isbister et al. 1966; Garraghty, Pons et al. 1987) and resides in the ansate sulcus and on the rostral aspect of the suprasylvian gyrus between SI, anteriorly, and parietal area 5, posteriorly. This region contains a somatotopically organized representation of the cat's entire body surface, with the head represented medial and the trunk/hindlimb representation lateral (Garraghty, Pons et al. 1987). For head and forelimb representations, there was a receptive field reversal as recording sites crossed the SI-SIII border, where SIII receptive fields also generally increased in size (Garraghty, Pons et al. 1987). Posteriorly, the caudal border of SIII was consistently characterized by the abrupt cessation of responses to tactile stimulation (Garraghty, Pons et al. 1987). Cortico-cortical connectivity of cat SIII includes inputs from somatosensory areas SI, SII and SIV as well as from M1, while thalamocortical projections arise primarily from the posterior thalamic nucleus (Garraghty, Pons et al. 1987).

Likewise, in ferret cortex, somatosensory responsivity posterior to SI has been noted by several studies (Rice et al. 1993; Hunt et al., 2000) where receptive fields were comparatively larger than in SI (Rice et al., 1993; present study). Further posterior along the suprasylvian gyrus, a sharp transition occurred where somatosensory activity ceased and robust visual responsivity was observed corresponding to the rostral posterior parietal area (Manger, Masiello et al. 2002). Thus, in terms of location and function, area SIII appears to be homologous in ferret and cat. Furthermore, the present study identified cortical inputs to SIII that arose from somatosensory areas SI and MRSS and M1 motor cortex, as well as thalamocortical connections to SIII from the posterior thalamic nucleus (PO). These connectional features of ferret SIII are essentially the same as those identified for area SIII of cats (Garraghty, Pons et al. 1987).

The present study has identified features of ferret SIII that appear to differ from those reported for cat SIII. Most striking is the difference in orientation of the somatotopy of the regions. Although the entire body surface was not examined in the ferret, its representation presents the top of the head most laterally with more ventral and posterior aspects of the body medial. In contrast, the somatotopy in cat SIII shows the head medial and the representation of the trunk/hindlimbs lateral (Garraghty, Pons et al. 1987). However, it should be noted that the mapping of sound frequencies in auditory cortex is rotated in ferret 90º from the well-known tonotopy seen in cat (Reale and Imig 1980). Together, these observations suggest that local, species-specific arrangements have occurred within the general pattern of their sensory representation distribution. In addition, the present study identified projections to SIII from PPr, that presumably represent feedback connections from visual-somatosensory bimodal neurons in the parietal area. These apparent crossmodal connections have not been examined in cats.

Relationships with other cortical fields:

Illustrations in recent studies of ferret cortex would give the impression that SIII is already a well established fact. However, most publications that directly examined the features of this somatosensory region (Leclerc, Rice et al. 1993; Rice, Gomez et al. 1993; Hunt, Slutsky et al. 2000) were reluctant to designate the region as SIII. Probably as a consequence, subsequent studies that have relied on the earlier descriptions have depicted SIII in various distributions in relation to their work on adjoining cortical fields (e.g., Figure 1,(Bizley, Nodal et al. 2007); Figure 1,(Manger, Engler et al. 2005); Figure 1-2,(Manger, Masiello et al. 2002)). The present study indicates that SIII occupies the full medial-lateral extent of the suprasylvian gyrus between SI (anteriorly) and PPr (posteriorly), as depicted in Figure 9. Although we did not

examine the representation on the lateral gyrus in detail, eight penetrations as well as previous reports (Leclerc et al., 1993; Rice et al., 1993) indicate that the SIII representation continues at this location. Another point of ambiguity in ferret cortex is the presence and location of somatosensory area SII. Preliminary results from our lab indicate somatosensory responsivity in the region anterior to the anteroventral auditory field (AVF; (Bizley, Nodal et al. 2005) and the AEV (Manger, Engler et al. 2005). Given the correspondence of this somatosensory location with that of SII in the cat (Burton and Kopf 1984), it seems logical to suspect this location to contain the ferret SII representation, as illustrated in figure 9 (see also (Manger, Engler et al. 2005). Furthermore, this portion of the anterior ectosylvian gyrus shows topographic connections with SI (unpublished data) much like SII does in the cat. Other ferret somatosensory regions have been described by Keniston et al., (2009) as the medial rostral suprasylvian area (MRSS) and by Keniston et al., (2008) as the lateral rostral suprasylvian area (LRSS). Like the other representations on or near the suprasylvian sulcus, these regions primarily represent the ferret head and face. However, the anterior borders of nearly all of these ferret somatosensory regions, along with the M1 domain, remain to be mapped. Accordingly, more attention needs to be directed toward elucidating the multiple somatosensory representations, as well as their connectional and hierarchical relationships, in ferret cortex.

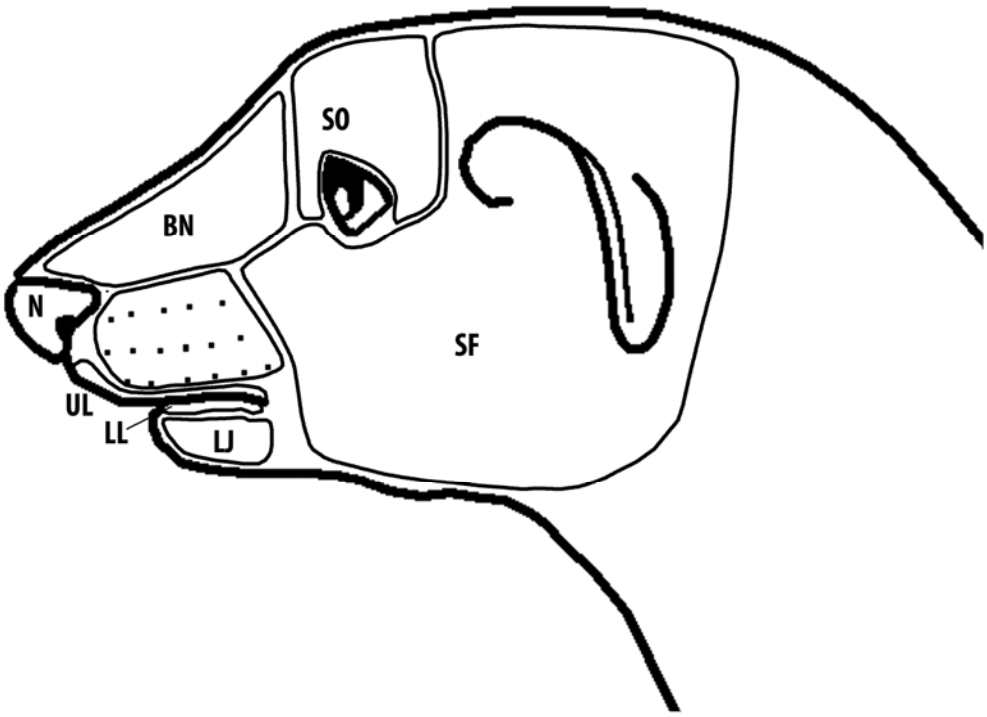

Figure 1: Scheme used to name the regions of the ferret face/head for defining recorded somatosensory receptive fields (after Leclerc et al 1993). SF, side of face; SO, supraorbital area; BN, bridge of nose; N, nose; UL, upper lip; LL, lower lip; LJ, lower jaw. Although not depicted on this schematic, the vibrissa responses were subdivided as: superior (SV), inferior (IV), rostral (RV), caudal (CV), or all (AV) if the entire vibrissa pad was responsive.

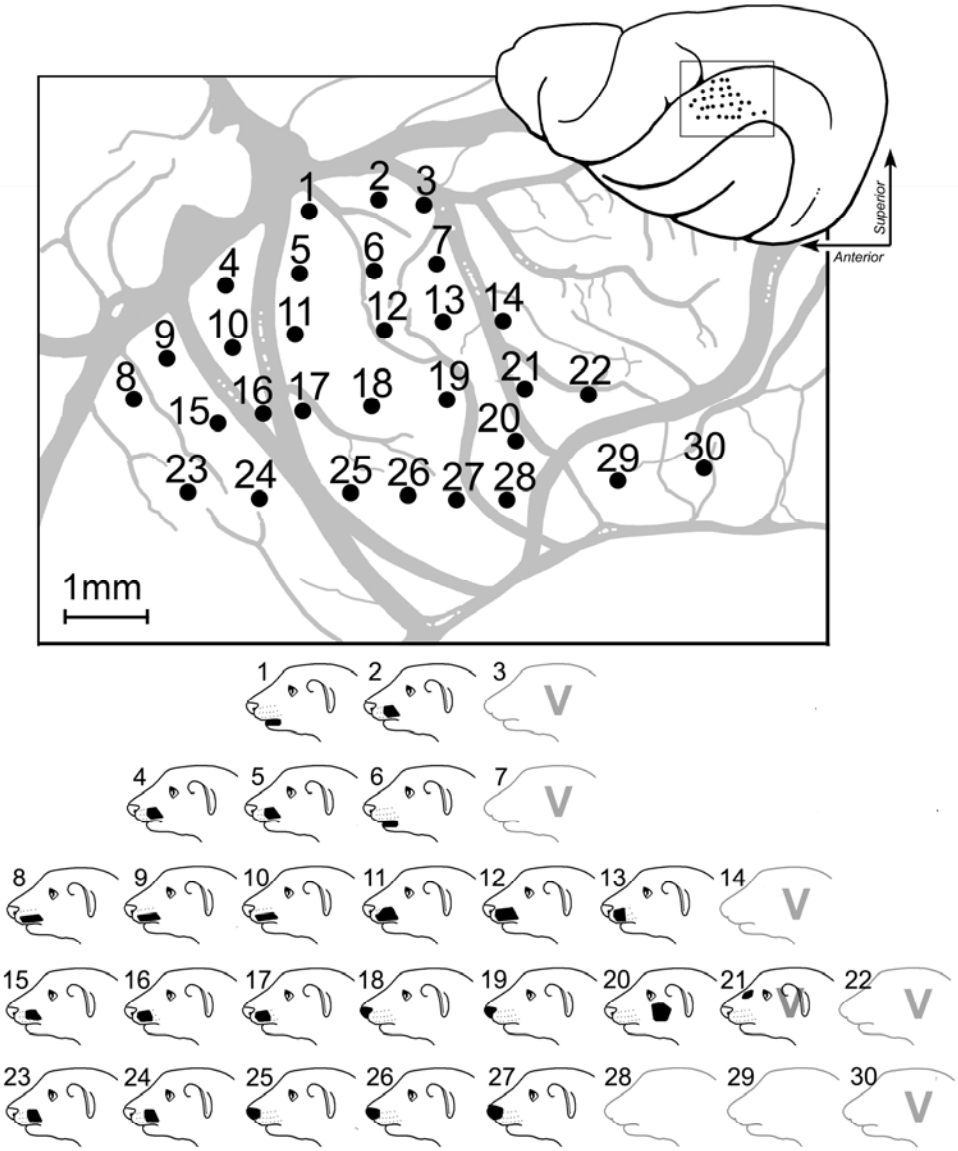

Figure 2: Recording penetrations and the corresponding receptive fields from SIII cortex of an adult ferret. In the top right image, a dorsal view of the left hemisphere shows the location of the recording penetrations (1 dot = 1 penetration). Each penetration was plotted onto a photograph of the cortical surface using vasculature and cortical landmarks. In the middle image, the photograph used for mapping (not pictured) has been traced and magnified for visibility, and the recording sites numbered. Somatosensory receptive fields were assessed at each penetration (at a depth of ~750-800um), where visual/auditory responsiveness was also tested. The bottom image shows receptive fields mapped at sites with corresponding numbers. Somatosensory receptive fields are indicated by solid black shapes. Sites with visual responsiveness are indicated with a "V." Unresponsive sites (28 and 29) are shown as an empty outline of the ferret face. Penetrations with bimodal responses (site 21) have somatosensory receptive fields mapped and also reliably responded to visual stimuli.

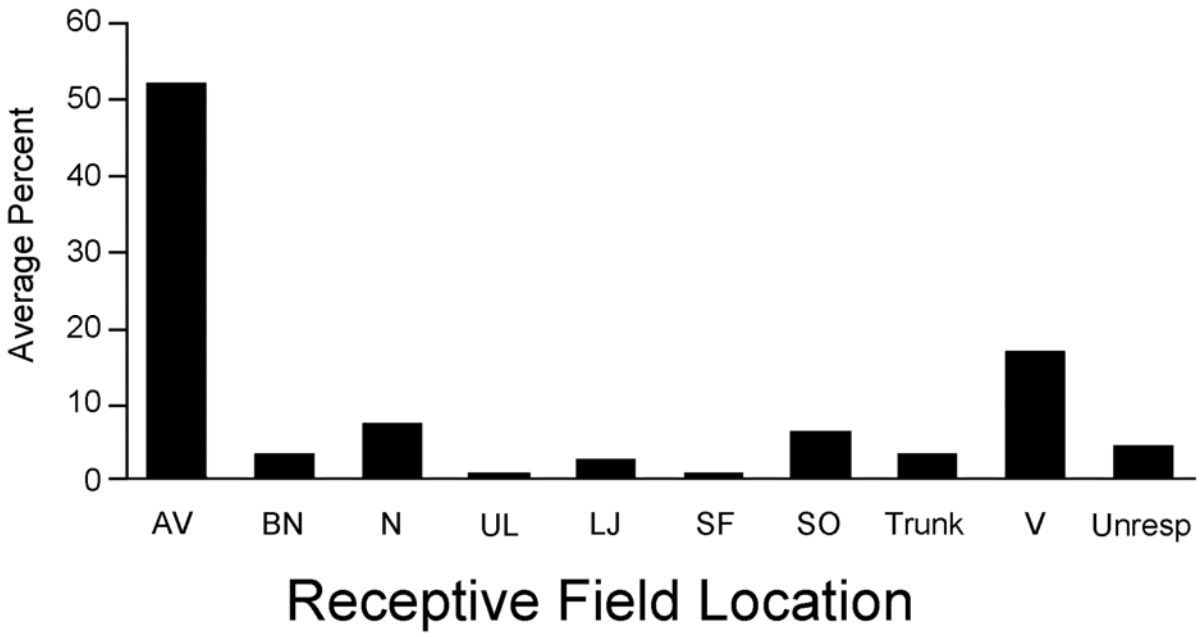

Figure 3: Somatosensory receptive fields of SIII neurons generally included the vibrissa. The bar graph shows the incidence of occurrence of each of the designated regions of the head/face (conventions same as Figure 1) in the somatosensory receptive fields of SIII neurons.

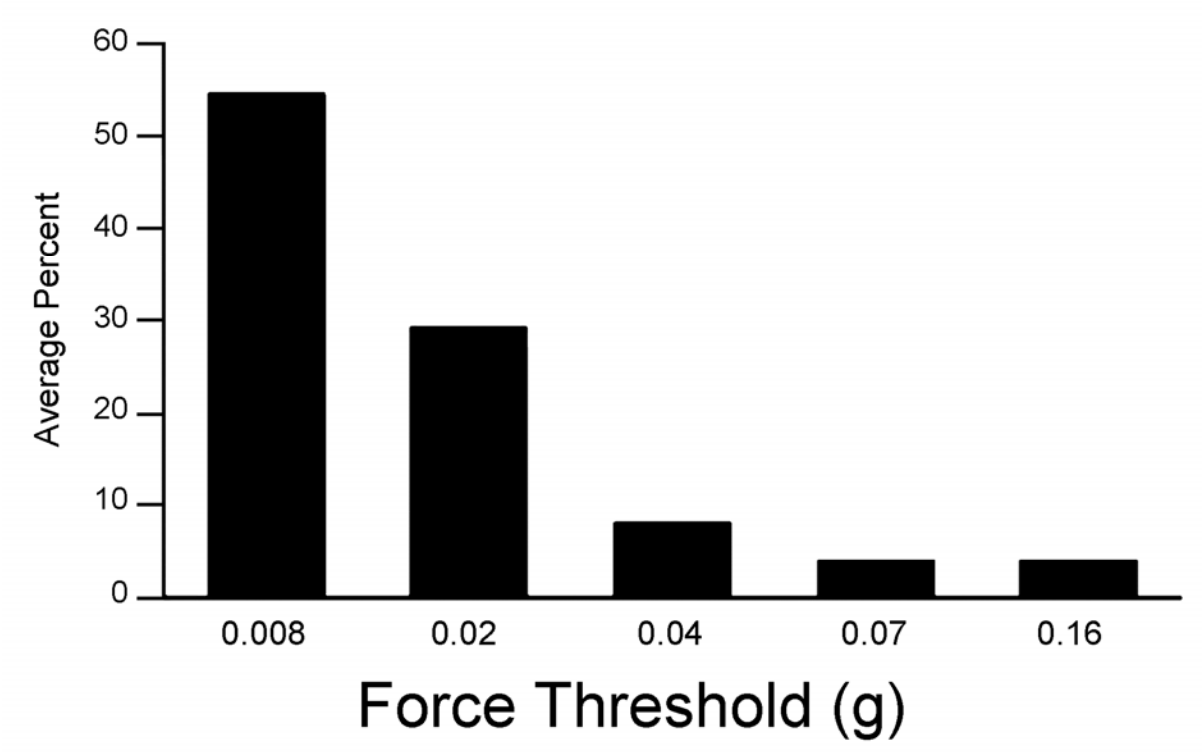

Figure 4: Force threshold for activation was very low for SIII neurons. Bars correspond with the proportion of recording sites responding with a specific force threshold (x-axis).

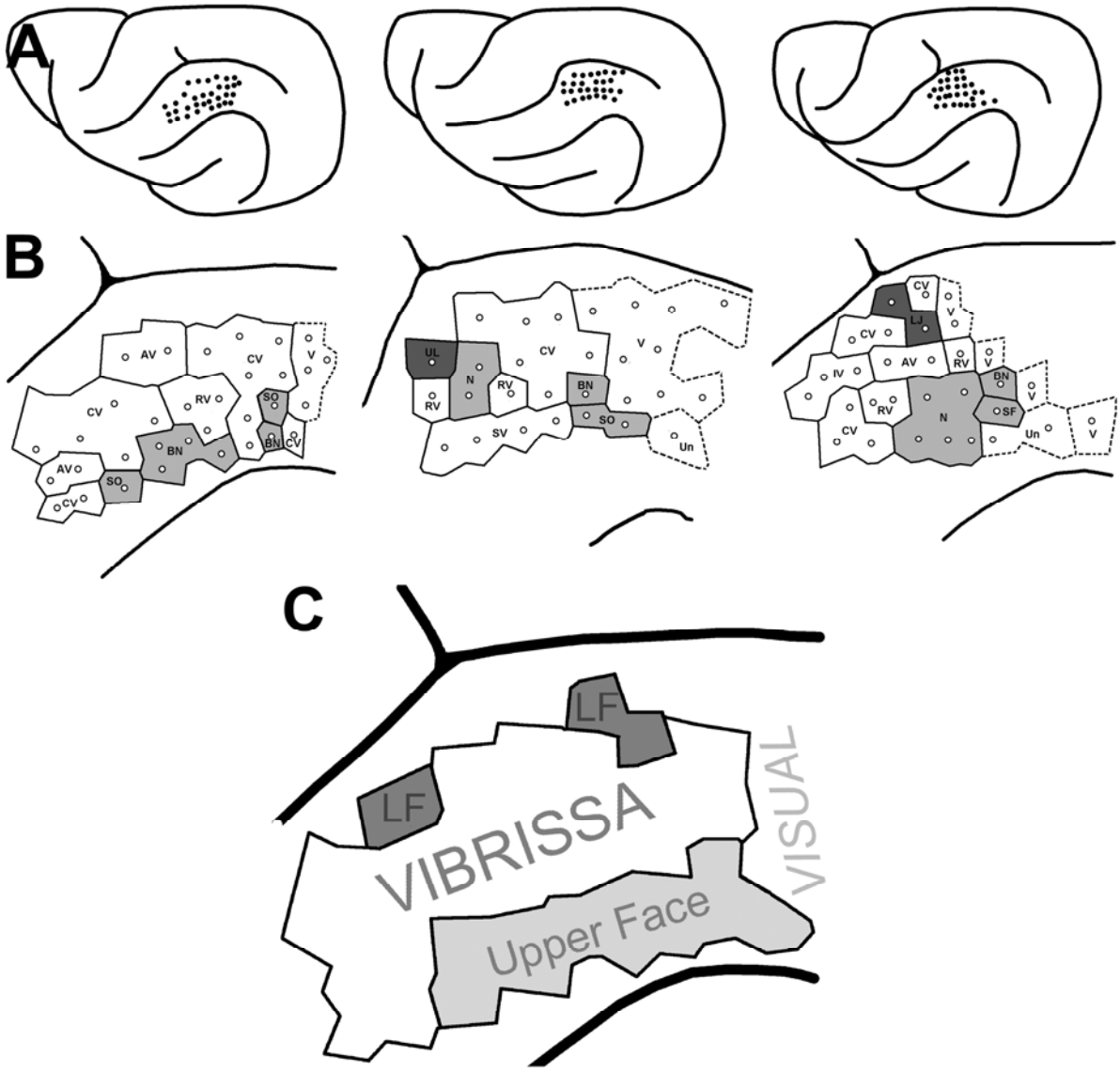

Figure 5: SIII recordings from 3 ferrets reveal a general somatotopic pattern. (Row A; top) Locations of electrode penetrations on the suprasylvian gyrus for each animal are shown of dorsal views of the recorded, left hemisphere. (Row B) Enlarged view of penetrations with Voronoi diagram and superimposed receptive fields (Conventions same as Figure 1). Dark shading indicates regions in the lower portion of the face; light shading indicates regions of the upper face; white represents any vibrissa. Dashed lines indicate unisensory visual responses or unresponsive penetrations. (Part C; bottom) A summary of three animals generated by overlapping the 3 plots depicted immediately above. This schematic indicates that the middle of the suprasylvian gyrus contains a representation of the vibrissa while the upper face is represented on the lateral portion of the gyrus and the lower face on the medial portion. Caudal to SIII is a region which is visually responsive, corresponding to PPr (Manger et al 2002).

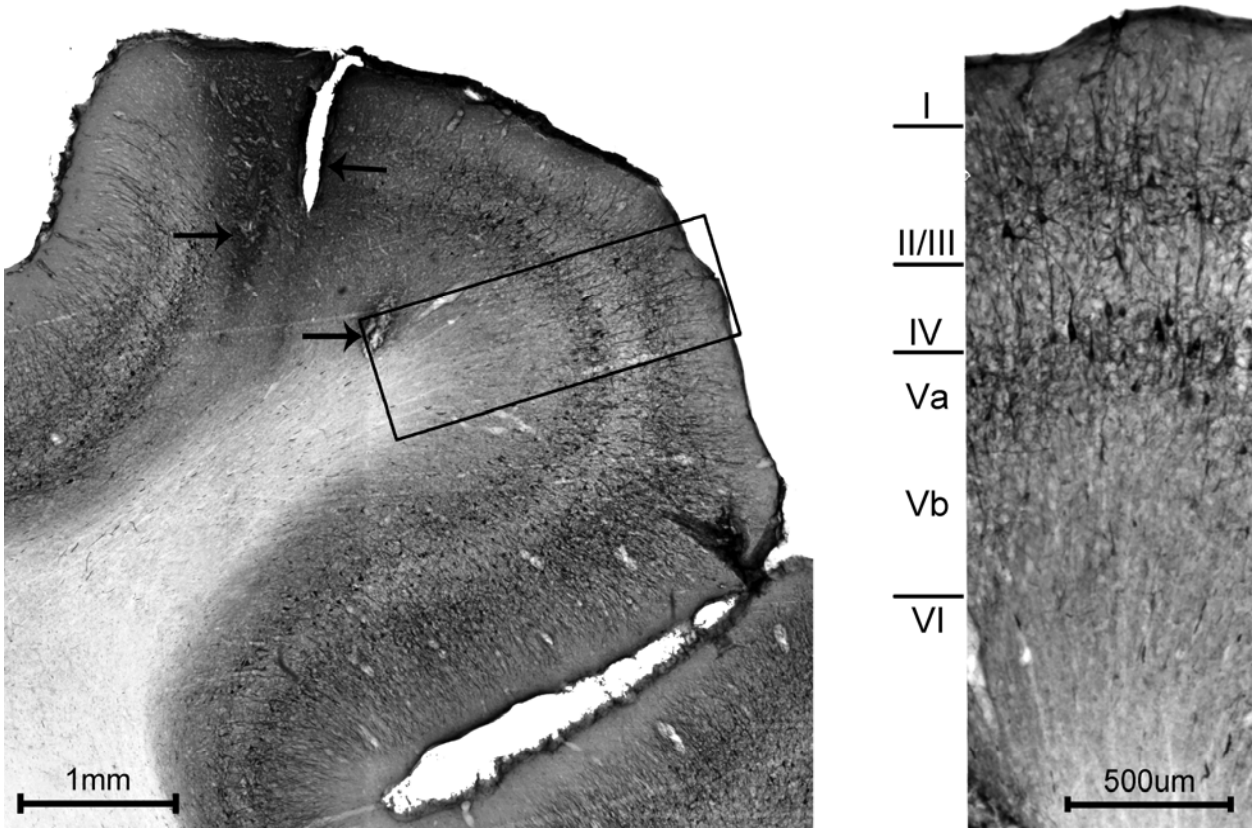

Figure 6: Cytoarchitectonic organization of SIII. (Left) The photomicrograph shows a coronal section through the suprasylvian gyrus in the SIII region. The cytoarchitecture of SIII was examined in tissue from the somatosensory mapping experiments, and arrows point to damage from electrode penetrations in which somatosensory receptive fields were mapped. A portion of the section through the suprasylvian gyrus (left, boxed area) is magnified (at Right) to reveal the laminar-specific staining. Layer I is thin and mostly devoid of label. Layers II/III contain a few, small, darkly stained pyramidal neurons and exhibit short stained fibers both parallel to and perpendicular to the pial surface. Layer IV is mostly devoid of label but demonstrates a few stained vertical fibers. Layers V-VI are relatively thick. Upper Layer V contains many darkly stained pyramidal cells with short labeled fibers of various orientations. Lower Layer V is comparatively light with few lightly stained fibers and cells while layer VI is mostly devoid of label.

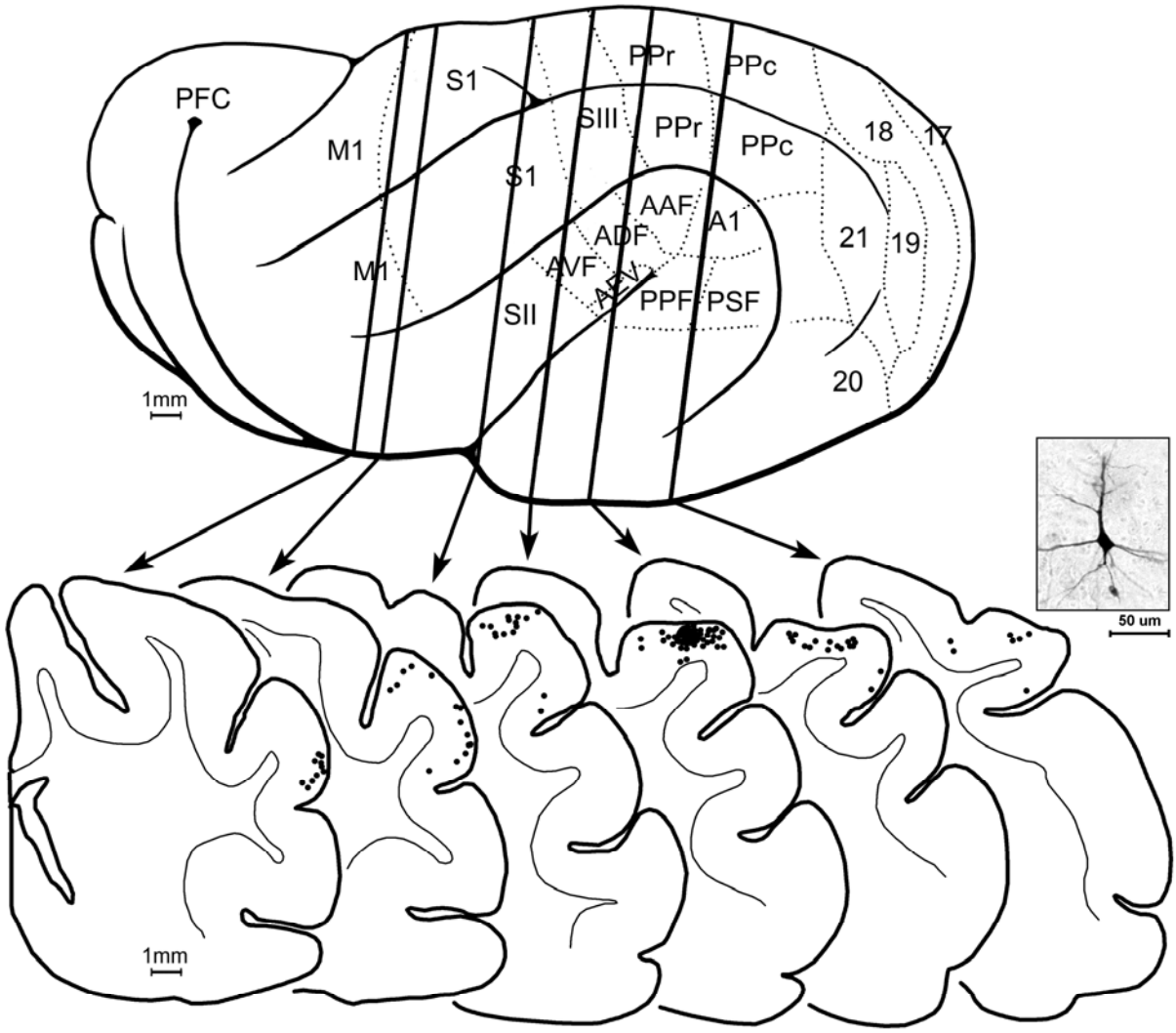

Figure 7: Projections to SIII demonstrated with tracer (BDA) injection. In (A), the lateral view of the hemisphere shows the known functional subdivisions (dotted lines). Vertical lines passing through the brain (TOP) correspond to the coronal sections s below. At bottom, the coronal sections are arranged serially (anterior=left) with the grey-white border of the cortical mantle indicated (thin line). The tracer was injected (black area) into the representation of the superior vibrissa recorded at that site. Each retrogradely labeled neuron (as shown in the example photomicrograph) was marked with a single black dot. Retrogradely labeled neurons are present in SI, MRSS, M1, and PPr**,** indicating the connectivity of these areas with SIII.

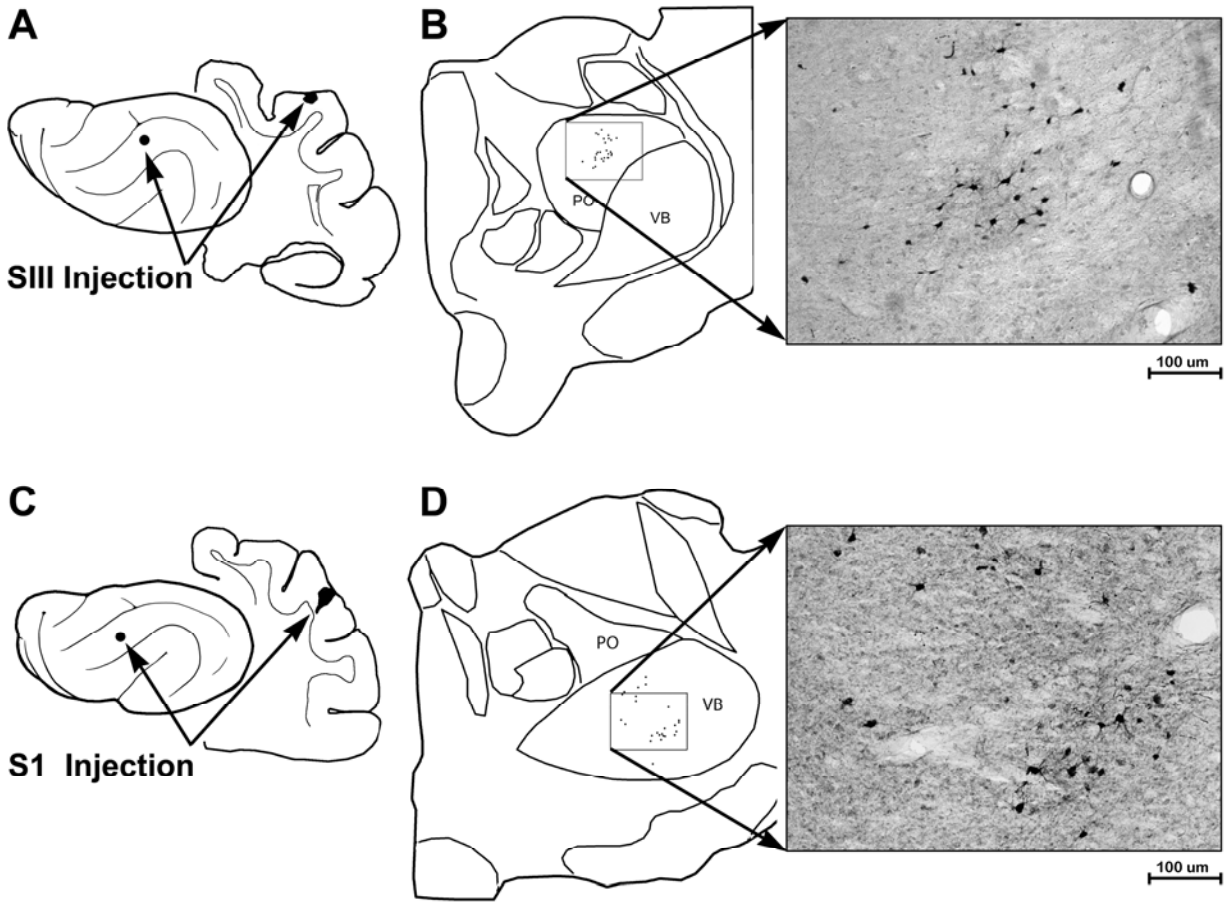

Figure 8: Thalamic connections with SIII are different from those with S1. (A) The lateral view of the ferret cortex, and the coronal section, indicates the location of tracer injection into SIII. Part 'B' shows a tracing of thalamus with the subnuclei of posterior thalamic nucleus (PO) and ventrobasal nucleus (VB) outlined. For tracer injections into SIII, labeled neurons were identified and plotted in PO (boxed area), which is enlarged in the photomicrograph of labeled neurons in. Part 'C' illustrates the injection site in S1 on lateral and coronal views of the brain. Part 'D' shows a tracing of thalamus with the subnuclei of posterior thalamic nucleus (PO) and ventrobasal nucleus (VB) outlined. For tracer injections into SI, labeled neurons were identified in VB (boxed area), which is enlarged in the photomicrograph of labeled neurons.

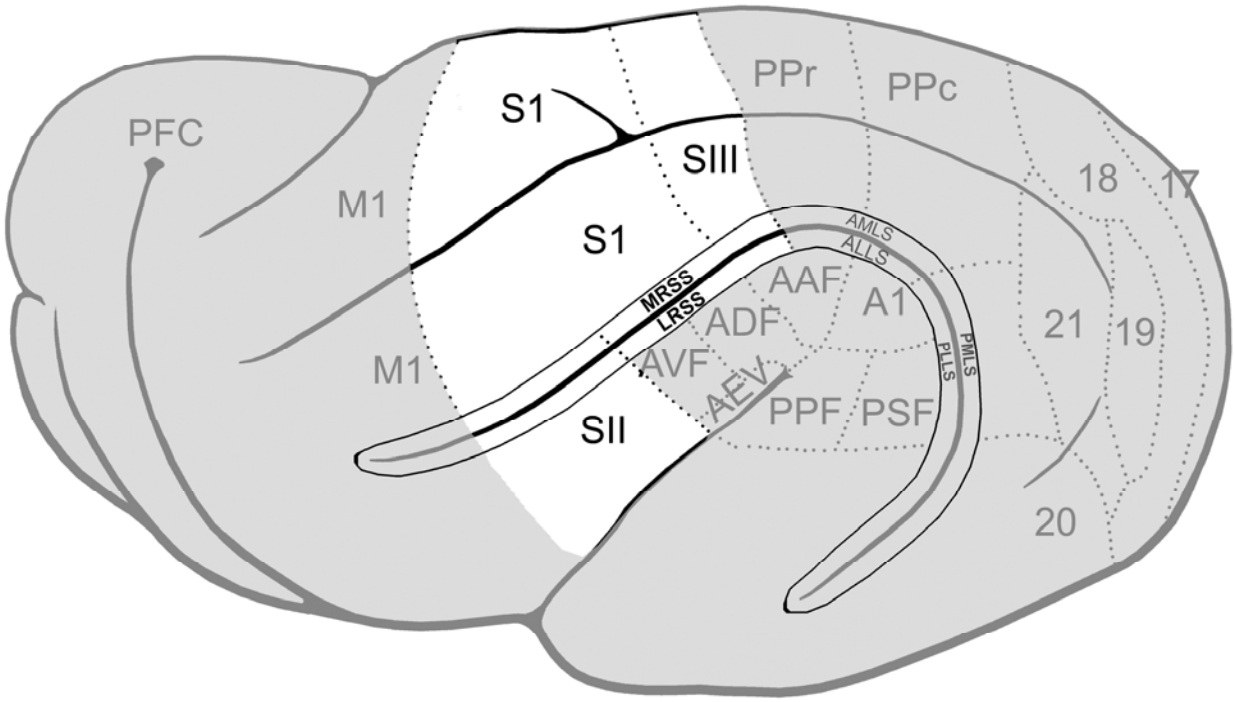

Figure 9: Summary of ferret cortical representations. On this lateral view of the ferret cerebral cortex (left hemisphere; anterior=left), the known somatosensory regions are highlighted in white. The borders of functional subdivisions are represented by the dotted lines. Abbreviations: S1, somatosensory area 1; SII, somatosensory area 2; SIII, somatosensory area 3; MRSS, medial rostral suprasylvian sulcus; LRSS, lateral rostral suprasylvian sulcus.

CHAPTER III

LAMINAR AND CONNECTIONAL ORGANIZATION OF A MULTISENSORY CORTEX

INTRODUCTION

It is well known that sensory signals are transformed by the circuitry of the neocortex to extract information about the physical nature of external stimuli. A great deal has been learned about how this process occurs by comparing the functional organization of the primary auditory, visual and somatosensory cortices. Perhaps the most fundamental similarity between these different areas is the laminar basis of their connectivity. In general, sensory information is relayed from the principal nuclei of the thalamus primarily to the excitatory spiny stellate neurons of cortical layer 4. From these gateway neurons, most local projections excite pyramidal neurons in layer 2-3 that, in turn, make translaminar connections to layer 5 neurons and finally to layer 6 neurons (see Callaway, 2004; Douglas and Martin, 2004; Thomson and Lamy, 2007 for detailed review). Output connections from these cortices have also been shown to be lamina dependent: layer 2/3 neurons project to other ipsilateral and contralateral cortical areas; layer 5 neurons project to subcortical structures (including non-specific thalamic nuclei, superior colliculus, caudate, pons, spinal cord); layer 6 neurons project to the principal and non-specific regions of the thalamus, the reticular nucleus of the thalamus, and the claustrum (see Callaway, 2004; Douglas and Martin, 2004; Reiner et al., 2003; Thomson and Lamy, 2007; Zhang and Deschenes, 1997 for review). This pattern is repeated across the different sensory cortices with such fidelity that it has become regarded by some as a "canonical" cortical microcircuit (but see Horton and Adams, 2005). Thus, for primary sensory cortices, thalamic principal nuclei target

layer 4 stellate neurons providing entry into the cortical circuit while subsequent neurons in other layers provide local processing and exhibit a stereotypical pattern of output projections.

Given this distinct laminar connectional pattern of the neocortex, it would be expected that neurons in each layer perform a unique functional transformation on the sensory signals passing through them. This notion is supported by a wealth of evidence which shows differential laminar responses to sensory stimulation (see Hirsch and Martinez, 2006; Linden and Schreiner, 2003 for review). For example, supragranular and infragranular neurons in primary somatosensory cortex exhibit larger receptive fields than layer 4 neurons (Brumberg et al., 1999). Similarly, in cat primary visual cortex, simple cells are found almost exclusively in layer 4 and 6, whereas supragranular and infragranular layers contain a preponderance of complex cells (Martinez et al., 2005). Neurons in layers 2 and 3 also appear to be more feature selective than their layer 4 counterparts whereby layer 4 neurons respond better to impoverished stimuli (such as noise) and their supra- and infragranular counterparts respond better to more specific stimuli such as punctate whisker deflections or visual motion in the preferred direction (Brumberg et al., 1999; Hirsch and Martinez, 2006). Layer 4 neurons have also been demonstrated to have a shorter response latency and greater response precision compared to supragranular and infragranular neurons in primary auditory (Atencio et al., 2009), visual (Hirsch and Martinez, 2006) and somatosensory cortices (Brumberg et al., 1999). Furthermore, the cortical circuitry also exhibits distinct parallel channels of submodal information, where separate processing modules deal with particular stimulus features (Nassi and Callaway, 2009; Schreiner et al., 2000; Sur et al., 1981) as well as exhibit neuronal type-specific connectivity (Thomson and Lamy, 2007; Xu and Callaway, 2009). Thus, specific neuronal connectivity appears to provide the basis

for the parallel transformation of different features of sensory information as well as the extraction of stimulus features as signals pass progressively through the neocortical circuit.

As described above, most efforts to understand the connectional basis of cortical sensory processing have focused almost exclusively on the primary and lower-level sensory cortices. However, the brain also uses information derived from combinations of different sensory modalities to influence perception and to guide behavior (for review see Stein and Meredith, 1993). Cortical areas dedicated to these tasks have been identified as multisensory (or classically as 'polysensory'). Although it was originally thought that these higher-level association cortices were the only sites in which multisensory neurons occurred (Jones and Powell, 1970), neurons that can be influenced by multiple sensory signals have now been found throughout the neocortex (Ghazanfar and Schroeder, 2006). However, while many areas contain neurons which can be *influenced* by more than one modality, some higher-level association cortices exhibit not only a majority of neurons that are multisensory, but also a large proportion of those that demonstrate bimodal properties; that is, they show suprathreshold spiking activity in response to more than one sensory modality (see Meredith et al., 2011a). Such multisensory cortical areas include primate superior temporal sulcus (Benevento et al., 1977; Bruce et al., 1981; Hikosaka et al., 1988) intraparietal sulcus (Avillac et al., 2007; Bremmer et al., 2002; Cohen et al., 2005; Duhamel et al., 1998; Russ et al., 2006; Schlack et al., 2005), frontal and prefrontal cortex (Fogassi et al., 1996; Graziano et al., 1999; Graziano et al., 1994; Romanski, 2007), and cat anterior ectosylvian sulcal regions (Clemo et al., 2011; Jiang et al., 1994; Wallace et al., 1992). As higher-level cortices, these areas receive thalamic inputs primarily from the non-specific nuclei such as the lateral posterior and pulvinar nuclei (Bucci, 2009; Matsuzaki et al., 2004; Roda and Reinoso-Suarez, 1983; Romanski et al., 1997; Takahashi, 1985; Yeterian and Pandya,

1989) that terminate within cortical layer 4 (Chomsung et al., 2010) or layers 3 and 5 (Rockland et al., 1999) or layers 1-2 (Rockland et al., 1999) depending on the area and the species (Jones, 2007a for review). In addition, inputs to higher-order cortices also arrive through cortico-cortical connections that terminate largely in layer 4 (Felleman and Van Essen, 1991; Van Essen, 2005; Zeki and Shipp, 1988). These observations indicate that association cortices differ from the lower-level, primary cortical counterparts not only in their thalamic activation, but also in the source of activation of layer 4. However, few studies have evaluated the laminar organization of higher-order cortices demonstrated to be multisensory.

Until recently, it might have been assumed that multisensory neurons and properties were uniformly distributed within multisensory cortices. However, a systematic examination of the spatial distribution of multisensory neurons within the superior temporal sulcal region revealed that neurons with multisensory properties tend to cluster (Dahl et al., 2009), although a laminar basis for this non-homogeneity was not evaluated. A laminar study of the timing of visual, auditory and somatosensory inputs to this same cortical region reported that layer 4 was activated first, but the actual published records also showed early current sinks (i.e., synaptic activity) at supra- and infragranular locations as well (Figure 4, Schroeder and Foxe, 2002). On the other hand, recent neuroanatomical studies of cat multisensory cortices have demonstrated a strong preference for cortico-cortical inputs to terminate within layers 2-3 (Clemo et al., 2007; Clemo et al., 2008; Dehner et al., 2004; Meredith et al., 2006; Monteiro et al., 2003; reviewed in Clemo et al., 2011). Collectively, these few observations indicate that the laminar basis for multisensory processing is unresolved and largely unexplored.

Just as information about the features of a sensory stimulus is transformed as it passes through a primary neocortical circuit, it should be expected that features of multisensory

responses likewise could differ by laminar location. What are the features of multisensory processing that might vary within a multisensory region? Although others certainly exist, three measures of multisensory processing have been already used for comparative purposes (Lim et al., 2011): the proportion of multisensory neurons present (see also Dahl et al., 2009), the proportion of multisensory neurons showing multisensory integration, and the magnitude of the integrative effects. In addition, these properties of multisensory processing are parametrically based on the features of neural connectivity that produced them (Lim et al., 2011). Therefore, the coupling of connectional properties (determined using neuroanatomical methods) with a systematic analysis of the measures of multisensory processing (determined using electrophysiological recordings) will provide unprecedented insight into the laminar and connectional bases for multisensory processing. To conduct this investigation, a well-documented (Manger et al., 2002) and robustly multisensory cortical region (Foxworthy et al., 2011), the rostral posterior parietal cortex of the ferret (PPr), was used as the experimental model.

MATERIALS AND METHODS

All procedures were performed in compliance with the Guide for Care and Use of Laboratory Animals (National Institutes of Health, publication 86-23), the National Research Council's Guidelines for Care and Use of Mammals in Neuroscience and Behavioral Research (2003), and with approval from the Institutional Animal Care and Use Committee at Virginia Commonwealth University.

Electrophysiological Studies

Surgical Procedures

Adult ferrets (n=13) were anesthetized, (8mg/kg ketamine; 0.03mg/kg dexmedetomidine intramuscularly), their heads were secured in a stereotaxic frame and a craniotomy was made to expose the rostral posterior parietal (PPr) region of the suprasylvian gyrus. Over this opening, a recording well/head supporting device was implanted using stainless steel screws and dental acrylic. The well/head support was attached such that the eyes and ears of the animal were not obstructed and no pressure points were present.

Electrophysiological Recording

For recording, the head-support implant was secured to an immobile supporting bar. The animals were intubated through the mouth, ventilated (expired CO_2: ~4.5%) and immobilized (pancuronium bromide; 0.3 mg/kg initial dose; 0.2 mg/kg h supplement i.p.). Fluids (lactated Ringer's solution) and supplemental anesthetics (4mg/kg h ketamine; 0.5 mg/kg h acepromazine i.p.) were administered continuously with an infusion pump. Anesthesia and paralytics were necessary to prevent movement of the body and eyes during the lengthy and repeated presentation of somatosensory and visual stimuli at fixed locations. Heart rate was monitored continuously and, if heart rate rose over a sustained period of 5-10 minutes, supplemental anesthetics were administered in addition to that supplied continuously by the infusion pump. Temperature was monitored and maintained at ~38°C with a heating pad. The pupils were dilated with 1% atropine sulfate and the eye was anesthetized with 0.5% proparacaine hydrochloride for the placement of contact lenses to adjust for refractive errors.

Neuron responses were recorded using a four shank, 32-channel silicon probe (A4×8-5mm 200–200-413 array; impedance ~1 MΩ; NeuroNexus Technologies, Ann Arbor, MI) that was advanced with a hydraulic microdrive. Neuronal activity was digitized (rate>25kHz) using a TDT System III Workstation (TuckerDavis Technologies Alchua, FL) running MatLab software and stored for off-line analysis. The raw signal was bandwidth separated (at 0.5-5kHz) to distinguish spiking activity from local field potentials. Spike signals were then de-noised by a two-stage multiple linear regression function to reject signals common to all channels. Waveforms were then clustered by principal component feature space analysis and then sorted into individual units using an automated Bayesian sort-routine. Spikes which failed to separate within a principal component cluster were marked as outliers and not included for further analysis. Also, spikes which exhibited interspike intervals < 2ms were rejected. This technique has been developed and used by our lab in explorations of other cortical regions in the ferret and has been demonstrated to reliably segregate single-units (neurons) (Allman et al., 2009; Keniston et al., 2009).

Once the PPr neurons were identified and templated, their responses to sensory stimulation were determined. First, each neuron was assessed independently with manually presented somatosensory (brush strokes, taps, and manual pressure) and visual stimuli (flashed or moving spots or bars of light from a hand-held ophthalmoscope projected onto a translucent hemisphere, 92cm diameter, positioned in front of the animal) to determine the neurons' receptive fields. These receptive fields were used to guide the placement of the subsequent electronically-generated, repeatable somatosensory and visual stimuli, which are described below. Auditory responsiveness was also evaluated using manually presented claps, hisses, whistles at different locations around the animal's head. However, auditory responses were never

observed, so quantitative sensory testing (below) progressed using only visual and somatosensory stimulation.

For quantitative sensory testing, somatosensory stimuli were produced by a calibrated 1 gram monofilament fiber moved by an electronically-driven, modified shaker (Ling, 102A) that displaced hair or indented the skin. Visual stimulation consisted of a bar or spot of light, whose movement direction, velocity and amplitude across the visual receptive field was computer-controlled and projected onto the translucent hemisphere. These somatosensory and visual stimuli were presented separately and in combination during recording. During combined presentations, the onsets of the stimuli were offset by 40ms (visual preceded tactile) to roughly compensate for the cortical latency disparity between these modalities. The separate and combined presentations of stimuli were randomly interleaved to compensate for possible shifts in baseline activity, interstimulus intervals randomly varied between 3-7 seconds to avoid response habituation, and each stimulus or combination was repeated 50 times. In this way, a given recording penetration in PPr simultaneously recorded neuronal responses for each recording channel to repeated presentations of effective visual, tactile, and combined visual-tactile stimulation. Extra attention was paid to maintaining the consistency of sensory stimulation between different experiments. The somatosensory stimulus was always positioned on the contralateral side of the face and moved at the same velocity and amplitude; visual stimulation always consisted of a moving (70 º/sec) bar (2x20º) of light that transited 10-15º of contralateral visual space in the nasal-to-temporal direction. These parameters were consistent in producing robust responses at the different recording sites across the dimensions of the probe, as demonstrated for one recording penetration in Figure 1.

When the recording session was completed, the recording probe was withdrawn and the animal was overdosed (Euthasol), perfused intracardially with saline and fixed (4% paraformaldehyde). The brain was blocked stereotaxically and the cortex containing the recording site(s) was serially sectioned (75 μm) in the coronal plane. The sections were mounted on slides and counterstained with cresyl violet to assist in locating the sites of electrode penetrations. Sections containing the electrode penetrations were photographed using a light microscope to identify those recording sites that were located within the gray matter of the suprasylvian gyrus. Any recording sites found in white matter, or not fully inserted into the cortex, were not used for further analysis. This yielded a total of 15 reconstructed penetrations in 13 animals. Additional steps were used to histologically reconstruct individual recording sites to determine their laminar location. Because the recording probe consisted of 4 parallel shanks that created 4 parallel tracks within the tissue, a digitized image of the probe could be superimposed over the tracks and aligned in two orthogonal planes: the probe image not only matched the depth of the recording tracks, but also precisely aligned with the M-L spacing of the parallel shanks. This produced a reconstruction of the recording probe that was scaled to the tissue section in which it was used. Accordingly, only cases in which all four shanks of the electrode were identified were used for laminar analysis (n = 10 animals; 10 penetrations). Once the recording electrode was scaled to match the tissue of the recording site, the cortical laminae of that section were plotted using a PC-driven digitizing stage controlled by Neurolucida software (Microbrightfield Biosciences, Inc., Williston, VT) and superimposed on the image. In this way, the individual recording pads of the recording electrode, spaced at 200 μm intervals on each of 4 shanks, were plotted in relation to the location of the different cortical laminae. The few electrode sites that fell on the border between laminae were considered ambiguous and were

excluded from analysis. Also, electrode sites located in the lower 2/3rds of the medial bank of the suprasylvian sulcus were excluded because of the border with the AMLS visual area (Manger et al., 2008). Finally, in a spreadsheet, each electrode pad and laminar location was correlated with the neuronal waveforms/responses obtained at that site, thereby matching their laminar location with neuronal response activity.

Data Analysis

To evaluate the neuronal responses to the somatosensory, visual and combined stimuli, custom software (MatLab) was used to compile and quantify the spiking activity of each identified neuron after the criteria of (Bell et al., 2005). A neuronal response was operationally defined as spiking activity which was >3 standard deviations from spontaneous activity, that lasted for 15ms duration, and ended when activity returned to baseline for at least 15ms. Neurons showing suprathreshold activation to more than one sensory modality were defined as bimodal forms of multisensory neurons. Neurons which showed suprathreshold activation by only one modality were identified as unisensory neurons that were further distinguished into one of two categories. Those unisensory neurons which exhibited responses that were significantly different in the combined stimulus condition than in the unisensory stimulus condition (determined by paired t-test) were classified as subthreshold multisensory neurons (after criteria of Allman et al., 2009). Alternatively, unisensory neurons not significantly affected by combined-modality stimulation were designated as unisensory neurons. Finally, neurons which failed to show activation by any sensory stimulus or combination were defined as unresponsive neurons. These criteria are consistent with other published studies of multisensory cortical neurons (Allman et al., 2009; Keniston et al., 2009).

Multisensory (bimodal and subthreshold) neurons were further analyzed to determine if they demonstrated integrated responses to multisensory stimulation. Responses showing a significantly greater activation (mean spikes/trial) to multisensory stimuli versus that elicited by the most effective single modality stimulus (determined by paired t-test) were classified as response enhanced, those showing a significantly reduced activation to multisensory versus the best unisensory stimulus were classified as response depressed. The magnitude of multisensory integration was calculated according to the method of (Meredith and Stein, 1986) using the formula: $(CM\text{-}SM_{max})/ SM_{max} \times 100 = \%$ Integration. In this equation, SM_{max} was the neuron's response to the most effective unisensory stimulus (mean spikes/trial) and CM was the response to the multisensory stimulus. Both the category and magnitude of multisensory integration were tabulated and examined by cortical lamina.

Anatomical Studies

Surgical Procedures

Ferrets (n=14) were anesthetized, (8mg/kg ketamine; 0.03mg/kg dexmedetomidine intramuscularly), their heads secured in a stereotaxic frame and, under aseptic conditions, a craniotomy was performed to expose the parietal areas of the suprasylvian gyrus. Supplemental anesthetics (8mg/kg ketamine; 0.03mg/kg dexmedetomidine intramuscularly) were administered as necessary. Temperature was maintained near 38°C with a circulating-water heating pad, and body temperature and heart rate were monitored continuously. Extracellular multiunit recordings were made to functionally identify the injection site using a glass-insulated tungsten electrode (tip exposure ~20µm, impedance<1MΩ) inserted to a depth (generally 750-850µm deep to the pial surface) that yielded vigorous neuronal activity. Neuronal discharges were amplified and

played on an audio monitor. Somatosensory responsiveness was assessed using manually presented displacement of the skin or hairs (tapping with calibrated Semmes-Weinstein monofilaments, blowing); visual responsiveness was assessed using manually presented bars of light (from a hand-held ophthalmoscope) and dark (moving a rectangular piece of black cardboard) stimuli. Relatively anterior recordings that identified only somatosensory activity were regarded as indicative of somatosensory area III (SIII) and were consistent with the previously identified location of the cortical area (Foxworthy and Meredith, 2011). More posterior recordings that encountered only visual responses indicated the caudal posterior parietal area (PPc) (Manger et al., 2002). Between these two unisensory regions, recordings that simultaneously identified both somatosensory and visual activity revealed the location of the rostral posterior parietal area (Manger et al., 2002). Once these different cortical areas were identified, one region was selected for injection.

Tracer injections consisted of a 10% mixture (in phosphate buffered saline) of 10,000 and 3,000 molecular weight biotinylated dextran amine (BDA; Invitrogen, Carlsbad CA), which promoted both anterograde and retrograde labeling with the same injection. The tracer was delivered iontophoretically through glass micropipettes with tip diameters between 20 and 40μm. The pipette was lowered to the desired depth (via hydraulic microdrive) under a continuous retaining current of -2.75 μA. Once a depth of 600-800μm was reached, positive current pulses (7s on, 7s off) of 6μA were delivered for 20 minutes. Then, the current was switched off for ten minutes before withdrawing the pipette. The cortex was then covered with bone wax, the wound sutured closed, and standard postoperative analgesic and antibiotic care was provided.

Histological Procedures

Following a 10-14 day post-injection survival period, animals were given a Euthasol overdose and perfused intracardially with saline followed by 4.0% paraformaldehyde. The brains were blocked stereotaxically, removed and cryoprotected. Coronal sections (75µm thick) were cut serially using a freezing microtome. One series of sections from each animal (at 150 µm intervals) was processed for BDA visualization using the avidin-biotin peroxidase method, according to the protocol of Veenman (1992), with added heavy-metal intensification. Reacted sections were mounted on standard chrome-alum gelatin pre-treated slides, dehydrated and coverslipped. An alternate series of sections was processed to visualize cytoarchitectonic features using the antibody SMI-32 (SMI-32R; Covance Inc.). An additional set of sections (n=3 ferrets) were processed for the antibody NeuN (Anti-NeuN, clone A60; Millipore; antibody to vertebrate neuron-specific nuclear protein), which reacts with most neuronal cell types.

Data Analysis

All processed tissue was examined using a light microscope and a PC-driven digitizing stage controlled by Neurolucida software (Microbrightfield Biosciences, Inc., Williston, VT). Each tissue section was traced to show its tissue outline and gray matter/white matter border. For injections made into the multisensory PPr (n=3 ferrets) to evaluate its anatomical inputs, the locations of retrogradely labeled neurons were plotted in every other BDA-processed section (300 µm interval). The injection site was defined as the region of densest label, usually at the end of the pipette track. BDA-labeled neurons generally were sharply black throughout their soma and dendrites. Labeled neurons were assigned to a specific cortical or thalamic region according to previously published reports of the functional organization of the ferret brain (Bajo et al.,

2010; Foxworthy and Meredith, 2011; Homman-Ludiye et al., 2010; Innocenti et al., 2002; Jackson et al., 1989; Keniston et al., 2009; Leclerc et al., 1993; Manger et al., 2008; Manger et al., 2002; Manger et al., 2004; Manger et al., 2010; McLaughlin et al., 1998; Rice et al., 1993) and local sulcal/gyral landmarks. All injections made into PPr in the different animals produced retrogradely labeled neurons in largely the same brain areas and, therefore, the data from the three animals was combined to determine the average number (and percent) of retrogradely labeled neurons in a given area. Plots of sections containing retrogradely labeled neurons were serially arranged and displayed using a standard graphics program. Anterogradely labeled projections from these same PPr injections were observed and assigned to a functional region using the same criteria as above.

For BDA injections made into somatosensory SIII (n=3 ferrets) or visual PPc (n=3 ferrets), labeled axon terminals (boutons) were visualized in the multisensory PPr using light microscopy and plotted with Neurolucida software. The location of each anterogradely labeled bouton was marked, taking care only to mark boutons which were clearly connected to axonal processes. To evaluate the laminar location and distribution of labeled boutons in PPr, adjacent SMI-32 treated sections were used to visualize and plot the cortical laminae. The plots of labeled boutons from one section were then superimposed on the tracings of the cortical laminae from the adjacent section. From this fused image, Neurolucida Explorer (Microbrightfield Biosciences, Inc., Williston, VT) was used to count the number of boutons falling within each layer. This process was repeated until at least 5 sections (per injection) from the PPr were evaluated. The laminar data was grouped by injection site (SIII, PPc) in a spreadsheet. Finally, data from the PPc injected animals was combined to obtain a mean (and percent) of the laminar distribution of the area's axon terminals within PPr. A one-way ANOVA was used to determine

if the mean bouton distribution in PPr differed by layer. A post-hoc Tukey test was used to adjust for multiple comparisons. The data from SIII injected animals was similarly combined and analyzed. Plots of PPr sections containing orthogradely labeled axon terminals were displayed using a standard graphics program.

Local connections within PPr were assessed from cases (n=5) in which tracer injection into PPr was observed to be restricted to the upper, supragranular layers. In these cases, tissue processing and data analysis of the laminar distribution of labeled axon terminals within the PPr was the same as for the assessment of projections to PPr from external sources (SIII, PPc – described above).

The thickness (superficial-deep dimension) of each of the cortical laminae in PPr was assessed using SMI-32 stained tissue in 5 animals (measurements made on 10 sections per animal), which has been shown to reliably visualize the six cortical laminae in ferret (Homman-Ludiye et al., 2010). Using a light microscope and a PC-driven digitizing stage controlled by Neurolucida software (Microbrightfield Biosciences, Inc., Williston, VT), outlines were made of the six cortical laminae as well as the white matter and the pial surface. To measure the thickness of the laminae in each tissue section, a line was digitally drawn through the cortical mantle perpendicular to the pial surface. The software was then used to measure the thickness of each of the cortical laminae along this line. Measurements were made in the same manner of the laminae from the primary somatosensory area (S1) identified according to the criteria of (Foxworthy and Meredith, 2011; Leclerc et al., 1993; Rice et al., 1993). The thickness of laminae in ferret primary visual cortex (area 17; VI) was measured from published reports of the area which also used the SMI-32 immunostain (Homman-Ludiye et al., 2010; Innocenti et al., 2002). Adjacent

sections processed for NeuN and SMI32 were photographed and compared to determine whether both stains revealed similar laminar dimensions.

RESULTS

Lamination of PPr

In agreement with previous studies (Manger et al., 2002; Foxworthy and Meredith, 2011), the rostral posterior parietal area (PPr) was identified between somatosensory area SIII (rostral) and visual area PPc (caudal), as illustrated in Figure 2. As in the other regions of ferret neocortex, the PPr exhibits six distinct layers that are particularly evident when processed with SMI-32 (Homman-Ludiye et al., 2010). As also shown in Figure 2A, layer 1 was mostly devoid of label; layer 2 had short stained fibers that ran mostly perpendicular to the pial surface; layer 3 contained darkly stained pyramidal neurons; layer 4 was extremely thin and mostly devoid of neurons and label; layer 5 contained darkly stained pyramidal neurons; layer 6 was mostly devoid of label and ended where the white matter began. In tissue reacted for NeuN, the same pattern of lamination was generally evident (Figure 2B) although the NueN labeling in layer 4 was now evident as sparse patches of small neuronal somata. Measurements of laminar thickness showed that, on average, about 52% of the cortical mantle was occupied by supragranular layers 1 (11.8%), 2 (17.2%) and 3 (22.5%) and 40% by infragranular layers 5 (20.1%) and 6 (20%), while the narrowest lamina was that of layer 4 which represented only an average 8.5% of the cortical thickness. These relative measures are depicted for PPr laminae in Figure 2C and are compared with laminar measurements from primary visual (V1) and primary somatosensory (S1) cortices in Table 1.

Sensory Responses of the PPr

To assess the laminar distribution of sensory and multisensory neuronal properties in the PPr, multi-channel single-unit extracellular recordings were performed in 15 different sites (n=13 ferrets) on the suprasylvian gyrus, as depicted in Figure 3. The recordings yielded a total of 451 sensory responsive neurons that were histologically verified within the PPr. All PPr recording sites were tested with standardized computer-generated visual, tactile, and combined visual-tactile stimulation. Responses to these sensory tests defined a given neuron as bimodal-multisensory, subthreshold-multisensory, unisensory tactile, or unisensory visual and representative examples of each are provided in Figure 4. Collectively, the majority of PPr neurons were multisensory (64%; 287/451), either as subthreshold neurons (14%; 62/451) or more commonly, as bimodal neurons (50%; 225/451). The remaining neurons were unisensory (36 %; 164/451), among which unisensory visual neurons (13%; 61/451) were encountered less frequently than unisensory tactile neurons (23%; 103/451). The proportions of neuron types in the PPr, summarized in Figure 5, were statistically different (ANOVA; $(F(3,52) = 10.17$, $p<0.0001$). A post-hoc Tukey test indicated that the proportion of bimodal neurons was significantly ($p<0.0001$) higher than all other groups, while the share occupied by the other neuron types did not differ significantly from each other. In the PPr, the latency of responses to visual stimulation averaged 93.7ms while latency to tactile stimulation averaged 51.5ms, with responses occurring significantly (t-test; visual $p=0.0049$; tactile $p=0.0092$) earlier in the supragranular than infragranular layers, as detailed in Table 2. These data confirm that the ferret PPr not only contains a mixture of visual and tactile neurons (as reported by Manger et al., 2002), but also establishes that the area contains a preponderance (64%) of neurons affected by both sensory modalities: multisensory neurons.

Several histologically-confirmed recording penetrations in the visual area PPc (n = 5) were also examined using the same standard presentations of visual, tactile, and combined visual-tactile stimulation, while additional penetrations (n = 3) in somatosensory area SIII received the same treatment. In the PPc, all neurons (118) exhibited suprathreshold activation in response to only visual stimuli, while a small proportion (13/118; 11%) had visual responses that were significantly altered by combined visual-tactile stimulation. For the PPc, visual response latency averaged 66.5ms. On the other hand, SIII neurons (78) responded to tactile but not visual stimulation presented alone, although a few (7/78; 9%) had somatosensory responses that were significantly modulated by combined tactile-visual stimulation. For SIII, tactile response latency averaged 40.7 ms. These results, summarized in Table 3, confirm previous experiments that identified SIII as an essentially unisensory tactile area (Foxworthy and Meredith, 2011) and PPc as an essentially unisensory visual area (Manger et al., 2002), while affirming the multisensory nature of the PPr.

Laminar Distribution of Sensory Properties in PPr

The laminar distribution of unisensory and multisensory neurons within the PPr was analyzed from the histological reconstructions of the recording sites, and the average percentage of each neuron type (multisensory, unisensory tactile, unisensory visual) was calculated by lamina. No penetrations identified sensory-responsive units in lamina 1. Additionally, only 3 penetrations had recording sites localized in layer 4, from which a total of 12 neurons were identified. Of those L4 neurons, 7 were found near the borders of either layer 3 or layer 5, where the responses of large pyramidal neurons could dominate the recording signal. Because recordings in layer 4 yielded an insufficient number of units and their laminar attribution could

be ambiguous, data from this layer were not included in the subsequent analysis. Based on data from layers 2, 3, 5 and 6, multisensory neurons were not uniformly distributed across the PPr laminae. As illustrated in Figure 6 (and summarized in Table 4), multisensory neurons were the majority of neurons in layers 2 (55%), 3 (65%) and 5 (65%), but not in layer 6 (35%). Conversely, unisensory neurons predominated in layer 6 (65%), but not in layers 2 (45%), 3 (35%) or 5 (35%). This distribution of multisensory and unisensory neurons varied significantly by laminae (ANOVA; ($F(3,36)=5$, $p <0.006$). A post-hoc Tukey test indicated that layers 3 and 5 had significantly more multisensory neurons than layer 6. Statistical tests (ANOVA; ($F(3,36)=5$, $p<0.006$) also showed that the proportion of unisensory neurons varied significantly by layer, with layer 6 showing the highest proportion (post-hoc Tukey test). However, the distribution of unisensory visual and unisensory tactile neurons did not significantly vary within layers (t-tests, $\alpha = 0.05$; Table 4). In summary, the majority of PPr neurons were found to be multisensory and this pattern of multisensory dominance was preserved predominantly within layers 2-3 and 5.

The average response (mean spikes/trial) to unisensory (visual alone, tactile alone) and multisensory stimulation (combined visual and tactile) was compared across the different laminae. These results are listed in Table 5. Statistical analysis (ANOVA) of laminar responses showed that the average magnitude of responses by layer did not differ to tactile ($F(3, 36) = 2.3$; $p = 0.07$), visual ($F(3, 36) = 2.4$; $p =0.07$), or multisensory stimuli ($F(3, 36) = 1.4$; $p =0.22$). In summary, the responses evoked by unisensory and combined stimuli did not vary significantly across the different laminae. However, increased average activity levels in response to combined stimulation were consistently observed in each layer.

Laminar Distribution of Multisensory Properties in PPr

Not every multisensory neuron generates integrated multisensory responses (Perrault et al., 2005). Accordingly, the percentage of multisensory PPr neurons that met the criterion for demonstrating multisensory integration was evaluated by layer. As in the analyses above, layer 1 and layer 4 lacked sufficient data to be included in these comparisons. Multisensory neurons in layers 2-3 tended to generate enhanced responses (L2=38%; L3=35%) to combined stimulation, while only few examples of response depression were observed (L2=0%; L3=16%). On the other hand, multisensory neurons in layers 5 and 6 showed enhanced (L5=22%; L6=20%) or depressed (L5=28%; L6=27%) multisensory responses. These results are depicted in Figure 7A and summarized in Table 6. Statistical tests (ANOVA) showed that the proportion of neurons showing enhanced ($F(3,36) = 0.6$; $p = 0.64$) or depressed ($F(3, 36) = 1.4$; $p = 0.27$) responses did not differ significantly by the individual laminae. When the data was re-grouped by supragranular (L2-3) and infragranular (L5-6), this treatment revealed that that the proportion of neurons showing multisensory enhancement did not significantly differ (t-tests, $p=0.31$) between supra- (36.7%) and infra-granular (23.8%) locations. However, a significant difference (t-test, $p=0.002$) was found in the share of neurons showing multisensory depression between supra- (6%) and infra-granular (25%) locations. Thus, laminar differences in multisensory processing were apparent within the PPr.

For neurons demonstrating multisensory integration, the magnitude (measured as percent of response increase or decrease) of multisensory integration was also analyzed by laminae. These results are depicted in Figure 7B and are summarized in Table 7. These analyses showed that the average level of multisensory enhancement tended to increase in the deeper laminae (L5=84%; L6=110%) versus the supragranular layers (L2=43%; L3=76%). A similar trend was

observed for neurons showing multisensory depression, where layer 2 neurons exhibited no response depression at all, layers 3 and 5 showed an average 43% and 46% (respectively) depression, while layer 6 neurons averaged 100%. Statistical tests (ANOVA) failed to show the magnitude of enhancement ($F(3, 36) = 0.6$; $p = 0.60$) or depression ($F(2,32) = 2.8$; $p = 0.08$) differed significantly among the individual layers. However, when the absolute magnitude of multisensory integration (includes both enhancement and depression) was grouped by supra- or infragranular location, multisensory neurons in supragranular locations showed significantly (t-test; $p=0.035$) lower integrative levels than their infragranular counterparts. Thus, these observations indicate a trend for levels of multisensory integration to increase with increasing laminar depth.

External Sources of Projections to PPr

Because multisensory processing is dependent on the convergence of information from different sensory systems, anatomical experiments were conducted to examine the connectional bases of sensory and multisensory activity in the PPr. To assess the sources of extrinsic inputs to the multisensory PPr, tracer (BDA) was injected (n=3 ferrets) into the PPr under electrophysiological guidance. Following processing, the injection sites (See Figure 8C) were determined to be confined to the gyral grey matter and exhibited an area of densely stained neuropil. Darkly stained, retrogradely labeled neurons were found in distinct areas of the cortex and thalamus. A representative case is summarized by the serially arranged coronal sections through the cortex ipsilateral to the injection site in Figure 8, and through the ipsilateral thalamus in Figure 9. As can be seen in Figure 8C, retrogradely labeled neurons were found anteriorly in primary motor cortex (M1), the medial rostral suprasylvian cortex (MRSS), the primary

somatosensory cortex (S1), and the third somatosensory cortex (SIII) and posteriorly in the caudal posterior parietal cortex (PPc), and the anteromedial lateral suprasylvian visual area (AMLS). In Figure 9, the retrograde tracer labeled the pulvinar (Pul), the lateral posterior nucleus (LP), and the ventral anterior nucleus (VA). When the data from all the cases with PPr injections was combined (n=3 ferrets; 1,205 neurons), a distinctive pattern of retrograde labeling was observed, as summarized in Figure 10. Overall, the greatest proportion of labeled neurons in a somatosensory region was found in the SIII (42.3% ± 9.3 SE). For the sources of visual inputs to PPr, the most labeled neurons were identified in the PPc (15.5% ± 5.2). Retrogradely labeled neurons were also found in somatosensory areas S1 (19.8% ± 5.8) and MRSS (4.7% ± 3.1) and in the visual area AMLS (5.6% ± 3.7). Few neurons were found in motor area M1 (1% ± 0.7). Relative to cortically labeled neurons, comparatively few neurons were identified in the thalamic nuclei: the lateral posterior-pulvinar thalamic complex (LP-Pulv, 4.8% ± 1.7) and the VA (6.3% ± 2.3). These results confirm that the present tracer injections were contained within PPr and were consistent with published thalamo-cortical connections to ferret PPr (Manger et al., 2002). Additionally, tracer injected into PPr in the present experiments did not label thalamic nuclei that are labeled from injections made into the adjacent areas SIII or PPc (Manger 2002; Foxworthy 2011). In summary, these data show that the major sources of somatosensory and visual inputs to PPr (Figure 10) are somatosensory area SIII and visual area PPc.

Anterograde Projections from PPr.

The areas to which neurons in the PPr project were determined by identifying labeled axon terminals resulting from tracer injections into the PPr (also under electrophysiological guidance; n=3). As indicated by the presence of labeled axon terminals, outputs from the PPr

project to all of the cortical areas identified (above) as sources of input to the region, including M1, MRSS, S1, SIII, PPc, and the AMLS. Reciprocal connections were also observed in all of the thalamic nuclei which contained neurons retrogradely labeled from the PPr, which were the LP, Pulv, and VA. Additionally axon terminals labeled from PPr were documented in the caudate, claustrum, reticular nucleus, as well as the superior colliculus and pons. Unlike the other projection targets of the PPr, projections to the caudate, claustrum, reticular nucleus, superior colliculus and pons were unidirectional.

Distribution of Axon Terminals in PPr from External Sources.

Because a majority (64%) of neurons in PPr exhibited visual-somatosensory multisensory properties, a potential substrate for this convergence would be for inputs from visual and somatosensory sources to overlap within the PPr. To examine this possibility, tracer (BDA) injections were made into the major cortical sources of somatosensory (area SIII; n=3) and visual (area PPc; n=3) inputs under electrophysiological guidance. After transport and processing, labeled axon terminals were visualized in the PPr using light microscopy. Boutons appeared as darkly stained swellings attached to axons either along the length of the axon (boutons in passage) or as terminal boutons at the ends of axonal processes, as demonstrated in Figure 11. The laminar distribution of labeled axon terminals was assessed using alternate sections through the rostro-caudal extent of the PPr, where the laminar boundaries traced from an SMI-32 labeled section were digitally superimposed onto the plot of an adjacent section containing BDA-labeled axon terminals. At least 5 merged sections per case were examined and a total of 187,228 BDA-labeled boutons were plotted. As depicted in Figure 12, labeled boutons from SIII and PPc were identified throughout the PPr. However, the distribution of labeled boutons in PPr differed by

cortical layer (ANOVA; SIII= $F(5,12)=37.2$; $p<0.0001$; PPc= $F(5,12)=20.7$; $p<.0001$), and post-hoc Tukey tests indicated that layers 2-3 received the strongest projections from each area. The differential laminar distribution of axon terminals labeled from SIII or PPc are graphed in Figure 13 where, in either condition, axon terminals occurred most densely within layers 2-3. In fact, 63% of all boutons labeled from SIII and ~58% of axon terminals labeled from PPc terminated in layers 2-3, indicating a dense overlap in their distributions. Thus, connections from somatosensory SIII and visual PPc both preferentially target layers 2-3 of PPr, where their overlapping distributions are most robust and appear to represent the substrate for the high levels of multisensory convergence that was evident in those layers. How the information received by the supragranular layers is transmitted locally is examined below.

Intrinsic Connections of PPr

Tracer (BDA) injections that were restricted to specific laminae in the PPr (n=5) were used to identify patterns of intrinsic connections within the PPr. All cases involved supragranular injections (layer 3 and above), as depicted in the example in Figure 14. Plots of labeled axon terminals revealed local supragranular projections to all layers. However, counts of the laminar distribution of labeled boutons showed that, in each case, supragranular injections produced the highest amount and density of terminal label within layer 5 (graphed in Figure 14). This observation is consistent with other studies of intralaminar cortical connections, where a major class of layer 5 neurons has been demonstrated to be the primary recipient of a highly focused and extremely dense excitatory projection from layer 3 neurons (Thomson and Lamy, 2007). It is possible that some labeled boutons resulted from collaterals of labeled layer 5 neurons, but few layer 5 neurons were retrogradely labeled in these cases, rendering this

possibility a minor effect. It should also be noted these injections labeled both excitatory and inhibitory neurons and their projections, which cannot be discriminated with this anatomical technique.

For the 5 cases examined in which a total of 43,402 BDA-labeled boutons were plotted, the preference for the supragranular layers to target layer 5 was consistent, as summarized in the bar graph in Figure 14. That the density of labeled boutons differed by laminae was statistically confirmed by an ANOVA ($F(5,24) = 10.4$, $p<0.0001$). Furthermore, a post-hoc Tukey test showed that layer 5 received a significantly higher density of projections from supragranular injections and that the projections to the other laminae did not significantly differ from each other. Collectively, these results demonstrate that translaminar projections originating from the supragranular layers of the PPr preferentially terminate locally in layer 5.

The question of whether connections from external sources or local projections could provide the substrate for multisensory properties in the PPr was assessed by plotting the data from these different experiments on the same graph. As plotted in Figure 15, the highest proportion of axon terminals from somatosensory area SIII and from visual area PPc occurred within the supragranular layers of the PPr (layers 2-3) where a majority of multisensory neurons were also identified (bar graphs) in each of those layers. In addition, the highest proportion of axon terminals originating from the supragranular, multisensory layers of the PPr were located in layer 5, which also exhibited a majority of multisensory neurons in that layer. Conversely, proportionally few extrinsic or local connections were observed to terminate within layer 6, where the fewest multisensory neurons were identified. These data are not only consistent with the hypothesis that multisensory convergence underlies multisensory function, but also that

different levels of connectivity and convergence provide the substrate for differential distribution of multisensory properties across the cortical laminae.

DISCUSSION:

As a model of cortical multisensory convergence and integration, the present study examined the rostral posterior parietal area of the ferret (PPr). This area exhibits 6 layers that were reliably observed using different staining techniques (see also Homman-Ludiye et al., 2010; Manger et al., 2002). As would be predicted from the location of the PPr between somatosensory area SIII (Foxworthy and Meredith, 2011) and visual area PPc (Manger et al., 2002), electrophysiological recordings in ferret PPr observed both unisensory somatosensory and visual neurons (see also Manger et al., 2002). Moreover, the present study identified the largest proportion of neurons in PPr to be multisensory (64%). For the most part, multisensory neurons showed suprathreshold activation by visual and somatosensory stimulation presented alone (bimodal neurons, 50%), but a smaller proportion also showed responses to only one sensory modality that were modulated by co-stimulation with cues from another modality (subthreshold multisensory neurons, 14%). It is important to note that this proportion of multisensory neurons is quite similar to the maximum identified for other mammalian multisensory areas (Meredith et al., 2011a; Meredith and Stein, 1986) as well as the proportion generated in computational models of multisensory processing (Anastasio and Patton, 2003; Lim et al., 2011). Furthermore, many multisensory neurons exhibited significant levels of response integration when presented multisensory stimuli. Together, these data indicate that the ferret PPr is a robustly multisensory region.

Laminar organization of multisensory properties

Analysis of the laminar distribution of unisensory and multisensory neurons within the PPr revealed that multisensory neurons predominated in layers 2-3 (55-65%), and V (65%), but not layer 6 (35%; too few neurons were encountered in layers 1 and 4 to be included in the comparison). Similarly, a segregation, or clustering of multisensory neurons has also been observed in multisensory superior temporal sulcal cortex, but a laminar analysis was not conducted in this study (Dahl et al., 2009). In the present study, multisensory processing showed a differential laminar distribution across the PPr, where both the proportion as well as the magnitude of multisensory integration varied between supra- and infragranular layers. Such differential distributions of multisensory response features in the PPr have significant implications for the connectivity and circuitry of the region. It must be pointed out, however, that although the present techniques can provide ***inferences*** based on broadcast labeling or extracellular recording techniques, actual demonstration of the proposed circuitry that follows will require measures of connectivity evaluated with more direct methods, such as paired cell recordings in whole animals. To our knowledge, such experiments have not yet been conducted in multisensory cortex.

Laminar organization of input connections

The ferret PPr is characterized by somatosensory and visual responses, and the greatest proportion of inputs from representations of the somatosensory and visual modalities arrived from areas SIII and PPc, respectively. Measures of tactile and visual response latency indicate that both SIII and PPc are activated earlier than responses in the PPr, which is consistent with the arrangement that inputs from SIII and PPc activate the PPr. In addition, the receptive fields in

the PPr demonstrate a superimposition of those found in SIII and PPc (Foxworthy and Meredith, 2011; Manger et al., 2002). Both of these input regions have been identified as unisensory (SIII, Foxworthy and Meredith, 2011; PPc, Manger et al., 2002; present study), as were most of the other sources of cortical inputs to the PPr. Only inputs from non-specific thalamus could be regarded as originating from multisensory areas, and these represent only a small fraction of total inputs to the PPr. Thus, it seems likely that the multisensory properties of PPr neurons are the result of convergence within the PPr rather than represent multisensory properties passed on from multisensory sources. Furthermore, as depicted in Figure 15, the preferential convergence of extrinsic inputs from SIII /PPc to layers 2-3 corresponded with the preponderance of multisensory neurons in those layers, while the reduced extrinsic projections to layer 6 were accompanied by reduced levels of multisensory neurons there. Thus, the layers (2-3) receiving the highest levels of convergence from different sensory sources are also those that exhibit the highest proportions of multisensory neurons. This relationship between converging inputs and multisensory incidence is supported by computational simulations of multisensory convergence (Lim et al., 2011), which also indicated that local connections contribute substantially to multisensory processing.

Laminar organization of intrinsic connections

Given the high proportion of multisensory neurons in layers 2-3 of the PPr, it is expected that outputs from these neurons relay multisensory signals to subsequent neurons in the circuit. The shorter latency of supragranular responses certainly supports this likelihood. In addition, tracer injections into the PPr supragranular layers revealed intrinsic connections to all other layers, but showed a strong preference for termination in layer 5. Multisensory neurons

predominate in layer 5, where their basilar dendrites neurons are strategically positioned to receive the massive local projection from the multisensory supragranular layers. In addition, layer 5 neurons have apical dendrites that extend directly into the supragranular layers, where they are positioned to receive connections from the extrinsic unisensory sources (Thomson and Lamy, 2007). Therefore, layer 5 multisensory neurons appear to be uniquely situated within the local PPr circuitry to receive both convergent (extrinsic: PPc/SIII) and converged (intrinsic) forms of multisensory inputs in a spatially segregated manner, as summarized in Figure 16. Of course, some extrinsic projections overlap with local connections within the other cortical laminae, but their distribution in those regions is more diffuse and less spatially restricted to one set of dendrites or another. In contrast, layer 6 neurons are located in a PPr region that receives neither extensive extrinsic inputs nor robust local supragranular projections, and exhibits comparatively few multisensory neurons. It remains to be determined whether local projections of layer 5 neurons innervate their subadjacent counterparts in layer 6, although there is evidence for this projection in primary sensory cortices (for review, see Thomson and Lamy, 2007). Ultimately, these collective results affirm the expectation that cortical multisensory neurons are the product of convergence of extrinsic inputs as well as local projections. While it seems likely that different ratios of these convergent and converged inputs may occur within different cortical laminae, how these varied contributions may affect multisensory responses and multisensory processing remains to be examined.

Laminar organization of output connections

It is well established that the individual cortical laminae differentially connect to particular cortical and subcortical targets. Numerous studies (for review, see Thomson and

Lamy, 2007) have established that outputs from layers 3-4 project to ipsilateral and contralateral (callosal) cortical locations, and some layer 5 neurons have ipsilateral cortical connections as well. Studies have also shown that layer 5 neurons project to non-specific thalamic nuclei (Sherman and Guillery, 2011; Thomson and Lamy, 2007; Van Horn and Sherman, 2004), caudate (Arikuni and Kubota, 1986; Fisher et al., 1984; Hedreen and DeLong, 1991; Jones et al., 1977; McGeorge and Faull, 1989; Oka, 1980; Reiner et al., 2003; Rosell and Gimenez-Amaya, 1999; Saint-Cyr et al., 1990; Tanaka, 1987; Veening et al., 1980; Wilson, 1987), superior colliculus (Fuentes-Santamaria et al., 2009; Kawamura and Konno, 1979; Manger et al., 2010; McHaffie et al., 1988; Meredith and Clemo, 1989; Stein et al., 1983) and pons (Albus and Donate-Oliver, 1977; Brodal et al., 1991; Perez-Samartin et al., 1995), while layer 6 neurons project to claustrum (Zhang and Deschenes, 1997; 1998), thalamus (Sherman and Guillery, 2011; Thomson and Lamy, 2007; Van Horn and Sherman, 2004) and the reticular nucleus of the thalamus (Zhang and Deschenes, 1998). All the listed regions were anterogradely labeled by PPr injections in the present study and it is presumed that the laminar-based origins of these projections are similar to those described (above) for other sensory cortical regions. Because there is a differential laminar distribution of multisensory properties in the PPr laminae, it is also expected that the different output projections will carry different multisensory properties. Specifically, since layers 2-3 and 5 of the PPr were dominated by multisensory neurons, it would be expected that many of these neurons would project multisensory information to their cortical, caudate, thalamic, superior colliculus, and pontine targets. Consistent with this notion, the caudate (Markus et al., 2008; Nagy et al., 2006), the lateral posterior and pulvinar thalamic nuclei (Avanzini et al., 1980), the superior colliculus (Meredith and Stein, 1986) and the pons (Amassian and Devito, 1954; Cazin et al., 1980; Keller and Crandall, 1983; Leergaard and

Bjaalie, 2007; Leergaard et al., 2000; Torigoe et al., 1986) are known to exhibit multisensory properties. On the other hand, because layer 6 neurons are predominantly unisensory, their projections are likely to carry unisensory signals to the claustrum (Remedios et al., 2010), and reticular thalamic (FitzGibbon, 2000; Jones, 1975; Zikopoulos and Barbas, 2007) targets which themselves exhibit multiple and distinct unisensory representations. Thus, the segregation of multisensory and unisensory properties by laminae in PPr apparently has a functional role in maintaining unisensory lines of information while, at the same time, providing the substrate for the processing and transmittal of multisensory information. Ultimately, as summarized in Figure 16, PPr cortex serves as a parallel processor of simultaneous multisensory and unisensory signals whose integrity is preserved among its output connections.

Laminar organization of multisensory integration

A unique feature of multisensory neurons is their potential to integrate responses to combinations of stimuli from different sensory modalities. Electrophysiological techniques have been used to observe multisensory integration in a variety of cortical association areas from a number of species (Allman et al., 2008; Allman et al., 2009; Allman and Meredith, 2007; Avillac et al., 2007; Barraclough et al., 2005; Brett-Green et al., 2003; Bremeglieri et al., 2008; Carriere et al., 2007; Clemo et al., 2007; Dehner et al., 2004; Meredith et al., 2006; Meredith et al., 2011b; Romanski, 2007; Sugihara et al., 2006). The present results indicate that this integrative feature is not homogeneous within a given multisensory cortical area, but instead exhibits laminar-dependent properties. Multisensory neurons in layers 2-3 more often exhibited response enhancement than response depression. In fact, no examples of response depression were observed for layer 2 neurons. It should be pointed out that the spatial and temporal parameters

that can reveal response depression were not manipulated in the present study, so it cannot be expected at this time that all forms of response depression would be minimized in the supragranular layers. On the other hand, proportionally more neurons showing response depression were observed in layers 5 and 6. This suggests that inhibitory neurons (or inhibitory effects) are increasingly recruited as signals pass through the translaminar circuit, although it has also been demonstrated that GABA-A mediated crossmodal inhibition can be evoked from extrinsic cortical sources (Dehner et al., 2004; Keniston et al., 2010; Meredith et al., 2006). In addition, the level, or magnitude, of multisensory integration (both depression and enhancement) also varied by layer and tended to increase with increasing laminar depth. However, neither the reason nor the mechanism for this effect is apparent at this time. For example, although higher levels of convergence promoted increased levels of integration in simulated multisensory neural networks (Lim et al., 2011), the laminae (infragranular) with the lower probability of convergence were the ones that generated the highest integrative effects in the present study. It might be tempting to propose that biophysical differences may exist between multisensory neurons in the supra- and infragranular layers, but the present study shows that sensory responses (visual, somatosensory) were not significantly different between neurons from these two regions. Given that highly integrative multisensory neurons tend to cluster (Dahl et al., 2009), the issue of the laminar effects of multisensory integration obviously merits further study.

Laminar properties of multisensory versus primary sensory cortices

The proportion of multisensory neurons, the share of neurons showing multisensory integration, and the magnitude of multisensory integration were all found to differ by cortical layer in a way that matched the functional or anatomical characteristics of the PPr. Coupled with a lack of input from principal thalamic nuclei and a minimal layer 4, these observations indicate that this higher-level multisensory cortex not only processes unisensory and multisensory information in parallel, but also shows unique functional and organizational modifications to the well-known laminar patterns identified for primary sensory cortical areas.

For example, the main generators of primary cortical sensory responses are thalamocortical projections derived from the principal thalamic nuclei (dorsal lateral geniculate,ventrobasilar, ventral medial geniculate) that preferentially target layer 4 (and lower layer 3). In contrast, the present study demonstrated that thalamic inputs to the PPr represent a small fraction (11%) of its total inputs and arise from the non-specific lateral posterior, pulvinar and ventral anterior thalamic nuclei (see also Manger et al., 2002). Given the significance of the thalamocortical inputs to primary sensory cortices, it is not surprising that layer 4 represents up to 21% of the primary sensory cortical thickness compared to only 8.5% in the PPr (see Table 1). It is possible that PPr layer 4 neurons could be more tightly packed into the available space than in other regions. However, while spiny stellate neurons densely populate layer 4 in primary sensory cortex, their presence in PPr was difficult to demonstrate. Using SMI-32, layer 4 in PPr was essentially devoid of labeled neurons, and NeuN staining revealed irregularly packed small, spherical neurons that, as such, could not be distinguished from inhibitory interneurons. Although the LP-Pulv has been demonstrated to have visual-somatosensory multisensory responses (Avanzini et al., 1980), the functional impact of pulvino-cortical projections remains unknown (Cappe et al., 2011; Sherman and Guillery, 2011; Van Essen, 2005). The ventral

anterior nucleus is a motor-related nucleus that has not been demonstrated to have connectivity or responses consistent with a visual-somatosensory/multisensory nature (Jones, 2007b) and, thus, seems an unlikely candidate to deliver multisensory information to PPr.

For multisensory cortex, the primary recipient layers for multiple sensory information appear not to be layer 4 but layers 2-3 (see also Clemo et al., 2007; Clemo et al., 2008; Dehner et al., 2004; Meredith et al., 2006; Monteiro et al., 2003). These inputs are mainly from other cortical regions and thalamic connections arrive not from principal but non-specific thalamus. It is of note that a current-source density analysis of the monkey multisensory cortex located in the superior temporal sulcal cortex (STS) described initial current sinks for visual, auditory and somatosensory responses to be centered on layer 4 (and lower layer 3; Schroeder and Foxe, 2002). However, these same published figures show current sinks above and below layer 4 in a pattern that is not consistent with that seen for primary sensory areas. Also, axons labeled from visual cortex have been described to terminate within layer 4/lower 3 of the STS (Montero, 1980), yet the same paper shows in 20 of 21 sections that terminal labeling of visual cortical inputs extended all the way to the pial surface/layer 1 and some terminal patches even exhibited a bi-laminar distribution. In the present study, correlation of axon terminal projections and current-source density analysis was attempted but was inconclusive because the electrode configuration could not resolve layer 4. These issues indicate that the basic organizational principles of multisensory cortex remain to be resolved. Nevertheless, the preponderance of data indicates that the well-known laminar and connectional arrangements of the primary sensory cortices are modified for at least the PPr, and perhaps for multisensory cortex in general.

Parietal cortex in other species

Multisensory cortical areas that reside between unisensory cortical areas have been found in all mammals studied (Krubitzer, 2007). Furthermore, a visual-tactile multisensory region between unimodal somatosensory and visual areas appears to be common to all eutherian (placental) mammals (Kaas, 2009; Manger et al., 2002). Although this area is greatly expanded in primates and carnivores (Kaas et al., 2011) it has been found in such diverse species as: the flying fox (Rosa, 1999), rodents (Reep et al., 1994; Reep and Corwin, 2009; Wallace et al., 2004), the tree shrew (Remple et al., 2007), cats (Avendano et al., 1988; Beloozerova and Sirota, 2003), and primates (Avillac et al., 2007; Bakola et al., 2010; Lewis and Van Essen, 2000). The best studied of these examples are regions in the parietal cortex of the rodent and the primate with which ferret PPr shares a number of commonalities. Comparing areas with similar anatomical connectivity and electrophysiological responses across species is important, as it provides insight into the basic cortical arrangements from which expanded cortical fields have evolved.

In the rodent, the posterior parietal cortex receives thalamic inputs from lateral dorsal, posterior, and lateral posterior thalamic nuclei (Reep and Corwin, 2009) which appear to be homologous to the LP-Pulv complex which innervates the primate posterior parietal cortex and ferret PPr (Bucci, 2009; Takahashi, 1985). The cortico-cortical connections of rodent posterior parietal cortex are also similar to those observed in ferrets with inputs arriving from somatosensory and secondary visual areas (Reep et al., 1994). Additionally, neuronal responses to both visual and somatosensory stimuli have been electrophysiologically demonstrated in rodent parietal cortex (Reep and Corwin, 2009; Wallace et al., 2004). The cortical areas immediately adjacent to the rodent posterior parietal cortex also exhibit similarities to ferret SIII and PPc. In the rodent, the area immediately caudal exhibits visual responsiveness and receives

thalamic afferents from the LGN – as is observed in ferret PPc (Manger et al., 2002; Reep et al., 1994). The area immediately rostral to the rodent multisensory area is somatosensory and receives input from the ventrobasal complex. This is somewhat different from the SIII area immediately rostral to the PPr in ferret which receives thalamic input from the posterior nucleus (Foxworthy and Meredith, 2011). However, S1 (which is immediately rostral to SIII in ferrets), receives input from the ventrobasal nucleus and sends a projection to PPr (Foxworthy and Meredith, 2011). This difference in somatosensory cortical connectivity is likely related to the expansion of cortical fields in the ferret versus the rodent. Similarly the number of cortical areas in the parietal cortex of the primate is greatly expanded when compared to the ferret, making establishment of direct homologies between cortical areas more difficult. Nevertheless, ferret PPr shares more features with the ventral intraparietal area (VIP) of the primate than other areas in the primate posterior parietal cortex. Like the ferret PPr, the VIP has cortico-cortical connections with motor, somatosensory and visual areas (Lewis and Van Essen, 2000). Also, the VIP is strongly influenced by both somatosensory and visual stimuli and contains a large proportion (70%) of multisensory neurons (Avillac et al., 2007). While the thalamic connectivity to this portion of the monkey intraparietal area has not been yet demonstrated, in general the primate intraparietal area receives thalamic projections from the LP, Pulv and the nucleus ventralis posterior lateralis pars caudalis (Matsuzaki et al., 2004). Thus the PPr of ferrets shares numerous anatomical and connectional features with parietal areas in rodents and primates.

Studies performed in primates and rodents have shown that the parietal cortex as a whole plays a role in attention and in rectifying spatial maps from different sensory modalities to achieve goal-directed behaviors such as reaching, navigation and gaze direction (Alais et al., 2010; Calton and Taube, 2009; Kaas et al., 2011; Nitz, 2009; Reep and Corwin, 2009; Save and

Poucet, 2009). The behavioral function of the PPr in the ferret is unknown, but the connections of the PPr with visual and somatosensory areas, and the correspondence of visual and somatosensory receptive fields (Manger et al., 2002) are consistent with the notion that the area rectifies spatial maps from different sensory modalities. Connections with motor cortex, the caudate, the ventral anterior nucleus, the pons and the superior colliculus are consistent with the performance of goal-directed motor behaviors.

Posterior parietal cortex is greatly expanded in carnivores (such as the ferret) and primates (Kaas et al., 2011). It is particularly enlarged in humans, and is proposed to provide the substrate for human tool use and the acquisition of complex new motor skills (Kaas et al., 2011). Thus studies of the ferret rostral posterior parietal cortex, in addition to furthering the understanding of cortical multisensory processing, may give insight into the expansion and evolution of cortical fields by providing additional data with which rodent and primate parietal cortex can be compared. It would also be informative to compare the laminar organization of multisensory properties of the ferret PPr to those found in other multisensory areas and also to similar parietal areas in other species. Such comparisons may reveal a general plan of organization for multisensory cortices and/or for parietal cortex.

SUMMARY & CONCLUSIONS:

The present study is the first systematic structural-functional examination of the laminar features of a multisensory cortex. The data show that the major sources of inputs to the multisensory PPr region are from its neighboring unisensory somatosensory (SIII) and visual (PPc) cortical areas. Collectively, these two projections were activated earlier than the PPr and constituted the majority of all inputs to the PPr. Axon terminals from both of these inputs preferentially targeted

layers 2-3. Corresponding to this high degree of input convergence in layers 2-3 was the high proportion of multisensory neurons identified in those layers. In turn, these predominantly multisensory layers projected to extrinsic cortical areas as well as locally to layer 5, which is known to connect with multisensory subcortical structures. In contrast, layer 6 of the PPr received the lowest amount of converging extrinsic inputs from SIII and PPc and the smallest projection from multisensory layers 2-3. Layer 6 neurons also demonstrated the highest laminar proportion of unisensory neurons that, in turn, connect with other unisensory structures. This differential distribution of unisensory and multisensory connections and functions not only reveals that the organization of multisensory cortex is altered from that of the well-studied primary sensory areas, but also indicates that unisensory and multisensory signals are processed in parallel as they pass through the PPr. Parallel processing is a ubiquitous feature of sensory cortex, and the present observations argue that multisensory cortex follows this same basic principle, albeit with modifications specific to its own processing tasks. These observations are important not only for the construction of computational simulations of multisensory processing, but also for a better appreciation of how the brain processes multisensory information.

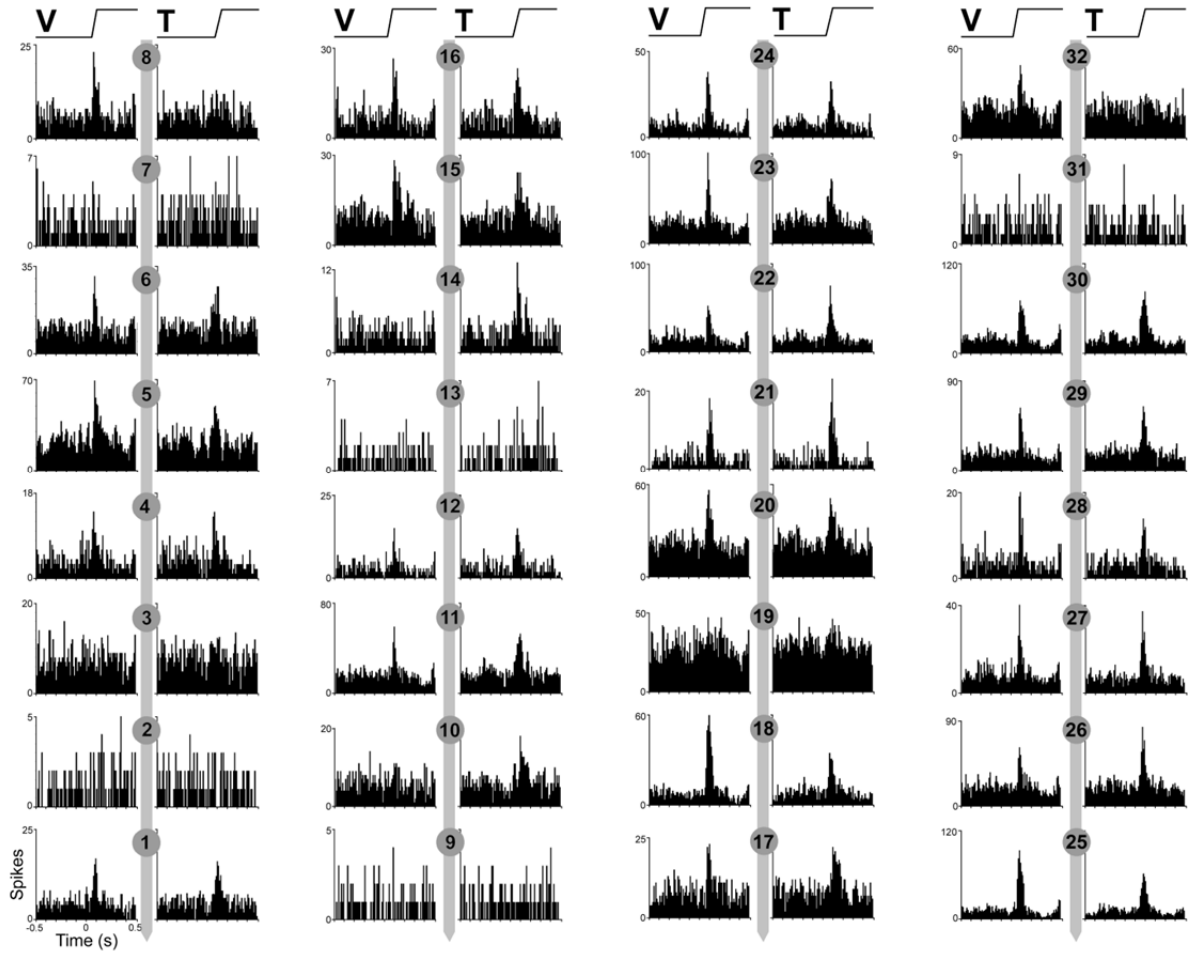

Figure 1. Simultaneous sensory recording in PPr using a 32-channel probe composed of 4 shanks (grey vertical lines) each with 8 recording sites at 200µm separation (numbered circles). Neuronal activity picked-up at each recording pad is illustrated by the histograms (10 ms time bin; y-axis = spike count) immediately adjacent to the numbered pad. Sensory activity was evoked by a visual (ramp labeled 'V,' top; representing a 2x20° light bar moved at 70°/sec nasal-to-temporal) or a tactile (ramp labeled 'T,' top; representing a 1 gram monofilament that displaced hair/skin on the cheek) stimulus. These same stimuli simultaneously elicited responses to visual, tactile, and combined visual-tactile (not-depicted) stimulation, revealing unisensory (respond to visual only, or to tactile only) or bimodal (respond to visual and to tactile separately) neurons at multiple locations on each shank. These results show that the stimulation parameters were appropriate to simultaneously activate neurons recorded at spatially different locations in PPr cortex.

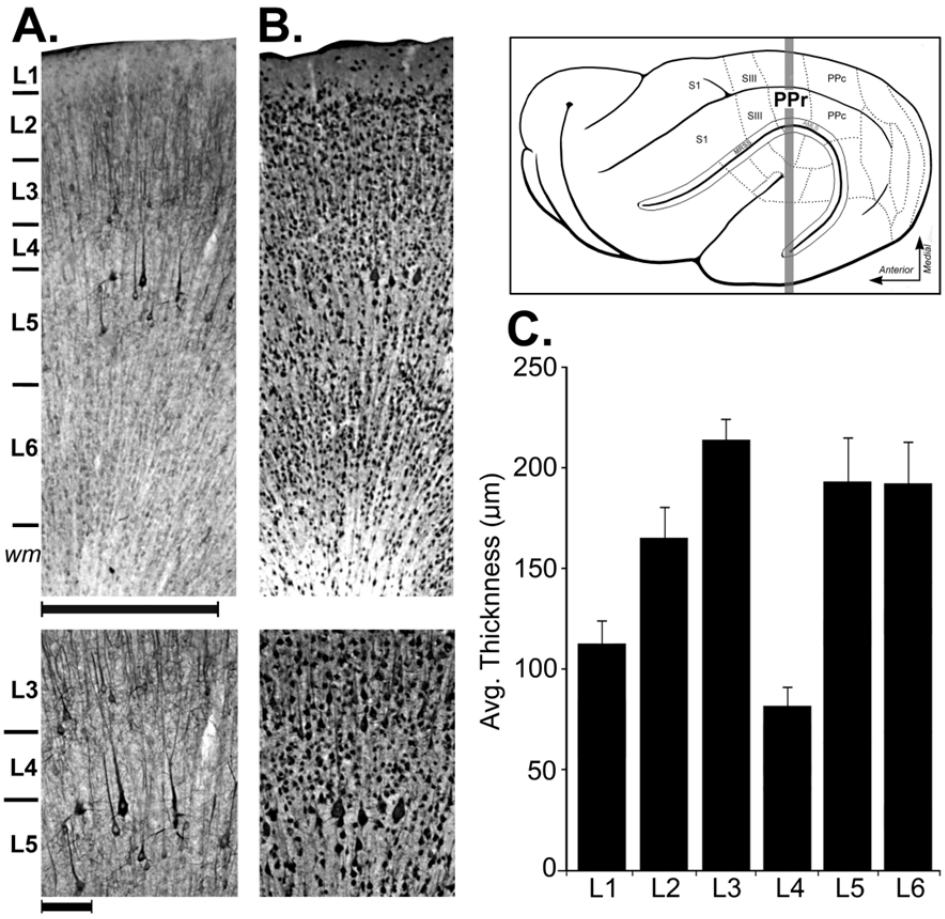

Figure 2. Location and lamination of ferret PPr cortex.
In the box, a lateral view of the ferret cortex shows the location of the rostral posterior parietal cortex (PPr), which is between somatosensory area III (SIII) anteriorly, and the visual caudal posterior parietal cortex (PPc), posteriorly. Also depicted: the primary somatosensory cortex (S1), and, inside the opened suprasylvian sulcus, the medial rostral suprasylvian sulcus (MRSS), and the anteromedial lateral suprasylvian sulcus (AMLS). The thick vertical gray line indicates the approximate level from which the photomicrographs were taken. The photomicrographs are from adjoining coronal sections through the PPr stained for SMI-32 (A) and NeuN (B), with enlargements (below) focused on layer IV. The laminar boundaries revealed by both SMI-32 and NeuN appear similar. In the enlargement of part (A), SMI-32-labeled pyramidal neurons of layers 3 and 5 are apparent, but layer 4 in between is devoid of label. In the enlargement of part (B), the pyramidal neurons of layers 3 and 5 are evident, as are patches of small, rounded neuronal somata in layer 4. Scale for upper images = 500µm; scale for lower images = 100µm. In (C), the bar graph summarizes the average thickness (from upper to lower border) of the different cortical laminae (measured from SMI-32 stained tissue). Approximately equal proportions of the cortical mantle are constituted by the supragranular (layers 2 and 3) and infragranular (layers 5 and 6) layers, while layer 4 is the thinnest. Error bars indicate standard error.

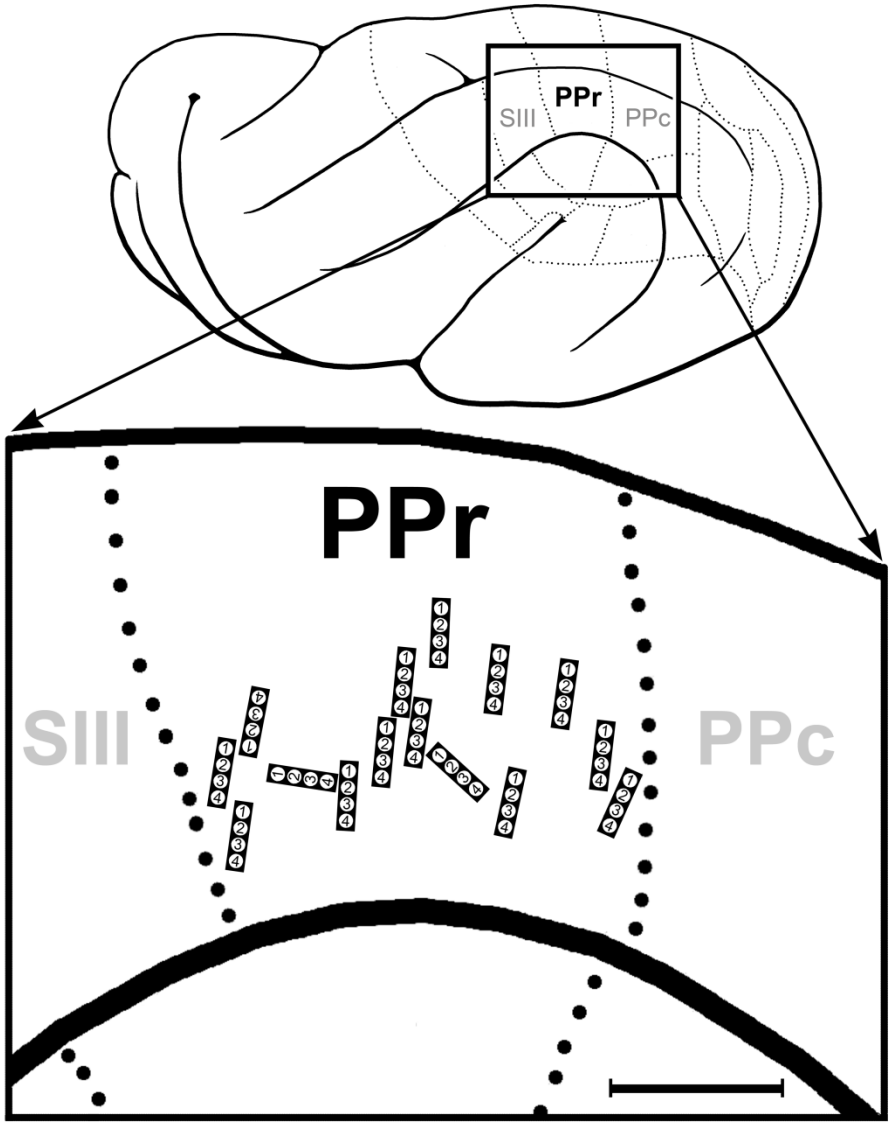

Figure 3. Recording penetrations in the PPr.
The lateral view of the ferret cortex (left = rostral; top = medial) shows the recording target: the rostral posterior parietal cortex (PPr) located between somatosensory area III (SIII) anteriorly, and the visual caudal posterior parietal cortex (PPc) posteriorly. The expanded view of the PPr shows the approximate locations of all of the recording sites (n=15) and depicts the orientation of the four-shank, 32-site recording electrodes used. (Scale bar = 1mm).

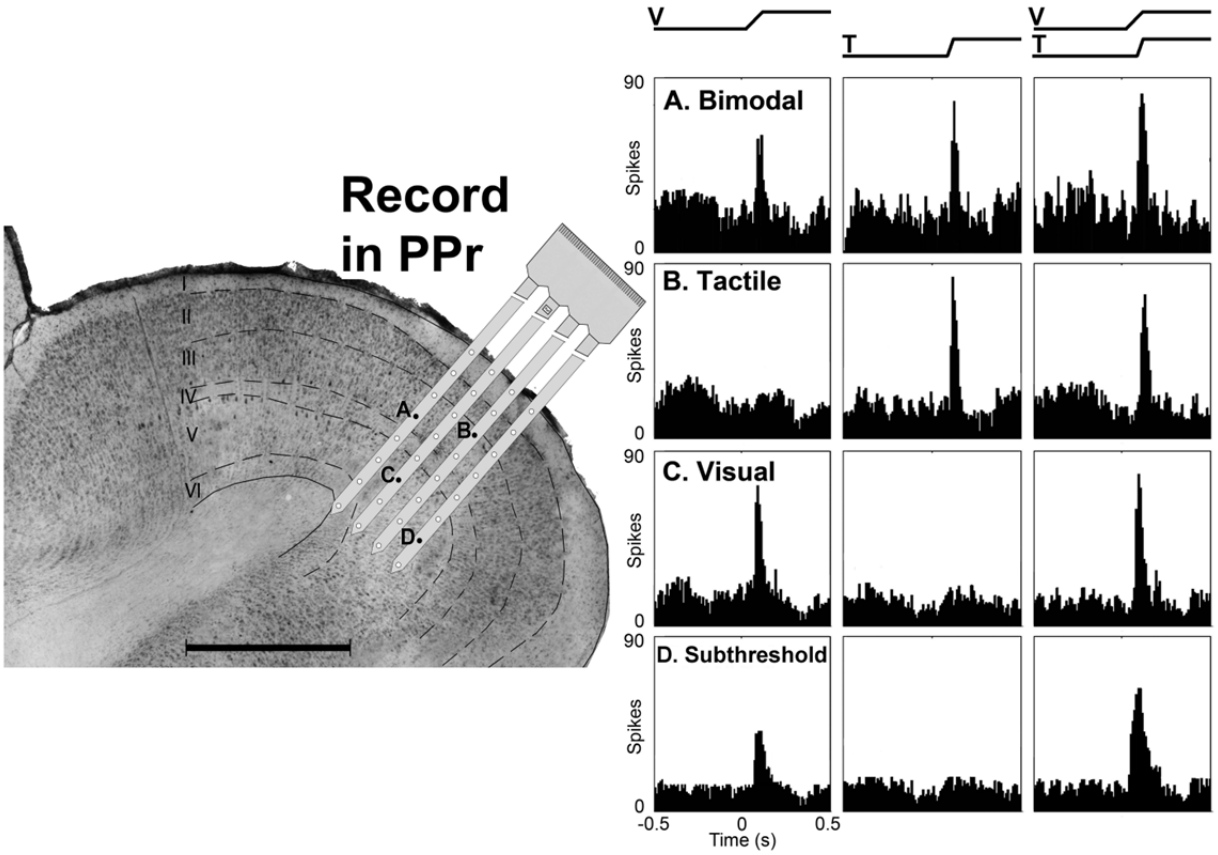

Figure 4. Electrophysiological recording and neuron classification of PPr sensory neurons. This cresyl violet stained coronal section through the PPr (left=medial; scale bar = 1000μm) shows the location of a scaled schematic of the 32-channel recording probe from one experiment. The black dots on the probe (A-D) indicate the recording locations that correspond with the neuronal activity represented by the histograms on the right. In these data panels, the stimuli are represented by the ramps above the histogram: V = visual; T = tactile; VT = combined. The bimodal neuron (A) responds independently both to V and to T stimulation. The unisensory tactile (B) and visual (C) neurons are activated or influenced by only one sensory modality. The subthreshold multisensory neuron (D) shows activation by one sensory modality (visual in this example) but not by the second sensory modality, yet shows significantly different spiking activity when the visual and tactile stimuli are combined. Histogram time-bins = 10ms.

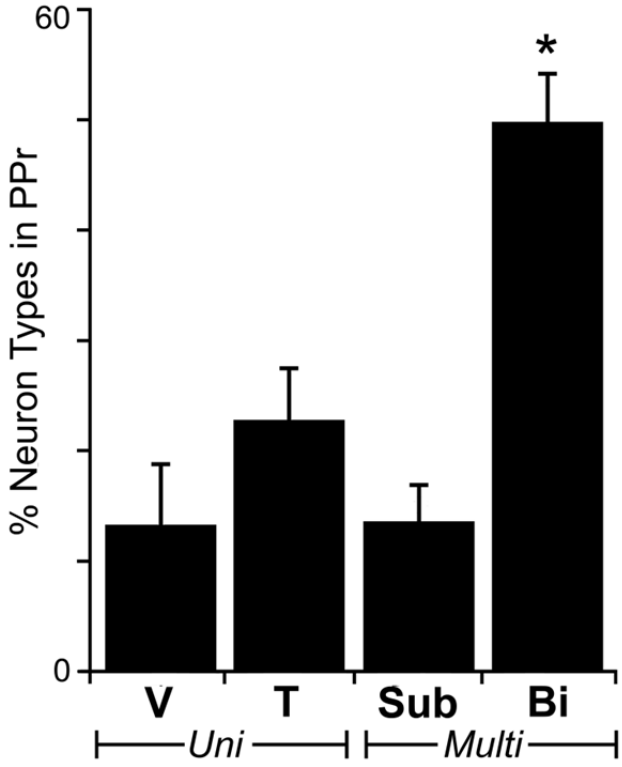

Figure 5. Sensory neuron types found in the PPr.
The bar graph shows the percentage (and standard error) of the different sensory neuron types found in PPr. Of the neurons responsive to sensory stimulation, the majority (64%) were found to be multisensory (*Multi*), either as subthreshold (Sub) or bimodal (Bi) neurons. Many fewer unisensory (*Uni*) tactile (T) or visual (V) neurons were encountered. The average percentage of bimodal neurons was significantly greater than the other neuron types (asterisk).

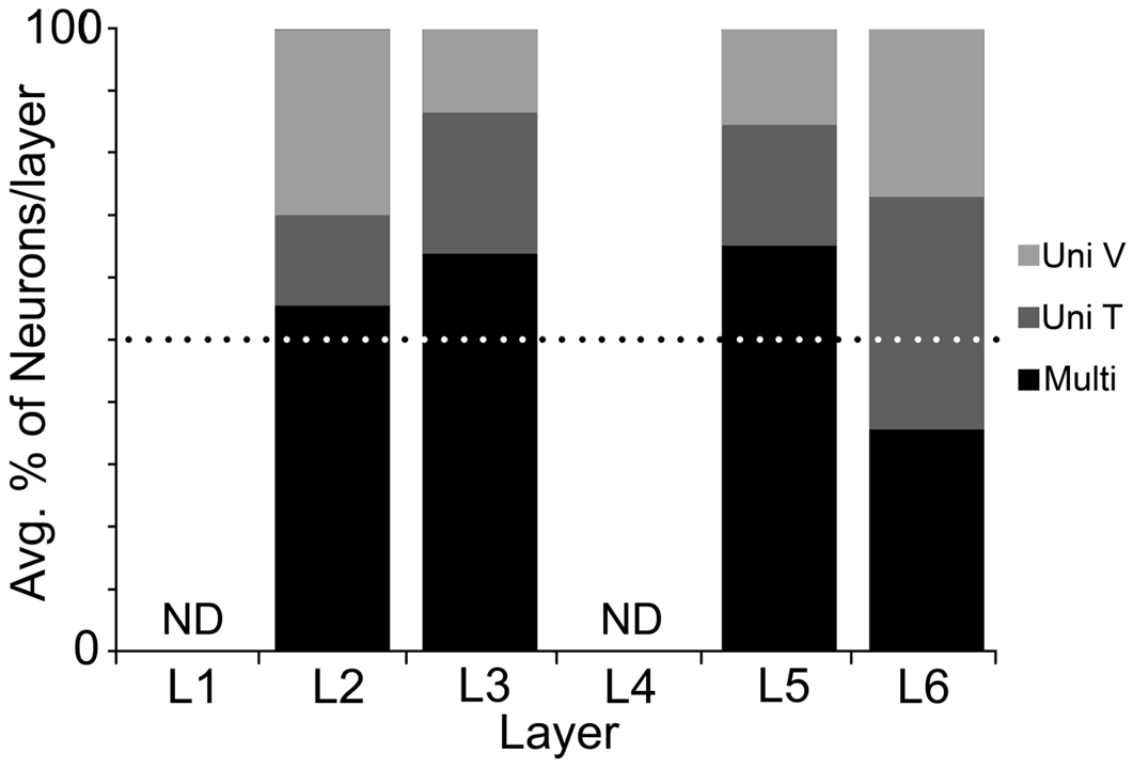

Figure 6. Laminar distribution of Multisensory and Unisensory neurons in PPr.
In the PPr, multisensory ('Multi;' black bars) predominate (>50%, above dotted line) in each layer except L6. Accordingly, proportionally fewer unisensory tactile (dark gray) neurons and unisensory visual neurons (light gray) were observed in all layers but layer 6. Values represent average percentage of neuron types by lamina. Too few neurons were localized to layers 1 and 4 to be included in these comparisons (ND = not sufficient data). See text for statistical treatments.

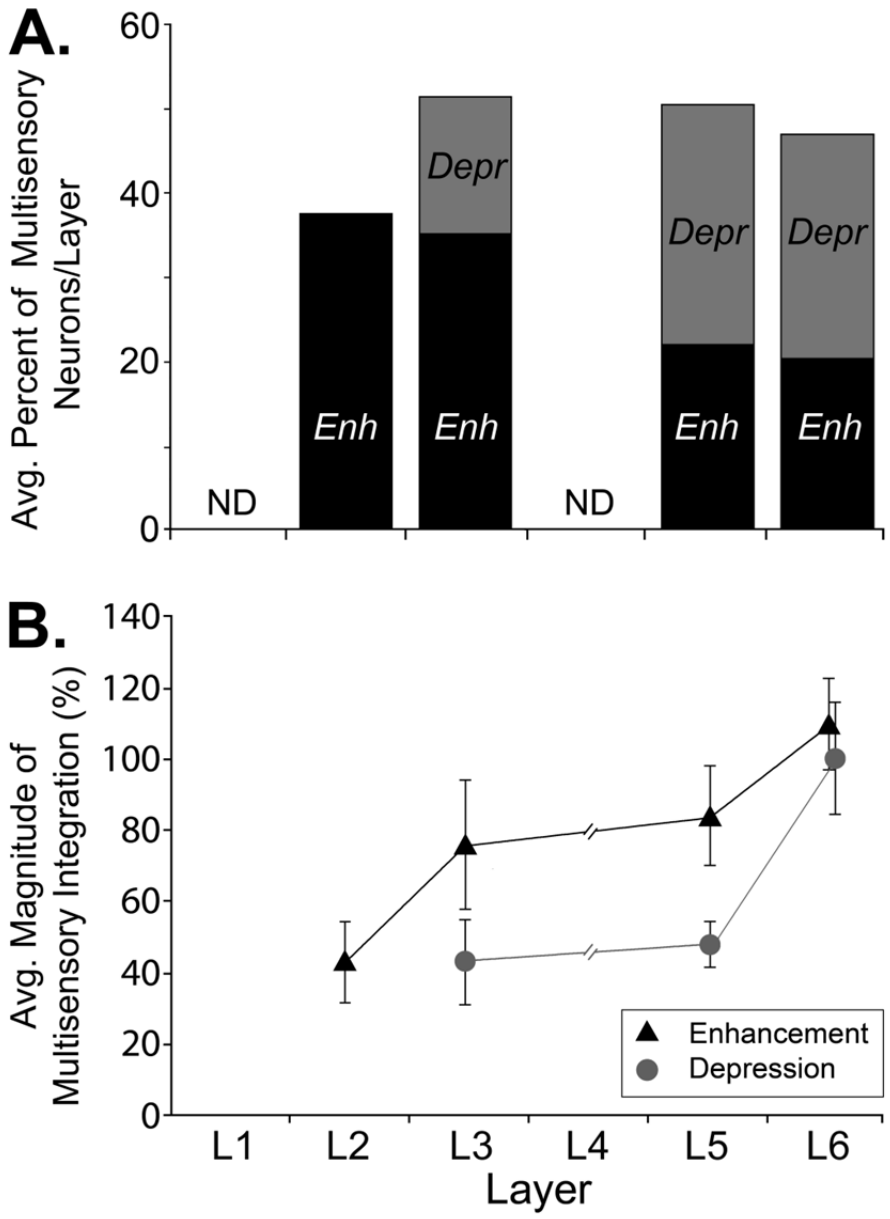

Figure 7. Laminar distribution of multisensory integration in PPr.
(A) Some neurons in PPr, when exposed to multisensory stimulation, show an enhanced (black with "Enh"), or depressed (grey with "Depr") response with respect to that elicited by the best unisensory stimulus. Values represent the average percentage of multisensory neurons. Supragranular layer (L2-3) neurons showing integrated responses mainly generated enhancement while those in infragranular layers (L5-6) showed a mixture of depressed or enhanced responses. (ND = not sufficient data). (B) The average magnitude of multisensory integration (Enhancement = black triangles; Depression = grey circles) tended to increase in the deeper laminae (error bars indicate SE). See text for statistical treatments.

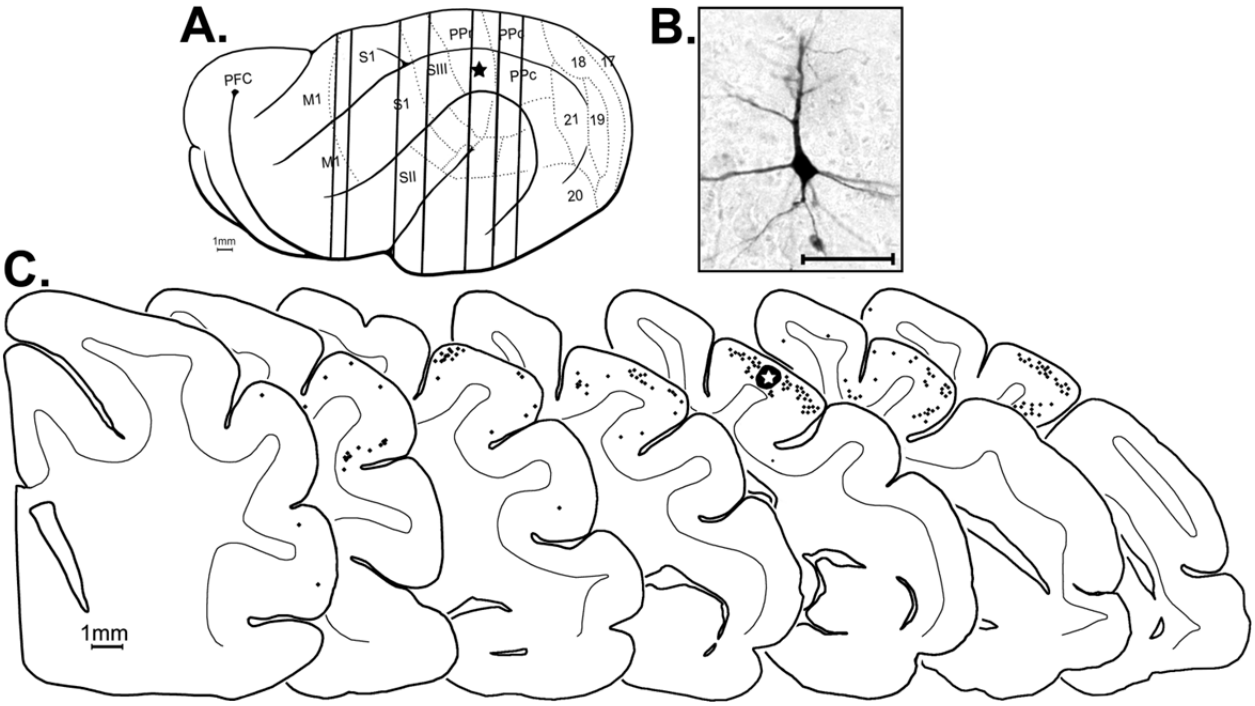

Figure 8. Retrogradely labeled cortico-cortical neurons from PPr tracer injection.
Tracer (BDA) injected into PPr produced retrogradely labeled neurons within the ipsilateral cortical hemisphere. Depicted is an example of a BDA injection made in PPr (indicated by star in lateral overview and the large, blackened/starred area on the 5th coronal section). (A) Vertical lines passing through the brain correspond to the coronal sections shown below. Each retrogradely labeled neuron (an example is shown in the photomicrograph (B); scale = 50 μm) was marked with a single black dot on the coronal sections (C; at bottom). The coronal sections are arranged serially (anterior = left) with the grey-white border of the cortical mantle indicated (thin line. Retrogradely labeled cortical neurons were present in functional areas SIII, MRSS, S1, M1, AMLS, and PPc.

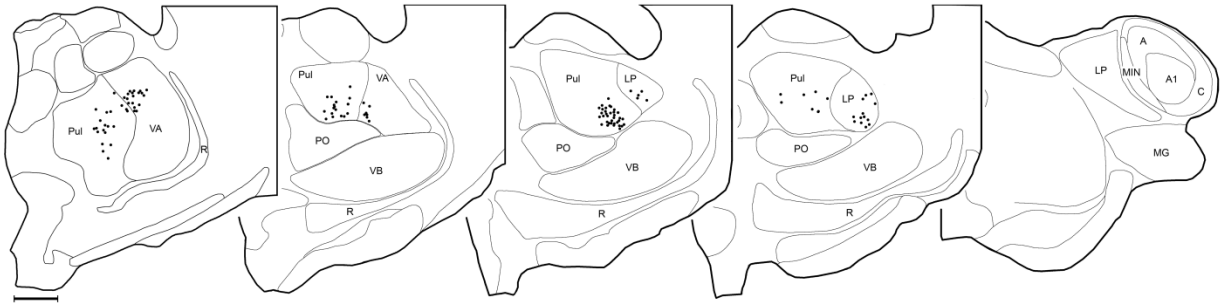

Figure 9. Retrogradely labeled thalamo-cortical neurons from PPr tracer injection.
The coronal sections through the thalamus are arranged with anterior (left) to posterior (right). Thalamic subdivisions were traced from each section and identified by the criteria of Manger et al., (2002; 2010). Each black dot represents the location of one retrogradely BDA labeled thalamo-cortical neuron. Labeled neurons were found in the pulvinar (Pul), rostral portions of the lateral posterior nucleus (LP), and the ventral anterior nucleus (VA). Importantly, no label was seen in the posterior nucleus (PO) or any portion of the lateral geniculate nucleus (A=A lamina of LGN; A1=A1 lamina of LGN; C=C lamina of LGN), MIN=medial interlaminar nucleus, MG=medial geniculate nucleus, R=reticular nucleus, or VB=ventrobasal complex. (scale bar = 1000μm).

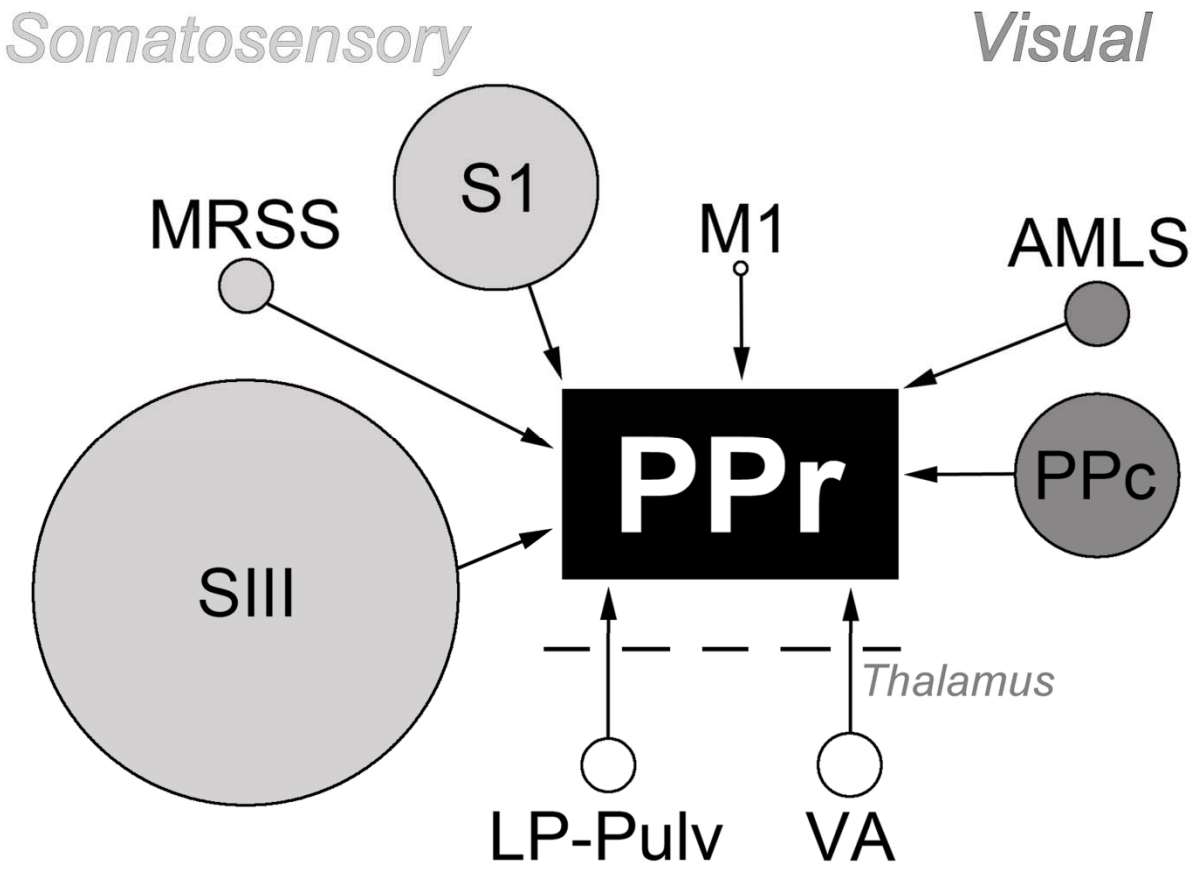

Figure 10. Summary of ipsilateral sources of projections to the PPr.
The PPr is represented by the central black rectangle. Each source of input to the PPr is represented by a circle. The sensory modality of each somatosensory (light grey), visual (dark gray), motor (M1) and thalamic area (bottom of diagram) is scaled to represent the proportion of the entire projection that originated from the indicated region. The majority of somatosensory inputs to the PPr arose from cortical area SIII and the majority of visual inputs are derived from cortical area PPc, while relatively few originated in the thalamus.

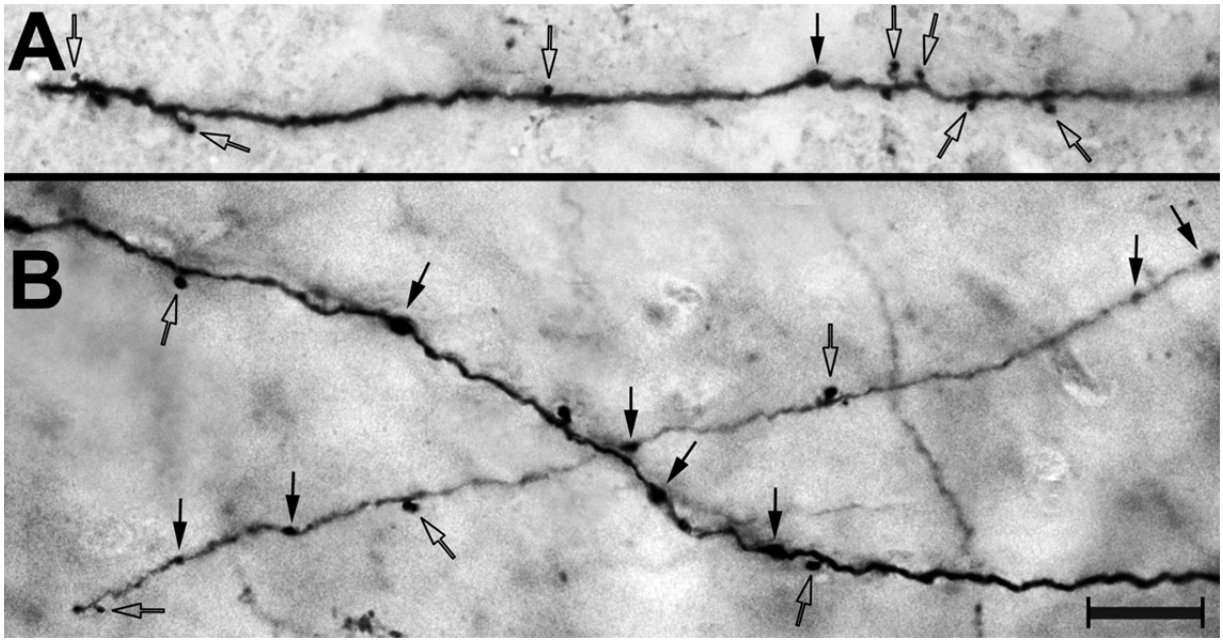

Figure 11. Labeled axon terminals in PPr.
Following BDA tracer injection in somatosensory area SIII (A) or visual PPc (B), labeled axon terminals (boutons) were visualized in the PPr using a light microscope (40x). Both terminal boutons (open arrows) and boutons in passage (closed arrows) were observed. Scale = 10μm.

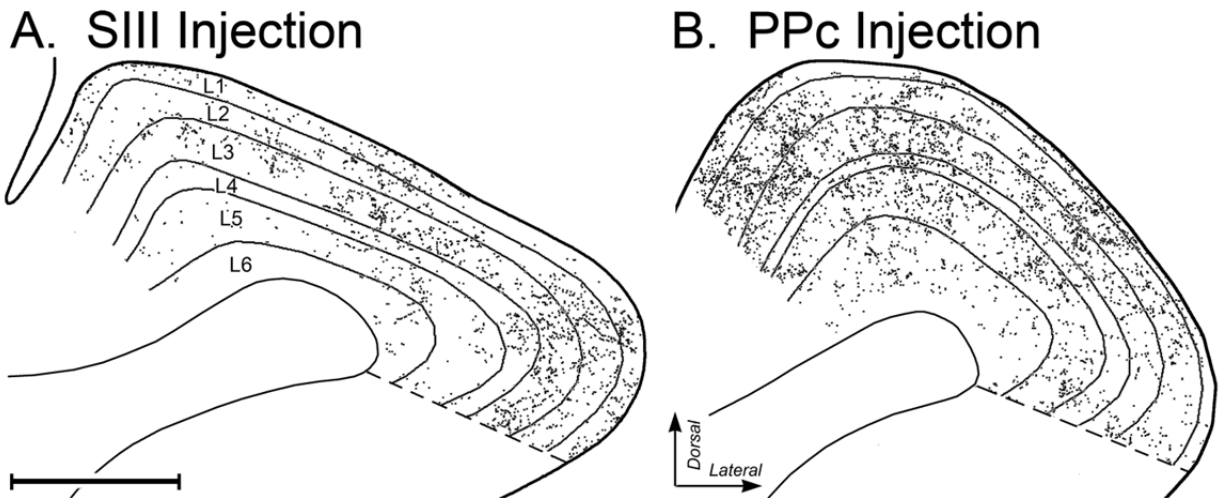

Figure 12. Axon terminal distribution in PPr labeled from BDA injections into SIII or PPc. Depicted are examples of digitally plotted coronal sections through PPr (left=medial; scale = 1000μm) showing the laminar distribution of axon terminals (1 dot = 1 labeled bouton) that were orthogradely labeled from somatosensory area SIII (A) or visual PPc (B).The thin black lines represent the laminar borders traced from an adjacent SMI-32 stained section.

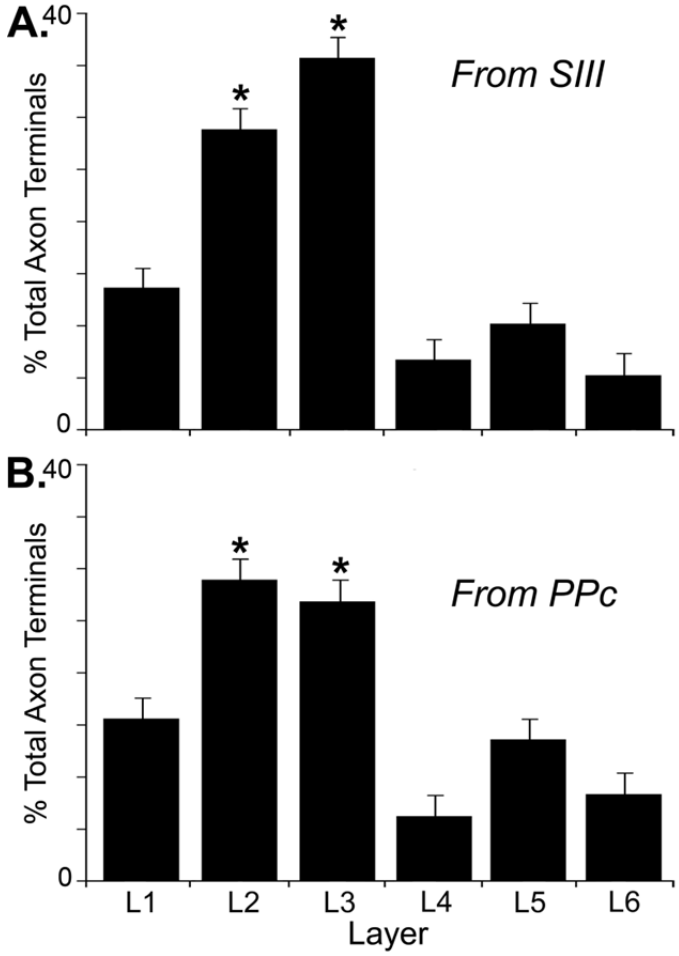

Figure 13. Laminar distribution in PPr of labeled axon terminals from SIII or PPc. (A) Labeled axon terminals in PPr from BDA injection into SIII were counted and grouped by their laminar location and were found to terminate primarily in layers 2 and 3. The histogram bars represent the average percentage of axon terminals by laminae in the PPr (error bars = standard error; asterisks = statistically significant). (B) Labeled axon terminals in PPr from BDA injection into PPc were counted and grouped by their laminar location and were found to terminate in all laminae, but predominated in layers 2-3. The histogram bars represent the average percentage of axon terminals by laminae in the PPr (error bars= standard error; asterisks = statistically significant). Importantly, the major SIII and PPc sources of projections to the PPr predominantly overlap in layers 2 and 3 of PPr.

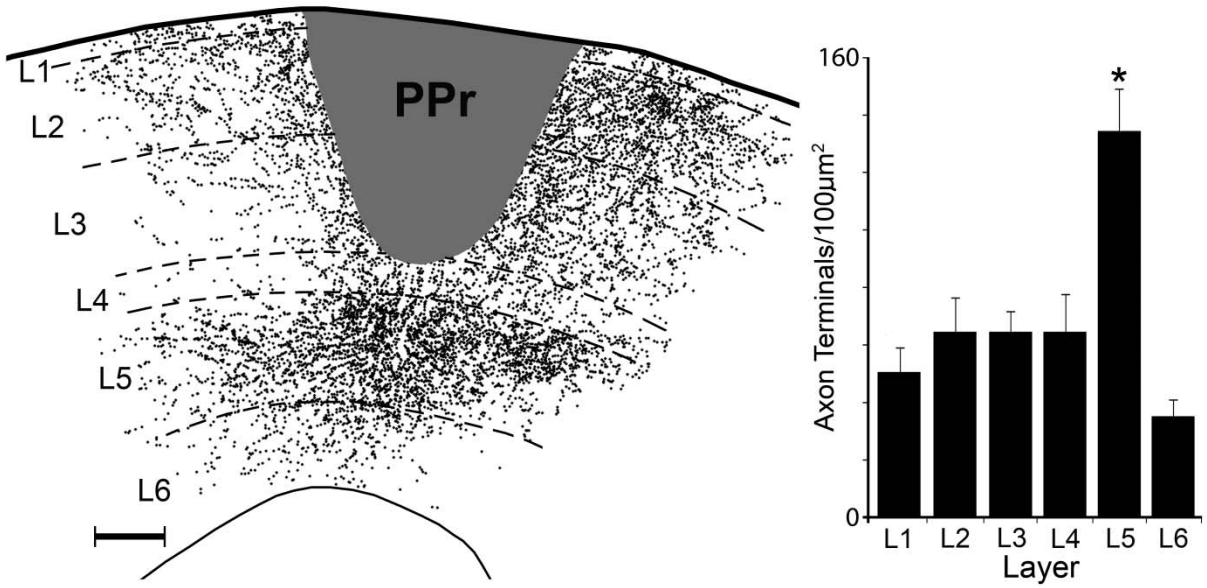

Figure 14. Local projections within PPr.
The coronal section through the PPr shows the center of a tracer injection (BDA, dark grey area) that was contained within the supragranular layers. This injection produced labeled axon terminals (1 dot = 1 bouton) across the different cortical laminae (1-6), but were most numerous and dense in layer 5. The bar graph (right; n = 5 ferrets) summarizes the distribution of local axon terminals labeled from injections in the PPr supragranular layers and shows the average laminar density of these boutons. The asterisk indicates that the density of projections to layer 5 was significantly greater than measured for all other layers, while the density of labeled terminals in the other layers did not differ significantly from each other (see text for statistics).

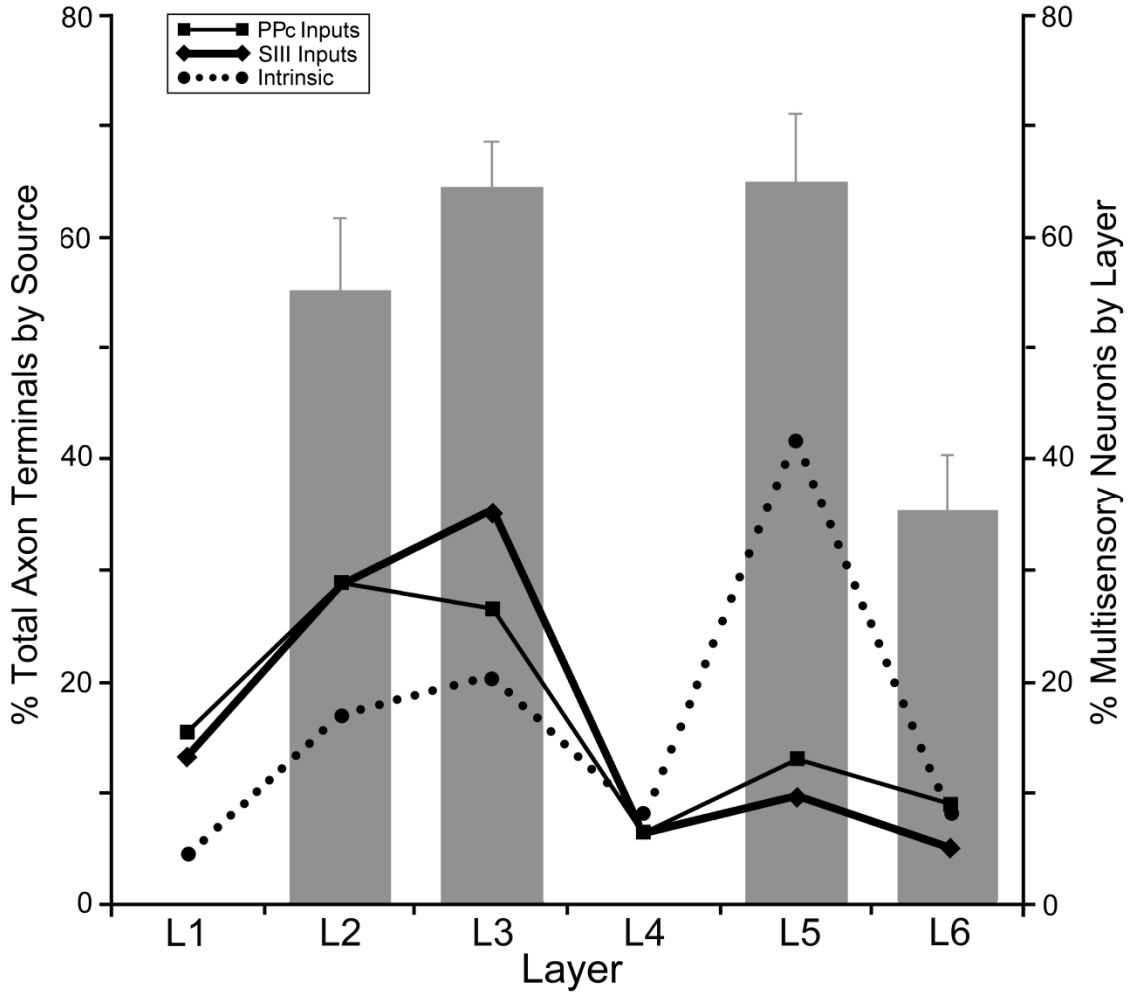

Figure 15. Correspondence of laminar connectional and functional properties of PPr. The preferential laminar distribution of converging extrinsic connections from SIII and PPc (solid black lines) into layers 2-3 favors the generation of multisensory neurons in layers 2-3 (histogram bars) while supporting mostly unisensory processing in layer 6. Intrinsic projections from supragranular layer 2-3 neurons (dotted line) carry converged multisensory signals primarily to layer 5, which is also characterized by a high level of multisensory neurons (histogram bar).

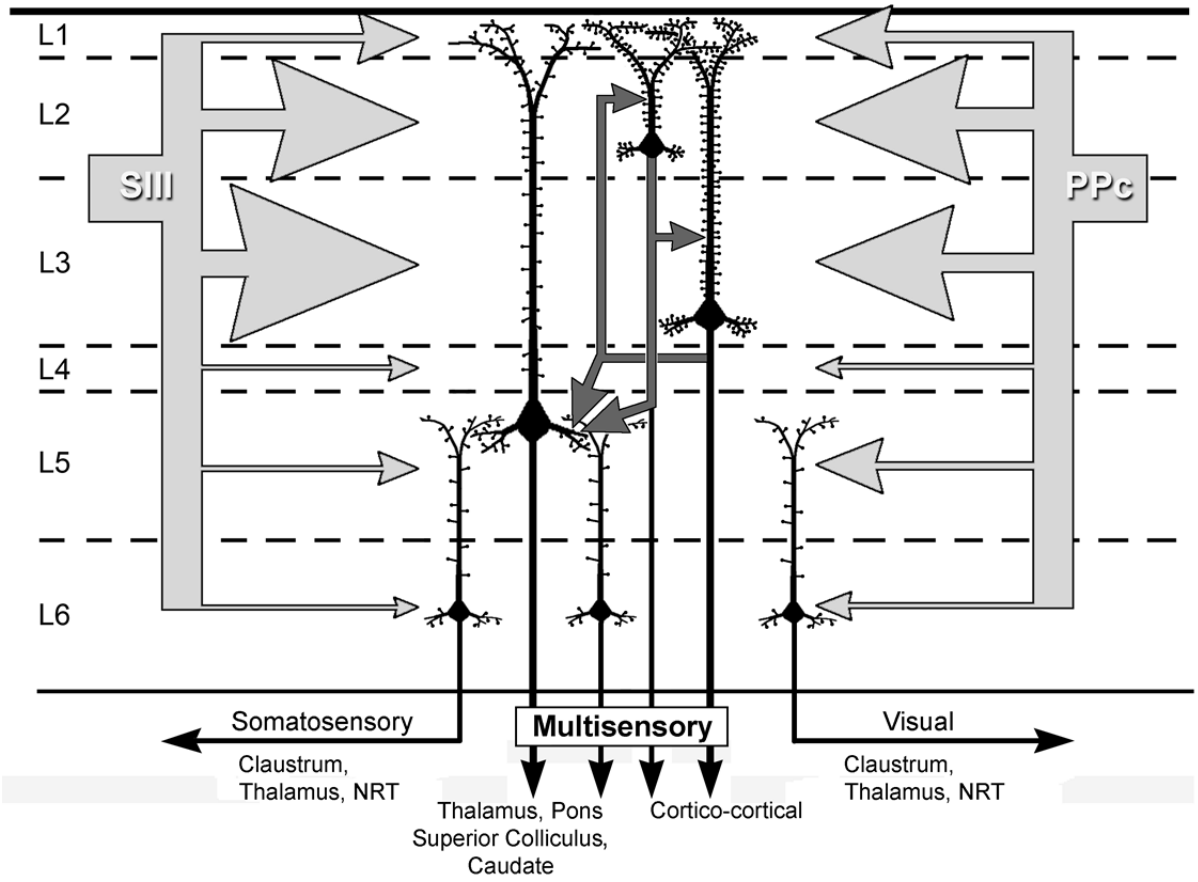

Figure 16. Summary of the laminar organization of connectivity and unisensory/multisensory properties of PPr.

The differential laminar distribution of converging extrinsic connections from SIII and PPc (large, light grey arrows scaled in proportion) favors the generation of multisensory neurons in layers 2-3. Intrinsic connections of supragranular layer 2-3 neurons carry converged multisensory signals (small, dark grey arrows) primarily to layer 5. In contrast, few extrinsic (convergent) or intrinsic (converged) projections reach layer 6, where most neurons were unisensory. Output targets of the multisensory layers of the PPr are known to be multisensory, while the output targets of the unisensory layer 6 largely target known unisensory areas. This arrangement suggests that unisensory and multisensory signals can be processed in parallel as they route through the PPr circuit. Roman numerals = cortical laminae. Dashed lines = laminar boundaries. SIII = somatosensory area III; PPc=visual caudal posterior parietal area. Light grey arrows = extrinsic inputs; dark grey arrows = intrinsic connections, black arrows=outputs.

Table 1. Average proportion of the total grey matter thickness spanned by individual layers by cortical region.

	Cortical Region		
Layer	PPr	V1	S1
I	11.8 ± 1.2	10.7	7.3 ± 0.4
II	17.2 ± 0.5	10.2	13.0 ± 1.2
III	22.5 ± 1.0	27.6	13.9 ± 0.9
IV	8.5 ± 0.3	20.9	18.3 ± 0.5
V	20.1 ± 1.2	11.4	27.0 ± 2.3
VI	20.0 ± 1.1	19.2	20.6 ± 2.3

Values indicate Avg. % ± SE

The average proportion (%) of the cortical mantle occupied by each of the six cortical laminae is shown for ferret PPr, as well as the ferret primary somatosensory area (S1). The data for ferret primary visual cortex (V1) were measured directly from published images(Homman-Ludiye et al., 2010; Innocenti et al., 2002) and, hence, do not have values of standard error (SE).

Table 2. Response latency to visual or tactile stimulation for neurons in SIII, PPr, or PPc.

Somatosensory Latency		**Visual Latency**	
SIII	**PPr**	**PPr**	**PPc**
40.7±1.25	51.5 ± 0.69	93.7 ± 2.76	66.5 ± 3.7
	Supragranular 47.4 ± 1.79	Supragranular 78.1 ± 4.24	
	Infragranular 53.3 ± 1.30	Infragranular 94.7 ± 3.88	

The latency of responses (average ± sd) to somatosensory stimulation and to visual stimulation are listed for somatosensory area SIII, visual area PPc and multisensory area PPr. These data indicate that responses in unisensory areas SIII and PPc significantly precede those which occur in multisensory PPr (t-test, tactile $p<0.0001$; visual $p<0.0001$). In addition, when response latency for neurons in PPr is further divided by their supragranular or infragranular location, activation of supragranular neurons occurs significantly earlier (t-test; tactile $p=0.0092$; visual $p=0.0049$).

Table 3. Neuronal Sensory Response Types in SIII, PPr and PPc.

	Unisensory		Multisensory		
			Subthreshold	**Subthreshold**	**Bimodal**
	Uni T	**Uni V**	**V_T**	**T_V**	**VT**
SIII	91 ± 10 (71)	0	0	9 ± 8.8 (7)	0
PPr	23 ± 3.9 (103)	14 ± 5.9 (61)	5 ± 4.0 (23)	9 ± 1.8 (39)	50 ± 4.5 (225)
PPc	0	89 ± 2.0 (105)	11 ± 2.1 (13)	0	0

Values indicate Avg. % ± SE (n).

Uni T = unisensory tactile; Uni V = unisensory visual; V_T = visual responses modified by tactile stimulation; T_V = tactile responses modified by visual stimulation; VT = independent suprathreshold responses to visual and to tactile stimulation.

Table 4. Laminar distribution of sensory and multisensory neurons in PPr.

	Neuron Type		
Layer	**Multisensory**	**Unisensory Tactile**	**Unisensory Visual**
I	ND	ND	ND
II	55.1 ± 6.7	14.6 ± 8.6	30.3 ±8.3
III	64.5 ± 4.1	23.0 ± 5.7	13.4 ± 5.5
IV	ND	ND	ND
V	65.0 ± 6.1	19.6 ± 3.8	15.4 ± 5.3
VI	35.2 ± 5.1	37.4 ± 11.7	27.4 ± 10.9

Values indicate Avg% ± SE; ND=Not sufficient data.

Table 5. Average Responses to Unisensory and Multisensory Stimulation by Lamina.

	Average Response to Sensory Stimulation		
Layer	**Tactile**	**Visual**	**Combined**
II	0.8 ± 0.31	2.1 ± 0.39	2.9 ± 0.57
III	1.4 ± 0.19	1.3 ± 0.24	2.4 ± 0.34
V	1.6 ± 0.15	1.4 ± 0.18	2.4 ± 0.26
VI	1.1 ± 0.27	0.8 ± 0.35	1.5 ± 0.47

Values indicate Avg. Mean spikes/trial ± SE

Table 6. Percentage of multisensory neurons in PPr showing multisensory integration by lamina

	Multisensory Integration Category		
Layer	**Enhanced**	**Depressed**	**Unchanged**
I	ND	ND	ND
II	37.5 ± 16.1	0	62.5 ± 15.7
III	34.9 ± 11.4	16.3 ± 7.7	48.8 ± 11.1
IV	ND	ND	ND
V	21.6 ± 8.2	28.4 ± 8.6	50.0 ± 11.1
VI	20.0 ± 12.5	26.7 ± 8.9	53.3 ± 12.8

Values indicate Avg. % ± SE; ND = Not sufficient data

Table 7. Magnitude of multisensory response enhancement or depression by lamina

Layer	**%Enhancement**	**%Depression**
I	ND	ND
II	42.8 ± 11.2	0
III	76.2 ± 18.1	43.4 ± 12.0
IV	ND	ND
V	83.6 ± 13.9	46.2 ± 6.2
VI	109.5 ± 12.9	100.0 ± 22.4

Values indicate Avg. % ± SE; ND = Not sufficient data

CHAPTER IV

BIMODAL AND UNISENSORY NEURONS EXHIBIT DISTINCT FUNCTIONAL PROPERTIES

INTRODUCTION

Since the identification of multisensory neurons a half century ago (Horn and Hill, 1966), the bimodal neuron has come to represent the basic (even iconic) unit of multisensory processing. These neurons, which show suprathreshold responses to stimuli from more than one sensory modality, have been found throughout the neuroaxis and across a wide variety of species ((Stein and Meredith, 1993) for review). Most of the early work on multisensory processing was carried out in the cat superior colliculus (SC). These studies showed that bimodal neurons integrate multisensory information (demonstrated by a statistically different number of action potentials in response to multisensory versus unisensory stimulation) according to the temporal and physical parameters of the stimuli. Specifically, stimuli in spatio-temporal coincidence produced integrative responses that were often super-additive (Meredith and Stein, 1983; 1985) (greater than the sum of the spikes elicited by the two unimodal stimuli presented alone). Furthermore, the tendency for weaker stimuli to evoke higher levels of integration when combined was described as the principle of "inverse effectiveness." The generality of these principles of multisensory processing, determined from SC studies, seemed to be confirmed by early similar findings in cortical bimodal neurons (Stein and Wallace, 1996; Wallace et al., 1992). While the principle of spatio-temporal coincidence seems to hold true for bimodal neurons studied in other brain areas – later studies of cortical bimodal neurons have shown that they do not demonstrate integration with the same predominance, or with the same levels as SC bimodal neurons (Avillac et al., 2007; Clemo et al., 2007; Jiang et al., 1994; Meredith and

Allman, 2009; Meredith et al., 2011a; Morgan et al., 2008; Sugihara et al., 2006). Although bimodal neurons in the SC show a range of response enhancement that in some cases exceeds 1200% (Meredith and Stein, 1986), with an average response enhancement of 88% (Meredith and Stein, 1983; 1985; 1986), cortical multisensory neurons (anterior ectosylvian sulcus (Jiang et al., 1994; Meredith and Allman, 2009), posterolateral lateral suprasylvian cortex (Allman and Meredith, 2007), rostral suprasylvian sulcal cortex (Clemo et al., 2007) exhibit a much lower range of integration (up to 212%) with an average level of enhancement of only 33% (Meredith et al., 2011a). In addition, while a majority of SC bimodal neurons exhibit integration, only a minority (39%) of cortical bimodal neurons exhibited integration and only 17% of these produced superadditive response levels. This is in stark contrast to the 55% of neurons in the SC which show superadditivity (Meredith et al., 2011a; Meredith and Stein, 1983; 1985). Thus, the multisensory properties of bimodal neurons appear to differ between the SC and cortex (reviewed in Meredith et al., 2011).

Within a given multisensory area, be it in brainstem or cortex, multisensory neurons coexist with unisensory neurons. However, because the two types of neurons are distinguishable, it is logical to expect that bimodal neurons provide a function that unisensory neurons do not. The early work performed on bimodal neurons in the SC has suggested that multisensory integration itself represents this unique function ((Alvarado et al., 2007; Meredith and Stein, 1983) for review), especially because unisensory neurons, by definition, were presumed to be insensitive to this integrative effect. However, more recent studies have shown (Allman and Meredith, 2007; Clemo et al., 2007; Jiang et al., 1994; Keniston et al., 2009; Meredith and Allman, 2009; Meredith et al., 2011a) that only a minority of cortical bimodal cells exhibit responses that meet the criterion for multisensory integration. Furthermore, some

'unisensory' neurons can be significantly influenced by multisensory stimulation, and have been identified as 'modulatory' or 'subthreshold' multisensory neurons(Allman et al., 2008b; 2009; Allman and Meredith, 2007; Avillac et al., 2007; Bizley et al., 2007; Carriere et al., 2007; Dehner et al., 2004; Driver and Noesselt, 2008; Keniston et al., 2009; Meredith et al., 2006; Sugihara et al., 2006). Therefore, multisensory integration can no longer be regarded as a distinguishing feature between bimodal from unisensory neurons. Moreover, the question of functional differences between bimodal and unisensory neurons has largely been unexplored because investigations of multisensory neuronal function have almost exclusively selected for and examined bimodal neurons while, at the same time, the vast majority of studies of unisensory functions test with only the effective stimulus modality to the exclusion of the others. Thus, missing from multisensory investigations are direct comparisons of unisensory and bimodal neurons. Therefore, it is the primary goal of the present experiments to compare the functional properties of neurons that are demonstrably unaffected by multisensory stimulation (i.e., unisensory) with those that are.

To investigate and analyze the function of these different neuron types, a suitable experimental model is one that expresses contains bimodal and unisensory neurons. The rostral posterior parietal cortex of the ferret (PPr) is such an area: it contains neurons which respond to either (i.e., unisensory) (Foxworthy et al., 2011; Manger et al., 2002) or both tactile and visual stimulation presented alone (i.e., bimodal) (Foxworthy et al., 2011). Also, both the visual and somatosensory receptive fields in PPr are large (visual = 20-45° diameter; tactile = mostly face and vibrissa) (Manger et al., 2002), such that a generic set of visual-tactile stimuli can activate all, or the majority of sensory neurons within a given penetration in the PPr (as demonstrated in Foxworthy et al, 2011). This is important because these arrangements permit activation of

sensory neurons at multiple, spatially-distinct sites (like those sampled by a multichannel recording probe) under the simultaneous and identical stimulus conditions (see previous chapter) necessary for direct comparison of their response properties. Multiple single-unit recordings also avoids the confound of serial sampling of sensory responses using repeated stimulation. The ferret PPr is also attractive because parietal cortex is well-studied in humans, monkeys and rodents that have demonstrated that the region plays a role in attention and in rectifying spatial maps from different sensory modalities to achieve goal-directed behaviors such as reaching, navigation and gaze direction (Alais et al., 2010; Calton and Taube, 2009; Kaas et al., 2011; Nitz, 2009; Reep and Corwin, 2009; Save and Poucet, 2009). Additionally, all eutherian mammals studied so far exhibit a visual-somatosensory multisensory area between visual and somatosensory representations (Kaas, 2009; Manger et al., 2002) and, therefore, the properties of bimodal/unisensory neurons in the ferret PPr can be generalized to a large number of species. Thus, the PPr is an appropriate cortical area in evaluate and compare the functional properties of bimodal and unisensory neurons.

METHODS

Surgical Procedures

Ferrets (male, adult n=17) were anesthetized (8mg/kg ketamine; 0.03mg/kg dexmedetomidine intramuscularly) and their heads were secured in a stereotaxic frame. Using aseptic surgical procedures, a craniotomy was made to expose the rostral posterior parietal (PPr) region, the caudal posterior parietal visual region (PPc) and the third somatosensory area (SIII) on the suprasylvian gyrus. Over this opening, a recording well/head supporting device was implanted using stainless steel screws and dental acrylic.

Electrophysiological Recording

For recording, the ferrets were secured to an immobile supporting bar via the cranial implant, such that their eyes and ears were not obstructed and no pressure points were present. The animals were intubated through the mouth, ventilated (expired CO_2: ~4.5%) and immobilized (pancuronium bromide; 0.3 mg/kg initial dose; 0.2 mg/kg h supplement i.p.). Fluids (lactated Ringer's solution) and supplemental anesthetics (4mg/kg h ketamine; 0.5 mg/kg h acepromazine i.p.) were administered continuously with an infusion pump. Paralytics were necessary to prevent movement of the body and eyes during the lengthy and repeated presentation of somatosensory and visual stimuli at fixed locations. Heart rate was monitored continuously and, if heart rate rose over a sustained period of 5-10 minutes, additional supplemental anesthetics were administered. Animal temperatures were continuously monitored and maintained at 38°C on a heating pad. The pupils were dilated with 1% atropine sulfate, the eyes were anesthetized with 0.5% proparacaine hydrochloride, and corrective contact lenses were placed on the corneas to adjust for refractive errors.

A 32-channel silicon probe (4×8- 5mm 200–200-413 array; impedance ~1 MΩ; NeuroNexus Technologies, Ann Arbor, MI) was positioned over the recording target (SIII, PPr or PPc) guided by sulcal and gyral landmarks described in published reports of the three brain areas (Foxworthy and Meredith, 2011; Manger et al., 2002). The probe was then advanced into the cortex to a depth of about 1750μm using a hydraulic microdrive. After allowing the probe to stabilize in the cortex for 30 minutes, neuronal activity was recorded and digitized (rate>25kHz) using a TDT System III Workstation (TuckerDavis Technologies Alchua, FL) running MatLab software and stored for off-line analysis. The raw signal was bandwidth separated (at 0.5-5kHz) to distinguish spiking activity from local field potentials. Spike signals were then denoised by a

two-stage multiple linear regression function to reject signals common to all channels. Waveforms were then be clustered by principal component feature space analysis then sorted into individual units using an automated Bayesian sort-routine. Spikes which failed to separate within a principal component cluster were marked as outliers and not included for further analysis. Also, spikes which had interspike intervals of less than 2ms were rejected. This technique has been developed and used by our lab in explorations of other cortical regions in the ferret and has been demonstrated to reliably segregate single-units (Allman et al., 2009).

After individual neurons were templated, their responses to sensory stimulation were determined. First, each neuron was assessed independently through the manual presentation of somatosensory (brush strokes, taps, manual pressure and joint movement) and visual stimuli (flashed or moving spots or bars of light from a hand-held ophthalmoscope projected onto a translucent hemisphere, 92cm diameter, positioned in front of the animal) to determine the each neuron's responsiveness to somatosensory or visual stimuli and its receptive field(s). Electrode penetrations which contained a mixture of visual and tactile responses on individual shanks were considered to be in the PPr. Penetrations immediately rostral to this location which had responses to only somatosensory stimulation were determined by established criteria (Foxworthy and Meredith, 2011) as being in SIII. Similarly, electrode penetrations caudal to the PPr which demonstrated only visual responses were defined by published criteria (Manger et al., 2002) as being located in the PPc. The receptive fields determined through manual stimulation were used to guide the placement of the subsequent electronically-generated, repeatable somatosensory and visual stimuli, which are described below. Auditory responsiveness was also evaluated using manually presented claps, hisses, whistles at different locations around the animal's head.

However, auditory responses were never observed, so quantitative sensory testing (below) progressed using only visual and somatosensory stimulation.

Electronically-generated, computer-controlled stimuli were used to acquire quantitative measures of neuronal functional properties in PPr, SIII and PPc. Stimulation parameters were kept as constant as possible (allowing for some minor adjustments due to preferred receptive fields in individual electrode penetrations) across different recording penetrations and among different animals. Somatosensory stimulation was produced by a calibrated 1 gram monofilament fiber moved by an electronically driven, modified shaker (Ling, 102A) that travelled 11mm and displaced hair or indented the skin on the contralateral side of the ferret's face at a velocity of 0.18 meters/second. Visual stimulation was projected onto the translucent hemisphere and consisted of a bar of light that moved (70 deg/sec) 10-15 degrees across the lower hemifield of the contralateral visual space in the nasal to temporal direction, and was 2x20 degrees in size. These stimuli were presented separately and in combination. During combined presentations, the onset of the visual stimulus preceded that of the tactile stimulus by ~40ms to compensate for the cortical latency disparity, such that the spike trains evoked by visual and somatosensory stimuli overlapped. The separate and combined presentations of stimuli were randomly interleaved to compensate for possible shifts in baseline activity, interstimulus intervals randomly varied between 3-7 seconds to avoid response habituation, and each stimulus or combination was repeated 50 times. In this way, a given recording penetration simultaneously sampled neuronal responses for each recording channel (n=32) to repeated visual, tactile, and combined visual-tactile stimulation. Operationally, (see Results) these stimulation parameters were appropriate to consistently elicit robust neuronal responses on a high proportion recording sites per penetration.

Once a recording session was completed, the animal was overdosed (Euthasol), perfused and fixed (4% paraformaldehyde). The cortex was blocked stereotaxically and serially sectioned (75 μm) in the coronal plane. The sections were mounted on slides and counterstained with cresyl violet. Sections containing recording sites were photographed using a light microscope and a scaled image of the recording probe was superimposed by aligning the depth and M-L dimensions with the electrode tracks. This produced a reconstruction of the tissue in relation to the recording probe and individual recording sites localized in white matter, or not fully inserted into the cortex, were not used for further analysis.

Data Analysis

To evaluate the neuronal responses to the somatosensory, visual and combined stimuli, custom software (MatLab) was used to compile and quantify the spiking activity of each identified neuron after the criteria of (Bell et al., 2005). A neuronal response was defined as spiking activity which was >3 standard deviations from spontaneous activity, that lasted for 15ms duration, and ended when activity returned to baseline for at least 15ms. For each neuron, the following specific response features were analyzed:

Sensory category: Neurons were defined by their different patterns of responses to the quantitative sensory tests, according to published criteria (Allman et al., 2008a; Allman et al., 2009). Neurons showing suprathreshold activation to more than one sensory modality were defined as bimodal multisensory neurons. Neurons that exhibit suprathreshold activation in only one modality, but were significantly influenced by the presence of a stimulus from another modality were designated as subthreshold multisensory neurons. Those which showed

suprathreshold activation by only one modality but failed to be influenced by stimulation in other sensory modalities were defined as unisensory neurons. Neurons which were not activated by any sensory stimulus or combination were defined as unresponsive neurons.

Response magnitude: The magnitude of response was calculated in terms of mean spikes per trial for each stimulation condition (visual; tactile; visual-tactile) for each neuron. A response was defined as activity that was time-locked to the onset of stimulation and that rose >3 standard deviations above baseline activity for at least 15 ms.

Response duration: Onset of a response was defined as activity that rises >3 standard deviations from baseline activity for 15ms duration. Offset was the point where activity returns to baseline for at least 15ms. Duration was defined as the time measured from response onset to offset.

Response latency: This was calculated as the time from the onset of the sensory stimulus to the beginning of a neuronal response.

Spontaneous activity level: The activity of the neurons in the absence of sensory stimuli was measured from spiking activity (spikes/second) captured from data records for the period of time 500ms prior to the onset of sensory stimulation.

Multisensory integration: Neurons classified as bimodal were further analyzed to determine if they demonstrated integrated responses to multisensory stimulation, which was defined as a response to combined stimulation that was significantly different (paired t-test; $\alpha=0.05$) than that

elicited by the most effective unisensory stimulus. Responses showing a significantly greater activation (mean spikes/trial) to multisensory stimuli versus that elicited by the most effective single modality stimulus (determined by paired t-test) were classified as showing response enhancement, those showing a significantly reduced activation to multisensory versus the best unisensory stimulus were classified as showing response depression. The magnitude of multisensory integration was calculated according to the method of (Meredith and Stein, 1986) using the formula: $(CM\text{-}SM_{max})/ SM_{max} \times 100 = \%$ Integration. In this equation, SM_{max} was the neuron's response to the most effective unisensory stimulus (mean spikes/trial) and CM was the response to the multisensory stimulus.

After neurons were categorized as unisensory (tactile or visual) or multisensory (subthreshold or bimodal) using the criteria above, statistical tests were used to assess functional differences between the groups using t-tests (when only two groups were compared) and ANOVAs (α=0.05) followed by Tukey tests (when multiple groups were compared; α=0.05). Tests of linear correlation were used to assess the relationships between different functional properties. For variables which correlated with multisensory integration, the relative strength of these correlations was assessed using multiple regression analysis and subsequent comparison of beta weights (standardized multiple regression coefficients).

RESULTS

Electrophysiological Recording Summary

To compare the functional properties of bimodal and unisensory neurons in the rostral posterior parietal cortex (PPr), multi-channel single-unit extracellular recordings (summarized in Fig. 1) obtained a total of 451 sensory responsive neurons. Of this neuronal sample, 50% (225/451) were bimodal neurons that were independently activated by visual and by somatosensory stimulation, while 36% were either unisensory visual (13%; 61/451) or unisensory tactile neurons (23%; 103/451). Examples of each response type are provided in Figure 2. Relatively few neurons activated by tactile (9%; 39/451) or visual (5%; 23/451) stimulation showed subthreshold multisensory responses. Recordings were also made in the adjacent somatosensory area SIII and the visual caudal posterior parietal cortex where 78 tactile and 118 visual neurons were identified, respectively. A few subthreshold multisensory neurons were also encountered in SIII (9%; 7/78) and in PPc (11%; 13/118).

Bimodal vs. Unisensory: Spontaneous Rate

Figure 2 shows the spiking activity of simultaneously recorded bimodal and unisensory neurons that includes periods of spontaneous discharge prior to the onset of stimulation. In these examples, the bimodal neuron had an average spontaneous rate of 24.9 spikes/second while the unisensory tactile and unisensory visual neurons had much lower spontaneous rates (13.7 spikes/second and 12.1 spikes/second respectively). These examples reflect the trend observed in the population of bimodal and unisensory neurons, as summarized in Table 1 and Figure 3A. Overall, bimodal neurons demonstrated an average spontaneous rate of 25±0.93 spikes/sec that was ~1.6 times that of unisensory neurons (Uni T = 18±1.38 spikes/sec; Uni V= 14±1.40

spikes/sec) within the PPr. An ANOVA ($F(2,386) = 25.6$; $p<0.0001$) followed by post-hoc Tukey tests showed that bimodal neurons had a significantly higher spontaneous rate than unisensory visual and unisensory tactile neurons, while the unisensory neurons did not differ significantly from each other. Subthreshold multisensory neurons did not occur with sufficient frequency to be included in these, and subsequent statistical comparisons (but see Multisensory Integration, below).

Bimodal vs. Unisensory: Response Magnitude

The levels, or magnitude, of evoked activity also varied among the different neuron types. For example, the bimodal neuron depicted in Figure 2 responded to the tactile cue with 1.8 mean spikes/trial and to the visual cue with 1.9 mean spikes/trial, while these identical stimuli evoked only 1.1 mean spikes/trial in the unisensory tactile neuron, and 1.4 mean spikes/trial in the unisensory visual neuron. These individual examples reflect the general trend observed in the overall sample. On average, bimodal neurons generated a greater response magnitude to tactile (2.7±0.15 mean spikes/trial) or to visual (2.7±0.18 mean spikes/trial) stimulation than did their unisensory counterparts (tactile=1.6±0.22 mean spikes/trial; visual =1.5±0.27 mean spikes/trial), as summarized in Table 1 and Figure 3B. In fact, bimodal neurons' average responses to separate sensory stimulation were nearly 2x that of the unisensory tactile or the unisensory visual neurons. These observations were statistically significant: t-tests showed that bimodal neurons had a greater average response magnitude to the same tactile stimulation compared to unisensory tactile neurons ($p<0.0001$); and bimodal neurons had a greater response to the same visual stimulation compared to unisensory visual neurons ($p=0.0003$).

Because the spontaneous activity of bimodal neurons was higher than that of unisensory neurons, it seemed likely that their elevated response magnitude simply reflected their higher spontaneous rate of firing. To evaluate this possibility, the average spontaneous activity for a given neuron was subtracted from the response magnitude recorded for that neuron, and these adjusted values were then compared between bimodal and unisensory groups. However, this manipulation did not change the direction or significance of the results. Bimodal neurons still exhibited a greater average response magnitude to tactile stimulation compared to unisensory tactile neurons (t-test; $p=0.0002$), and to visual stimulation compared to unisensory visual neurons (t-test; $p=0.0045$). In summary, these results showed that bimodal neurons had a greater response magnitude to the same visual or tactile stimulation than their unisensory counterparts, and this difference did not depend on spontaneous activity levels.

Bimodal vs. Unisensory: Response Duration

Given that bimodal neurons showed greater response magnitudes than their unisensory neighbors, one mechanism by which this change could be effected would be for the response duration of bimodal neurons to increase. Using the same visual and tactile responses described above, the response duration was assessed for bimodal and unisensory neurons. In the example provided in Figure 2, the bimodal neuron had a response duration of 38ms to tactile stimulation while the unisensory tactile neuron exhibited a duration of only 29ms to the same stimulus. With visual stimulation, however, the bimodal neuron revealed a response duration of 38ms that was similar to that of the unisensory visual neuron (39ms). These examples mimic the trend seen in the overall sample, where bimodal neurons had a greater mean response duration to tactile stimulation (39±1.19 mean ms) than did unisensory tactile neurons (28±1.72 mean ms), and this

difference was statistically significant (t-test, $p<0.0001$). But for visual stimulation, the average duration of response of all bimodal neurons (40±1.70 mean ms) was similar to that of unisensory visual neurons (40±2.54 mean ms), which was not significantly different (t-test, $p=0.79$).

Bimodal vs. Unisensory: Response Latency

The latency for responses to tactile and to visual stimulation was compared between bimodal and unisensory PPr neurons, as listed in Table 1 and illustrated in Figure 3D. For the simultaneously recorded examples provided in Figure 2, the visual responses of the bimodal neuron (latency = 87ms) were much shorter than those of the unisensory visual neuron (98ms), but the tactile responses of bimodal (45 ms) and unisensory tactile (44 ms) neurons were not very different from one another. These latency patterns were reflected in the overall population. Bimodal neurons responded on average 17ms faster to visual stimulation (87±4.24 mean ms) than did the unisensory visual neurons (104±5.02 mean ms), and this latency difference was statistically significant (t-test; $p=0.0116$). For responses to tactile stimulation, bimodal neurons exhibited an average response latency (51±0.97 mean ms) that was similar to that measured for unisensory tactile neurons (53±1.33 mean ms), and these values were found to not significantly differ from each other (t-test, $p=0.31$).

Correlations Among Response Features

To evaluate whether response features of cortical bimodal and multisensory neurons might covary, data from the different response measures were examined for correlative relationships using Pearson's correlation to allow for comparisons with the extant data that examines correlations in multisensory processing (Perrault et al. 2003; Perrault et al., 2005;

Avillac et al., 2007). Additionally, because the scatterplots of the data did not always appear to show linear relationships – Spearman's rank correlation coefficient was also utilized to evaluate potential correlations. In Figure 4, response magnitudes for tactile and visual stimulation were plotted against spontaneous discharge rates. For tactile stimulation, both bimodal (Pearson $r=0.57$, $p<0.0001$; Spearman $\rho=0.60$, $p<0.0001$) and unisensory tactile (Pearson $r=0.57$, $p<0.0001$; Spearman $\rho=0.66$, $p<0.0001$) neurons showed a significant positive linear correlation between spontaneous rate and response magnitude (Figure 4A). With visual stimulation, both bimodal (Pearson $r=0.39$, $p<0.0001$; Spearman $\rho=0.53$, $p<0.0001$) and unisensory visual (Pearson $r=0.41$, $p=0.0002$; Spearman $\rho=0.44$, $p<0.0001$) neurons also showed a significant positive linear correlation between spontaneous rate and response magnitude (Figure 4B). Thus, response magnitude tended to increase with increasing spontaneous rate for bimodal and unisensory neurons alike.

As shown in Figure 5, the relationship of the temporal variables of response duration and response latency was analyzed (Pearson's correlation; Spearman's rho). No significant correlation was found between tactile response latency and tactile response duration for either bimodal ($r=-0.08$; $p=0.33$), or unisensory tactile neurons ($r=-0.13$; $p=0.24$) (Figure 5A). With visual stimulation, a significant negative linear correlation was found between visual response latency and visual response duration for bimodal neurons ($r=-0.34$; $p=0.0088$) as shown in Figure 5B. The negative correlation between these variables was confirmed by Spearman's rho ($\rho=-0.37$; $p=0.0004$). However, no significant correlation was found for unisensory visual neurons ($r=-0.29$; $p=0.65$) as is also illustrated in Figure 5B. Thus, except for visual responses of bimodal neurons, there seemed to be little relationship between the temporal features of response latency and response duration.

Multisensory vs. Unisensory Areal Comparisons

Because the unisensory somatosensory (SIII) or unisensory visual (PPc) areas combine to provide ~58% of the afferent input to the PPr (Meredith et al., 2011b) (Foxworthy et al., 2012), comparisons of the functional properties of neurons between the different areas were also conducted. However, bimodal neurons were not observed in SIII or PPc, so only the measures from their unisensory tactile or unisensory visual (respectively) neurons were available for these comparisons (too few subthreshold multisensory neurons were recorded for statistical evaluation). As shown in Figure 6A and summarized in Table 1, the spontaneous rate of the unisensory neurons in SIII (18±1.82 mean spikes/sec) and PPc (19±1.54 mean spikes/sec) was about 1.4 times less than that of bimodal neurons in PPr (25±0.93 mean spikes/sec). The neurons in visual area PPc exhibited a higher spontaneous rate than the unisensory visual neurons of the PPr. SIII neurons, on the other hand, had a mean spontaneous rate nearly equivalent to that of unisensory tactile neurons in PPr. Statistical comparisons of these data (ANOVA $F(4, 560) = 8.95$; $p<0.0001$) showed that bimodal neurons in the PPr indeed showed a significantly higher spontaneous rate than unisensory neurons in PPr, PPc and SIII, but that the spontaneous rates of activity of unisensory neurons from these areas did not differ significantly from each other (post-hoc Tukey tests). In other words, bimodal PPr neurons showed higher spontaneous rates than did any of the unisensory neurons examined within and outside the PPr.

When the response magnitude was compared between neurons in the PPr and its afferent regions (PPc and SIII), an interesting dichotomy was observed. The average response magnitude of bimodal neurons in the PPr (tactile 2.7±0.15; visual 2.7±0.18 mean spikes/trial) was similar to the responses of unisensory neurons in area SIII (2.4±0.23 mean spikes/trial) and to unisensory

responses of neurons in area PPc (3.1±0.29 mean spikes/trial), as depicted in Figure 6B (Table 1). However, the response of unisensory PPr neurons (Uni T 1.6±0.22; Uni V 1.5±0.27 mean spikes/trial) was 1.5-2 times less than the same unisensory responses obtained in the afferent areas (SIII and PPc). Statistical tests (ANOVA; Tukey tests) showed that the responses of bimodal neurons in the PPr and unisensory tactile neurons in SIII did not differ significantly than each other, and that both had a significantly higher magnitude of response as compared to the unisensory tactile responses of the PPr ($F(2,396)=11.65$; $p<0.0001$). Also, visual responses in the unisensory PPc did not differ significantly from those of bimodal neurons in the PPr, and both groups had a significantly greater magnitude of response as compared to unisensory visual neurons in the PPr ($F(2,388)=7.09$; $p = 0.001$). In summary, the responses of bimodal neurons in the PPr were similar in magnitude to those of unisensory neurons from its input regions of SIII and PPc, while these same unisensory neurons generated greater response magnitudes than their unisensory counterparts within the PPr.

Measures of response duration were also examined between the different cortical areas. In response to tactile stimulation, SIII neurons (38 ±1.78 mean ms) had a similar response duration to PPr bimodal neurons (39±1.19 mean ms), but were an average 10ms longer duration than unisensory tactile neurons in PPr (28±1.72 mean ms). With visual stimulation, PPc neurons (52±2.42 mean ms) had an average response duration that was 12ms longer compared to both bimodal (40±1.70 mean ms) and unisensory visual neurons (40±2.54 mean ms) in the PPr. These relationships are displayed in Figure 6C and the data summarized in Table 1. Statistical tests (ANOVA; post-hoc Tukey) showed that the response duration of SIII neurons and PPr bimodal neurons (to tactile stimulation) did not differ from each other, and that they were significantly longer than the average duration of unisensory tactile neurons in PPr

($F(2,396)=15.87$; $p<0.0001$). PPc neurons had a greater average response duration (to visual stimulation) than both bimodal and unisensory visual neurons in the PPr, which did not differ significantly from each other ($F(2,388)=8.06$; $p=0.0004$). Thus, the response duration of bimodal neurons in the PPr was similar to that of the unisensory neurons in area SIII, but PPc neurons showed a greater duration of response than either bimodal or unisensory neurons in the PPr.

Because areas SIII and PPc are sources of projections to PPr, it would be expected that response latency in the source areas would be shorter than those observed in the target. This expectation was confirmed by the data. The average response latencies to tactile or to visual stimulation were shorter in SIII (41±1.25 mean ms) and PPc (67±3.7 mean ms) than was measured for both unisensory (Uni T 53±1.33; Uni V 87±4.24 mean ms) and bimodal neurons (tactile 51±0.97; visual 87±4.24 mean ms) in the PPr. These results are illustrated in Figure 6D and summarized in Table 1. In response to tactile stimulation, SIII neurons responded, on average, 10ms faster than PPr bimodal neurons and 12ms faster than PPr unisensory tactile neurons. In response to visual stimulation, PPc neurons responded, on average, 20ms faster than PPr bimodal neurons and 37ms faster than PPr unisensory visual neurons. Statistical comparisons (ANOVA; Tukey tests) of SIII tactile response to both unisensory and bimodal PPr tactile responses showed that these differences were significant ($F(2,396)= 28.32$; $p<0.0001$). Similarly, PPc responses to visual stimulation showed significantly (ANOVA; Tukey tests) shorter latency than both bimodal and unisensory visual neurons in the PPr ($F(2,388)=22.39$; $p<0.001$). Thus the average response latencies of afferent areas SIII and PPc were shorter than any of the neuron types measured in the PPr.

Multisensory Integration of Multisensory Neurons in the PPr

The responses of individual unisensory neurons were not significantly changed by combined stimulation. On the other hand, bimodal multisensory neurons showed a range of changed responses to combined stimuli. The range of multisensory processing effects has been analyzed elsewhere in the brain (Avillac et al., 2007; Stein and Meredith, 1993; Stein and Stanford, 2008; Stein and Wallace, 1996; Wallace et al., 1992) and in synthetic neural networks (Lim et al., 2011) with respect to the proportions of multisensory neurons, the share of multisensory neurons that exhibit multisensory integration, and the magnitude of multisensory integration generated. In the present study, of the 225 PPr neurons identified as bimodal multisensory, 105 (47%) generated responses to combined stimulation that met the statistical criteria for demonstrating multisensory integration. Multisensory integration in bimodal PPr neurons ranged in magnitude from -100 to 296% (avg. absolute value = 69%). Using another measure of integrative magnitude, the percentage of integrative neurons exhibiting super-additive responses (response to combined stimulation greater than the sum of the responses to the separate unisensory stimuli) was 32% (34/105).

Subthreshold multisensory neurons were infrequently encountered in all the regions studied. However, by definition (see Methods), all subthreshold neurons exhibited multisensory integration. For PPr neurons that were activated by tactile stimulation, their spiking responses were significantly modified by combined stimulation (9%; 39/451) that ranged in magnitude from -100 to 238% (avg. absolute value = 22%). Visual PPr neurons which showed subthreshold multisensory responses (5%; 23/451) showed a range of multisensory integration from 35 to

217% (avg. = 55%). These subthreshold multisensory neurons tended to exhibit functional measures more akin to unisensory neurons than their multisensory counterparts. Specifically, tactile neurons with subthreshold multisensory responses had, on average, a spontaneous rate of 19.38±2.25 spikes/second, a response magnitude of 1.58±0.17 spikes/trial, a response duration of 29.89±1.9 ms, and a response latency of 51.58±1.16 ms. Visual neurons with subthreshold multisensory responses had an average spontaneous rate of 14.99±2.25 spikes/second, a response magnitude of 1.21±0.28 mean spikes/trial, a response duration of 36.03±3.4ms, and a response latency of 109.56±11.4ms. When compared with values from the other neuron types (see Table 1), all response measures of subthreshold multisensory neurons were similar to their unisensory counterparts, but these data could not be statistically confirmed due to small numbers.

Correlations Among Response Features and Multisensory Integration

To determine which response features of bimodal neurons might be predictive of their capacity to exhibit multisensory integration, the following correlations were tested with Pearson's correlation coefficient and Spearman's rho. For bimodal neurons in the PPr that demonstrated multisensory integration, values for spontaneous rate and response magnitude were plotted against the measures of multisensory integration exhibited by those same neurons. Spontaneous rate was found to have a significant negative linear correlation with the level of multisensory enhancement (Figure 7A) (Pearson's correlation $r=0.43$, $p=0.006$) and a significant positive linear correlation with the magnitude of multisensory depression (Figure 7B) (Pearson's $r = 0.43$, $p = 0.006$). In other words, bimodal neurons with lower spontaneous rates tended to exhibit greater levels of multisensory integration. These above described relationships were confirmed by Spearman's rho for enhancement ($\rho=-0.37$; $p=0.0004$) as well as for depression

(ρ=0.41; p=0.0075). Next, the response magnitudes to separate tactile or visual stimulation were examined in relation to the level of multisensory integration generated by their combination. These relationships are illustrated in Figure 8. Specifically, the response magnitudes to separate tactile (Pearson's r=-0.47, p<0.0001; Spearman ρ=-0.66, p<0.0001) or visual (Pearson's r=-0.34, p=0.0028; Spearman ρ=-0.52; p<0.0001) stimulation showed a significant negative correlation with multisensory enhancement, as plotted in Figures 8A-B.Similarly, the response magnitudes elicited by tactile (Pearson's r=0.47, p=0.006; Spearman ρ=0.38, p=0.031) or visual (Pearson's r=0.51, p=0.0079; Spearman ρ=0.52, p=0.006) stimulation produced a significant, but positive, linear relationship with multisensory depression. Thus, there is an inverse relationship between response magnitude of the components of a multisensory stimulus and the levels of multisensory integration their combination evoked.

Because the relationship between response magnitude elicited by the components of a multisensory stimulus and multisensory integration was similar to that seen between spontaneous rate and multisensory integration, the relative strength of these factors to contributions to multisensory enhancement and depression were compared with a multiple regression analysis. This treatment demonstrated that, for bimodal PPr neurons, tactile responsiveness (standardized partial correlation coefficient β = -0.44, p = 0.0035) and visual responsiveness (β = -0.10, p = 0.04) were larger contributors to multisensory enhancement when compared with spontaneous activity (β = 0.046, p =0.75). Similarly tactile (standardized partial correlation coefficient β = 0.35, p = 0.02) and visual (β = 0.60, p =0.012) responsiveness were larger contributors to multisensory depression when compared with spontaneous activity (β = -0.27, p =0.279). In summary, both sensory response magnitude and spontaneous rate were correlated with

multisensory integration (both enhancement and depression), but sensory response magnitude was more predictive of integration than spontaneous rate.

DISCUSSION

Using neurons recorded from ferret multisensory cortex that were presented a standard set of visual, somatosensory and combined visual-somatosensory cues, the present study sought to compare the functional properties of bimodal and unisensory neurons. These comparisons demonstrated that bimodal and unisensory neurons within PPr cortex were distinct from one another on essentially all of the features examined. Specifically, when compared to the properties of unisensory neurons, bimodal neurons had, on average, a significantly greater spontaneous discharge rate, greater response magnitude, greater response duration to tactile stimulation and decreased response latency to visual stimulation. Similar results are apparent as ancillary observations in a few other reports. In the ferret medial rostral suprasylvian sulcus, bimodal neurons exhibited a level of spontaneous activity that was more than double that of unisensory neurons (Keniston et al., 2009). Additionally, in monkey ventral intraparietal cortex, the raw data and figures show that response latency was shorter for bimodal neurons than for unisensory visual neurons (Avillac et al., 2007), although statistical comparisons were not made. Altogether, because these results were derived from different cortical areas and different species, distinctions between bimodal and unisensory neurons may represent a general property of the neocortex. Furthermore, since most studies of multisensory processing have focused almost exclusively on the integrative properties of multisensory neurons, the present findings represent a completely novel set of features by which bimodal and unisensory neurons can be distinguished.

The mechanisms underlying these functional differences between bimodal and unisensory neurons remain to be demonstrated. However, cortical neurons are not only heterogeneous in their distinctive discharge patterns, but also in morphology and the expression of voltage-gated ion channels (Bekkers, 2000; Storm, 2000; Sugino et al., 2006). For example, in some neurons, the membrane current most closely associated with spontaneous activity results from hyperpolarization-activated channels (Chan et al., 2004; Forti et al., 2006) (Bennett et al., 2000; Maccaferri and McBain, 1996; McCormick and Pape, 1990) while in other neuron types, spontaneous activity is dependent on a TTX-sensitive persistent sodium current that flows at voltages positive to -65mV (Bean, 2007; Bevan and Wilson, 1999; Do and Bean, 2003; Jackson et al., 2004; Raman and Bean, 1997; Raman et al., 2000; Taddese and Bean, 2002). Furthermore, layer 5 thick tufted neurons, which have distinctive membrane properties, exhibit both increased spontaneous activity as well as elevated response levels when compared with the other neurons in barrel (de Kock et al., 2007) or visual cortex (Groh et al., 2010). Whether any of these intrinsic factors are responsible for elevated spontaneous activity in bimodal neurons remains to be determined.

In addition to the influence of intrinsic neuronal properties, extrinsic features such as connectivity are also likely contributors to the distinctions between bimodal and unisensory neurons. Indeed, there is a robust literature describing differential inputs to laminar-specific neuron types (e.g., (Krook-Magnuson et al., 2012; Schubert et al., 2007; Thomson and Lamy, 2007), and it has been established that bimodal and unisensory neurons differentially distribute within and across the cortical laminae (Foxworthy, 2012). This same study showed that layer 6 neurons in the PPr were most likely to be unisensory and were also the least likely to receive convergent inputs from adjoining visual and somatosensory areas. On the other hand, layer 2-3

neurons were highly likely to be multisensory as well as receive convergent inputs from the afferent visual and somatosensory areas. Thus, differential connectivity appears to correlate with the unisensory and bimodal neurons identified in the PPr which, in turn, exhibit different activity levels.

During a recording session, because a single stimulus evoked different responses in the constituent bimodal and unisensory neurons of a region, these data also support the hypothesis that multisensory and unisensory information is processed in parallel as it passes through the local cortical circuit. Specifically, bimodal and unisensory neurons were found intermingled within each layer within the PPr, but bimodal neurons predominated in the layers 2/3 and 5, while unisensory neurons represented the majority of neurons in layer 6 (see previous chapter). For unisensory signals to be maintained through layer 6 indicates that unisensory information somehow remains segregated as it passes through the earlier levels of the circuit. This effect seems to be confirmed by the current finding that the signals processed by unisensory neurons are quantitatively and significantly different from their bimodal neighbors. Alternatively, it might be possible for a multisensory circuit perhaps to filter-out the inputs from a weaker modality, but this condition has not yet been proposed or observed, and the data do not suggest that one modality has weaker effects in the PPr than the other. Ultimately, these observations of co-extensive but distinct unisensory/multisensory functional features and circuits have serious implications for the interpretation of macroscopic measures of multisensory processing (such as EEG or fMRI, or computational models). In all forms of multisensory study, establishment of response levels to unisensory stimulation is an essential baseline measure. However, the present results demonstrate that it is no longer appropriate to assume that a given unisensory stimulus will evoke the same response from bimodal and unisensory neuronal subpopulations.

Correlates of Multisensory Integration and Inverse Effectiveness

Bimodal neurons have the capacity to integrate multisensory signals, while unsensory neurons, by definition, do not. Since bimodal neurons also exhibit elevated spontaneous rates and response levels (relative to their unisensory counterparts), the relationship between these features and multisensory integration was examined. For bimodal neurons, both response magnitude and spontaneous rate were correlated with the magnitude of multisensory integration. Specifically, bimodal neurons which exhibited vigorous sensory responsiveness to tactile or visual stimulation tended to generate low levels of multisensory integration while other neurons which displayed low levels of sensory-evoked activity were more likely to produce higher degrees of multisensory integration. Similarly, neurons with low levels of spontaneous activity tended to demonstrate the greatest degree of multisensory integration whereas different neurons with high spontaneous rates exhibited lower levels of multisensory integration. These relationships were observed for neurons that showed multisensory response enhancement (see also (Perrault et al., 2003), as well as those demonstrating multisensory response depression. Moreover, although both response magnitude and spontaneous rate were inversely correlated with the magnitude of multisensory integration, response magnitude was the better predictor of multisensory integration (Perrault et al., 2003; Stanford et al., 2005). That similar functional features co-vary with both response enhancement and depression (and affects unisensory neurons *as well)*, supports the notion that these contrasting effects actually fall along a broad continuum of response activity (Allman et al., 2009).

The described relationships between groups of highly (or weakly) responsive neurons and multisensory integration also correspond with a fundamental property demonstrated by individual multisensory neurons. Termed the "inverse effectiveness principle," individual

multisensory neurons tend to exhibit higher levels of multisensory integration when the separate components of the stimulus are minimally effective, while lower levels of integration tend to result from the combination of highly effective stimuli (Avillac et al., 2007; Kayser et al., 2005; Meredith and Stein, 1986; Perrault et al., 2003; 2005; Wallace et al., 1996). The present study extends this principle to populations of differentially sensitive bimodal neurons. Specifically, bimodal neurons that, as a group, showed low levels of response to separate visual and somatosensory stimulation, exhibited proportionally higher magnitudes of multisensory integration, while other neurons that were more highly activated by the separate-modality stimuli generated lower levels of multisensory integration when those same stimuli were combined. In addition, this group inverse effect was observed for neurons showing multisensory response enhancement as well as for those that generated response depression. To our knowledge, these are the first indications that inverse effectiveness applies to expressions of multisensory response depression.

Areal Comparisons of Response Properties

The results discussed thus far indicate that bimodal neurons have distinct functional properties compared to unisensory neurons within a given multisensory area. However, this raises the question as to whether bimodal neurons are distinct in these measures from unisensory neurons in general. When compared with unisensory neurons of the adjoining somatosensory area III (SIII) and the visual caudal posterior parietal cortex (PPc), bimodal neurons of the PPr exhibited higher spontaneous rates but similar response levels. Bimodal PPr neurons were also found to have a similar response duration compared to SIII neurons, although they exhibited a significantly shorter duration of response than PPc neurons. Additionally, all neurons (both

unisensory and bimodal) in PPr had a greater response latency than neurons in SIII and PPc, but this may have more to do with serial connectivity as discussed below. Given these observations, spontaneous rate appears to be the only feature that reliably distinguishes bimodal from unisensory neurons across different regions. Although this relationship has also been observed in another cortical region (MRSS; Keniston et al., 2008), further empirical comparisons of different multisensory regions are needed.

It has been demonstrated anatomically that the majority of somatosensory and visual inputs to PPr arrive from SIII and PPc, respectively (Chapter III), while comparatively few connections (~11%) arrive from thalamus. Thus, comparisons of response latency can provide an indication of serial cortical connectivity into and within the PPr. As predicted by the anatomical observations, measures of tactile and visual latency indicate that both SIII and PPc regions were activated prior to the PPr. In addition, PPr bimodal neurons were activated earlier by visual stimulation than their unisensory counterparts in PPr, suggesting that bimodal neurons, at least in part, may occupy an earlier segment of the PPr cortical circuit. In fact, the bimodal neurons are most concentrated in the supragranular layers of the PPr that directly receive the convergent SIII/PPc inputs, while the unisensory PPr neurons largely occur in L6, which is much later in the cortical circuit. These data are also consistent with the hypothesis, mentioned earlier, that multisensory and unisensory signals are processed in parallel as they transit the circuitry of the PPr.

Response variation to standardized stimulation

The present study has shown that a single external stimulus produces different responses in populations of bimodal and unisensory neurons of the PPr. Specifically, a given unisensory

stimulus (visual or somatosensory) elicited, on average, a significantly larger response in bimodal than in unisensory neurons. It is also important that a single set of combined stimuli (visual and somatosensory) produced a wide range of responses in bimodal neurons, with no response integration occurring in some, and response enhancement and depression occurring in others; an effect that was observed across the entire sample as well as within individual recording penetrations. These observations indicate that cortical bimodal neurons have distinct operational modes, much like that demonstrated for the brainstem (Perrault et al., 2005). Importantly, because these operational modes of multisensory neurons are independent of the stimulus features that are involved, (Perrault et al., 2005), it is unlikely that the present observations in cortical neurons would be substantially different if a larger set of stimulation parameters had been employed.

Despite representing part of the continuum between response enhancement and response depression, bimodal neurons that did not integrate multisensory information raise an important conceptual issue. Non-integrating bimodal neurons, despite having the ability to represent information from different sensory modalities, appear to respond to multisensory stimulation as they would to their preferred unisensory stimulus. Accordingly, it has been suggested (Sabes, 2011) that at least for some bimodal neurons, there is *competition* for representation of a sensory modality rather than integration. Alternatively, bimodal neurons with different integrative capacities may occupy distinct locations and perform distinct functions within a local circuit. This notion is supported by data from the previous chapter, that demonstrated a tendency for supragranular multisensory neurons to generate enhanced responses (relative to depressed responses) while infragranular neurons were more evenly distributed in their tendency to exhibit either enhanced or depressed responses. Furthermore, the magnitude of the integrated

multisensory responses (both enhanced and depressed) increased with increasing laminar depth. Because cortical layers each exhibit distinct connectional patters (both inputs and outputs), these data suggest that integrated multisensory information is processed and relayed in a laminar-dependent fashion.

Another feature of the examined sensory activity is that of response latency. Contributing factors to variation in response latency are differences in a neuron's position within the cortical circuit, its unisensory/bimodal status, and its responsiveness to a given sensory modality. The ability for neuron's latency to encode specific stimulus features has been demonstrated in auditory (Bizley et al., 2010; Brasselet et al., 2012; Nelken et al., 2005), visual (Gawne et al., 1996; Shriki et al., 2012), and somatosensory cortices (Panzeri and Diamond, 2010; VanRullen et al., 2005). In a multisensory region, a given bimodal neuron encodes response latency for two sensory modalities, and it is an intriguing possibility that these differential delays also encode information about the stimuli involved. These possibilities, however, remain to be examined.

SUMMARY AND CONCLUSIONS

While bimodal neurons have long been regarded as unique in their ability to integrate responses to multisensory stimuli, the present study has revealed completely novel set of features that also distinguish bimodal from unisensory neurons. When compared with neighboring unisensory neurons, bimodal cortical neurons exhibit significantly higher spontaneous discharge rates and greater magnitudes of response. These observations have important implications for understanding multisensory cortical processing. Because functionally distinct bimodal and unisensory neurons co-exist within a given cortical region, these data support the postulate that multisensory cortex operates as a parallel processor of unisensory and multisensory signals (see

also Foxworthy et al., 2012). Furthermore, because of intrinsic differences in sensitivity, a given multisensory stimulus can evoke different levels of response enhancement and response depression within different subsets of bimodal neurons; both of which follow the principle of inverse effectiveness. Ultimately, these results have serious implications for the interpretation macroscopic studies of multisensory processing, such as fMRI, EEG and computational simulations, because it can no longer be presumed that a given sensory stimulus evokes the same responses in multisensory neurons and their unisensory counterparts, nor do multisensory neurons process a particular stimulus combination in a uniform manner.

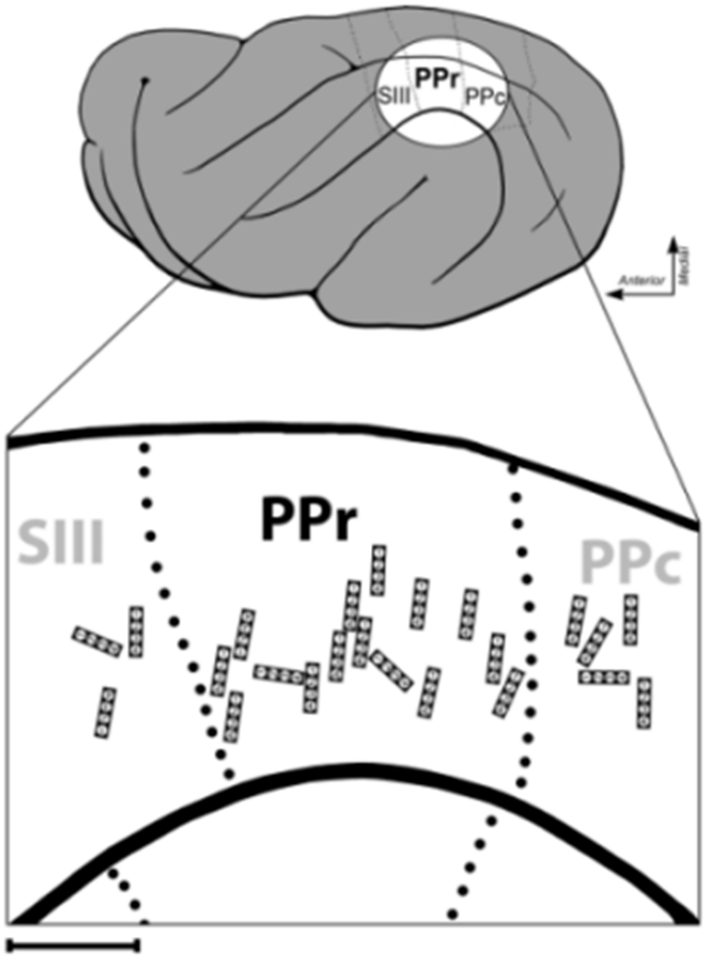

Figure 1. Summary of recording penetrations.

The lateral view of the ferret cortex indicates the three brain regions examined: somatosensory area III (SIII), the multisensory rostral posterior parietal cortex (PPr), and the visual caudal posterior parietal cortex (PPc). The expanded view shows the approximate location of all the recording sites as well as the orientation of the electrodes. Scale bar = 1mm.

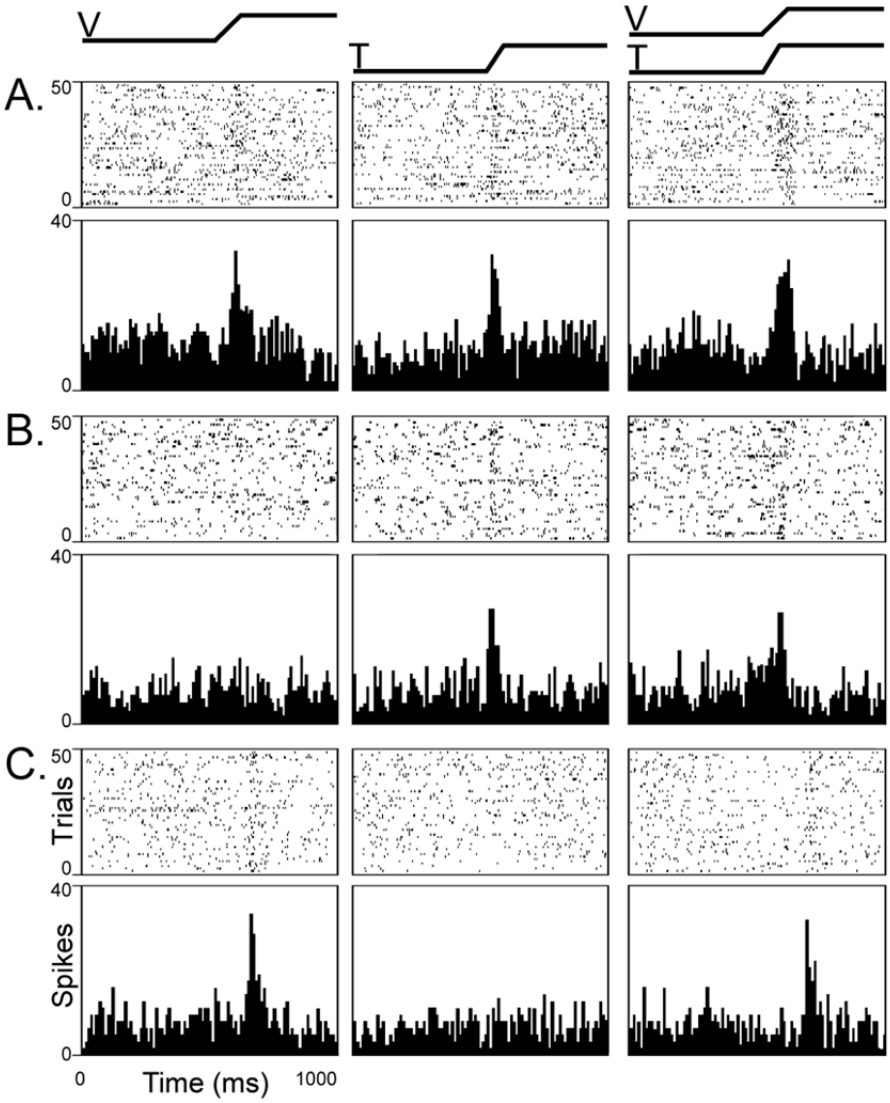

Figure 2. Sensory responses of PPr neurons.

Responses of typical bimodal (A), unisensory tactile (B) and unisensory visual (C) neurons in the PPr are depicted. All of these responses were elicited by the same set of visual and somatosensory stimuli (indicated by the traces at top; V=visual, T=tactile), and were recorded simultaneously. In (A), the bimodal neuron responded to visual and tactile stimulation presented alone and its response to combined stimulation was significantly greater than that elicited by either separate stimulus. In part (B), the neuron did not respond to the visual stimulus, but responded to the tactile stimulation presented alone; this response was not significantly altered when the visual-tactile stimuli were combined. In part (C) the unisensory visual neuron (C) showed a suprathreshold response only to the visual stimulus presented alone that was not significantly changed when combined stimuli were. In each of the panels, spontaneous activity was evaluated in the 500ms period before stimulus onset. Raster: 1 dot = 1 spike; 50 trials. Histogram: 10ms time bins.

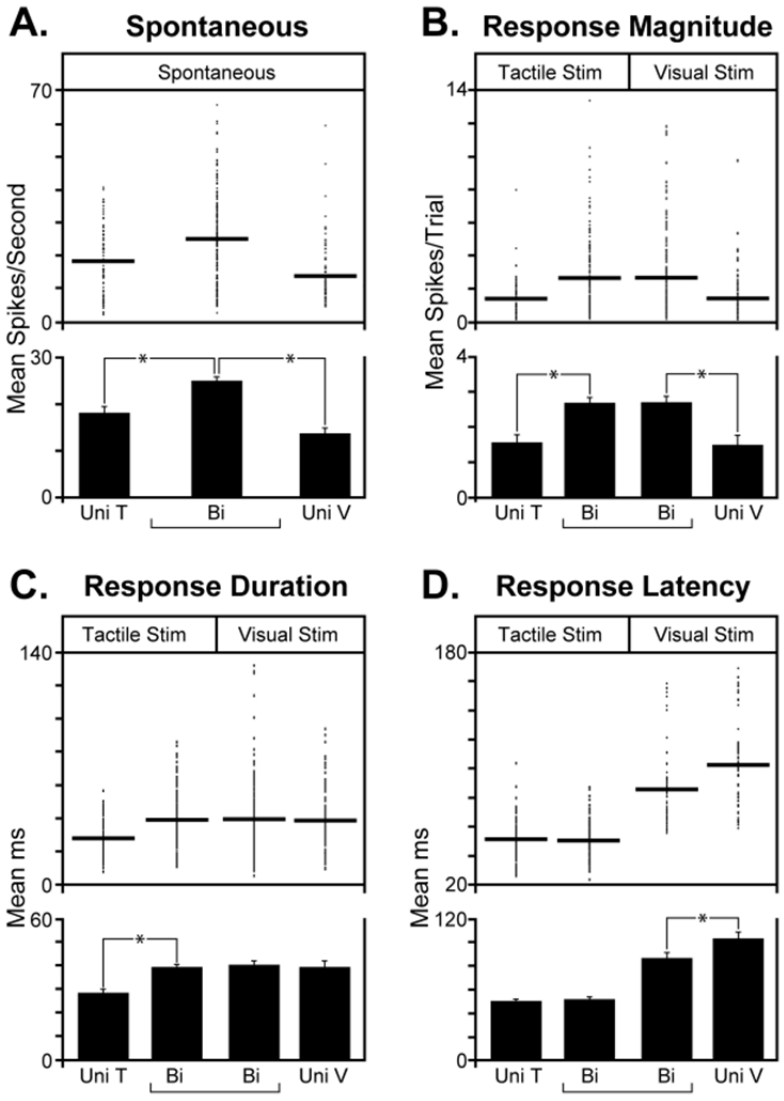

Figure 3. Functional properties of bimodal neurons are distinct from those of unisensory neurons in the PPr.

Each panel (A-D) shows a dot plot (individual neuron data=dot; population mean=horizontal line) with a summary bar graph (mean ± se) below; significant differences are indicated by an asterisk. (A) The rate of spontaneous activity for bimodal (Bi) neurons was significantly greater than that of unisensory tactile (Uni T) or unisensory visual (Uni V) neurons. (B) The response magnitude of bimodal neurons was significantly greater to tactile or visual stimulation than that of unisensory tactile or visual neurons, respectively. (C) The average response duration of bimodal neurons to tactile stimulation was significantly greater than that of unisensory tactile neurons, but the bimodal visual response duration did not differ significantly that of unisensory visual neurons. (D) The response latency to tactile stimulation did not significantly differ between bimodal and unisensory tactile neurons, but bimodal neurons did have significantly shorter average response latency than unisensory visual neurons.

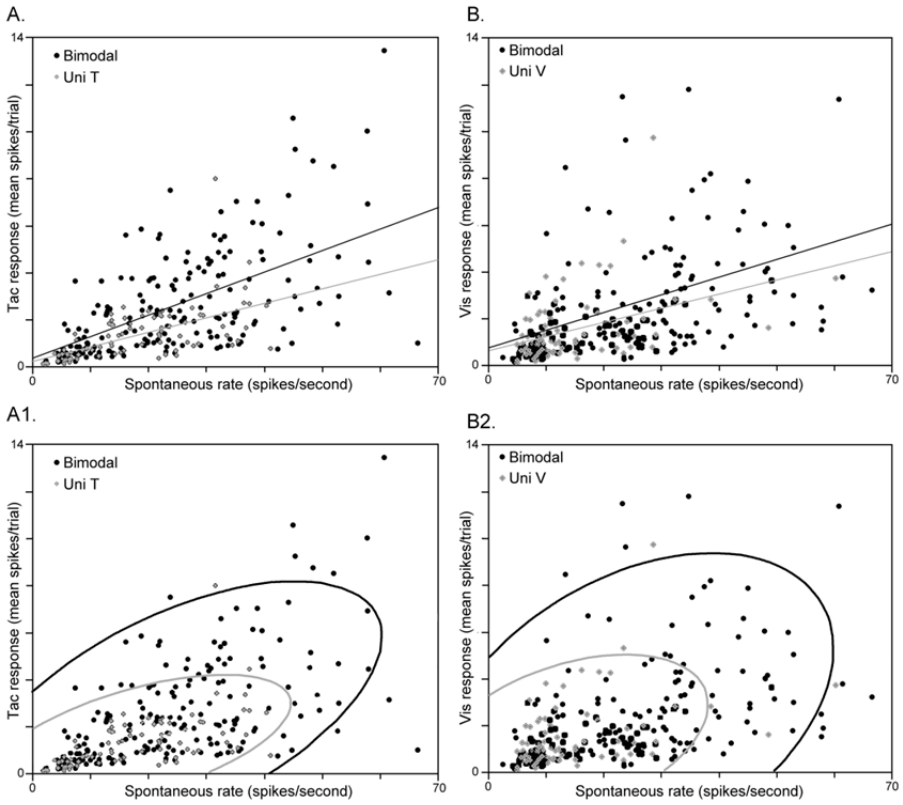

Figure 4. Correlations of spontaneous rate and response magnitude for bimodal and unisensory PPr neurons.

The scatterplots shows the relationship between spontaneous rate and sensory response magnitude for bimodal neurons (black dots) and unisensory neurons (gray symbols). The lines in the upper row of graphs indicate the linear line of best fit for bimodal (black) and unisensory (gray) neurons. The curves in the bottom graphs represent 95% confidence ellipsoids for bimodal (black) and unisensory neurons (gray). (A) With tactile stimulation, both bimodal (Pearson's correlation, $r = 0.57$; $p<0.0001$) and unisensory tactile neurons ($r = 0.57$; $p<0.0001$) showed a significant positive linear correlation between spontaneous rate and response magnitude. (A1) The correlation in (A) was confirmed by a statistical test that does not depend on the existence of a linear relationship between the variables (Spearman's rho; $\rho=0.60$; $p<0.0001$) (B) For visual stimulation, both bimodal (Pearson's correlation, $r = 0.39$; $p<0.0001$) and unisensory visual ($r = 0.41$; $p = 0.0002$) neurons showed a significant positive linear correlation between spontaneous rate and response. (B1) The correlation in (B) was confirmed by Spearman's rho ($\rho=0.44$; $p<0.0001$)

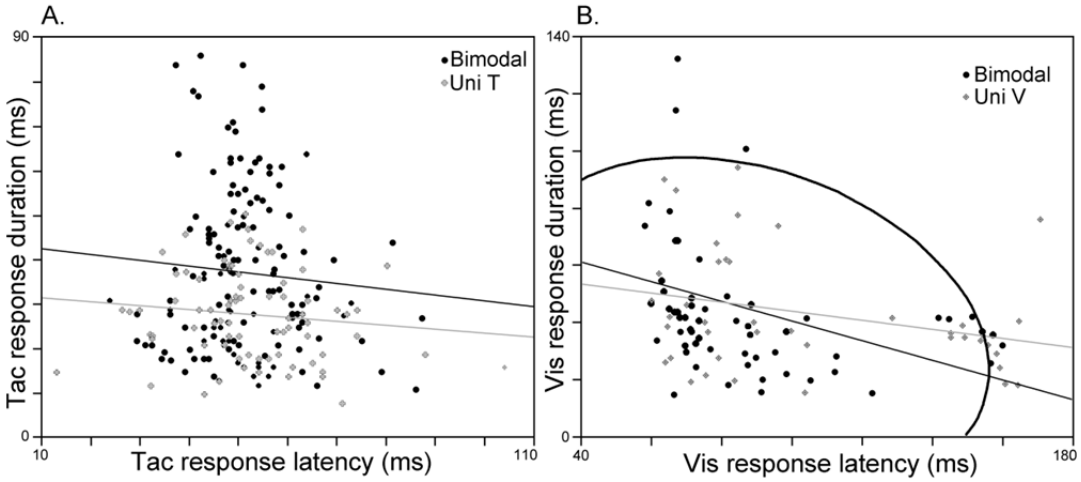

Figure 5. Response latency correlated with response duration for visual but not for tactile responses in bimodal neurons.

The scatterplots show the relationship between response latency and response duration for bimodal neurons (black dots) and unisensory neurons (gray symbols). The lines indicate the linear line of best fit for bimodal (black) and unisensory (gray) neurons. Where Spearman's rho tests were significant, 95% density ellipsoids are indicated with curved lines (A) For tactile stimulation, no significant correlation (Pearson's correlation) was found between tactile response latency and tactile response duration for either bimodal (black dots, black line; $r = -0.08$; $p = 0.33$), or unisensory tactile neurons (grey +, grey line; $r = -0.13$; $p = 0.24$). These results were consistent with those produced by the Spearman Rho test of correlation. (B) With visual stimulation, a significant negative linear correlation was found between visual response latency and visual response duration for bimodal neurons (Pearson's correlation, $r = -0.34$; $p = 0.0088$; Spearman $\rho=-0.54$, $p<0.0001$). On the other hand, no significant correlation was found for these measures in unisensory visual neurons (Pearson $r = -0.29$; $p =0.65$; Spearman $\rho=-0.29$, $p=0.061$).

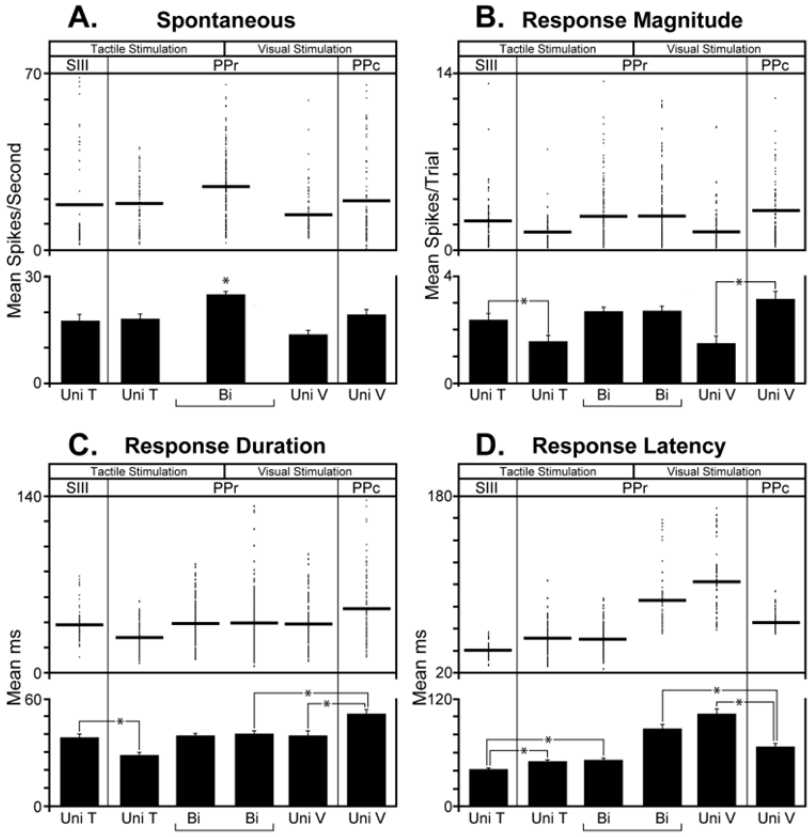

Figure 6. Functional properties of neurons in areas SIII, PPr, and PPc.

Each panel (A-D) shows a dot plot (individual neuron data=dot; population mean=horizontal line) with a summary bar graph (mean ± se) below; significant differences are indicated by an asterisk. Differences among data from PPr neurons already illustrated in Figure 3 are not depicted here. Data from unisensory tactile neurons of SIII are displayed on the left side of the graphs; data from the unisensory visual neurons of the PPc are displayed on the right side of the graphs. (A) The spontaneous rate of bimodal (Bi) neurons in PPr was found to be significantly higher than that of any other group. (B) Average response magnitudes were found to be similar between bimodal PPr neurons and the unisensory neurons of SIII and PPc. However, the average magnitude of SIII neurons was significantly higher than that of the unisensory tactile (Uni T) neurons in PPr, and PPc neurons had a significantly greater response magnitude than the unisensory visual (Uni V) neurons of the PPr. (C) Visual neurons of the PPc had a greater duration of response than either the bimodal or unisensory visual neurons within the PPr. The somatosensory neurons of SIII on the other hand, had similar average response duration to PPr bimodal neurons, but had a significantly greater duration than the PPr unisensory tactile neurons. (D) Both SIII and PPc neurons had shorter response latencies, to tactile and visual stimulation respectively, than either the bimodal or unisensory neurons of the PPr.

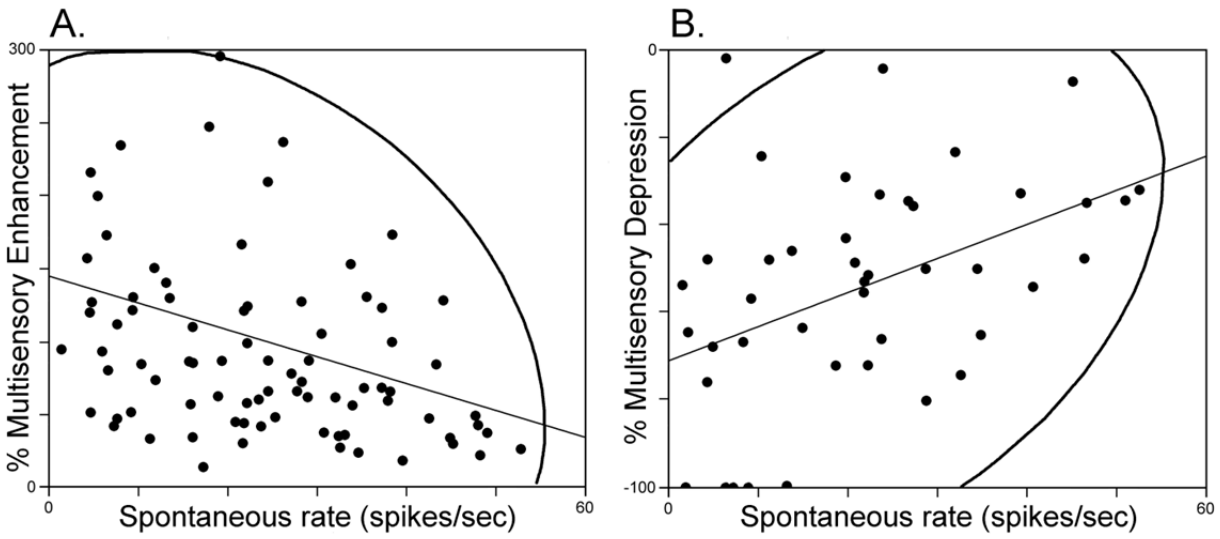

Figure 7. Spontaneous rate correlates with levels of multisensory enhancement and depression in bimodal PPr neurons.

The scatterplots show the relationship between spontaneous rate and the magnitude (percent) of multisensory enhancement (A) or multisensory depression (B) for bimodal neurons (black dots) that met the criteria for demonstrating multisensory integration. The lines indicate the linear lines of best fit. Curved lines indicate the 95% density ellipsoids. (A) The spontaneous rate of bimodal neurons showed a significant negative linear correlation with the magnitude of multisensory enhancement generated by these same neurons in response to combined stimulation (Pearson's correlation; $r = -0.31$; $p = 0.0044$). This correlation was confirmed by Spearman's rho (ρ=-0.37; p=0.0004). (B) The spontaneous rate of bimodal neurons showing multisensory depression demonstrated a significant positive linear correlation with the magnitude of multisensory depression (Pearson's correlation; $r = 0.43$; $p = 0.006$). This correlation was confirmed with Spearman's rho (ρ=0.41; p=0.0075).

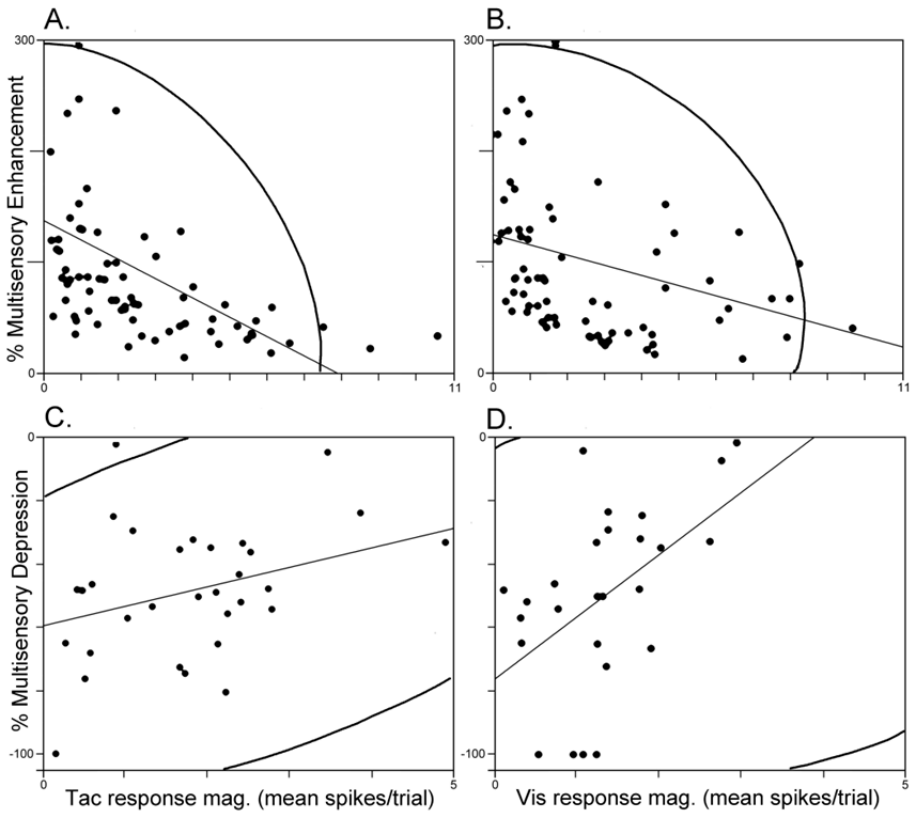

Figure 8. Response magnitude correlates with multisensory enhancement and depression. The scatterplots show the relationship between sensory response magnitude and the magnitude (percent) of multisensory enhancement (A, B) or multisensory depression (C, D) for bimodal neurons (1 dot=1 neuron) that met the criteria for demonstrating multisensory integration. The lines indicate the linear lines of best fit. Curved lines represent 95% density ellipsoids. (A) The relationship of tactile response magnitude to multisensory enhancement showed a significant negative relationship ($r = -0.47$; $p<0.0001$), whereby bimodal neurons with lower tactile response magnitudes tended to have a higher percent multisensory enhancement. This correlation was confirmed by Spearman's rho ($\rho=-0.66$; $p<0.0001$). (B) A significant negative linear relationship was found between visual response magnitude and multisensory enhancement ($r=-0.34$; $p=0.0028$). Thus, bimodal neurons with weaker visual responses tended to generate higher levels of multisensory enhancement. This relationship was confirmed by Spearman's rho ($\rho=-0.52$; $p<0.0001$). (C) The relationship of tactile response magnitude with multisensory depression showed a significant positive linear relationship ($r = 0.47$; $p=0.006$), such that bimodal neurons with weaker responses to tactile stimulation tended to show greater levels of multisensory depression. This relationship was confirmed by Spearman's rho ($\rho=0.38$; $p=0.031$). (D) A significant positive linear relationship was found between visual response magnitude and multisensory depression ($r=0.51$; $p =0.0079$), where bimodal neurons with relatively weak visual responses tended to show greater levels of multisensory depression. This relationship was confirmed by Spearman's rho ($\rho=0.52$; $p=0.006$).

Table 1. Summary of data for PPr, SIII and PPc

		Stimulus					
		Tactile			**Visual**		
Category	**Spontaneous**	**Magnitude**	**Duration**	**Latency**	**Magnitude**	**Duration**	**Latency**
PPr Bi	25.12 ± 0.93	2.67±0.15	39.4±1.19	50.8±0.97	2.69±0.18	40.4±1.70	86.7 ±4.24
PPr Uni T	18.27 ± 1.38	1.56±0.22	28.4±1.72	52.5±1.33	NA	NA	NA
PPr Uni V	13.68 ± 1.40	NA	NA	NA	1.50±0.27	39.6±2.54	103.6±5.02
SIII Uni T	17.72 ± 1.82	2.35±0.23	38.5±1.78	40.7±1.25	NA	NA	NA
PPc Uni V	19.41 ± 1.54	NA	NA	NA	3.12±0.29	51.5±2.42	66.5 ± 3.7
Mean ± SE							

Spontaneous = spontaneous rate in spikes/second; Magnitude = response magnitude in mean spikes/trial; Duration = average response duration in milliseconds; Latency = average time from stimulus to response onset in milliseconds; '±' = standard error; NA=not applicable.

CHAPTER V

GENERAL DISCUSSION

The present experiments examined fundamental features of neuronal processing and organization of a multisensory cortical area, the ferret posterior parietal cortex (PPr). A detailed discussion of the results of these experiments are described in each of the associated Chapters (II-IV) and what follows is a broad overview of the significance of this work. Four main hypotheses were tested in these experiments. First, since convergence of inputs onto individual neurons from separate sensory modalities is the first requisite step in the generation of multisensory neurons, it was hypothesized that overlap of extrinsic inputs from somatosensory (identified in Chapter II) and visual cortical sources would correspond with the presence of multisensory neurons in the PPr (evaluated in Chapter III). Second, given the differential distribution of converging inputs, it was hypothesized that multisensory neurons and properties would be heterogeneously distributed across the layers and that the laminar organization of PPr would differ from the commonly described pattern observed in primary sensory cortices (evaluated in Chapter III). Third, multisensory neurons and multisensory properties were heterogeneously distributed within and across layers, suggesting that unisensory and multisensory signals are processed in parallel as they pass through the PPr, this hypothesis is evaluated in Chapter III. Finally, given that bimodal and unisensory neurons coexist within a given multisensory area, that many bimodal neurons do not perform multisensory integration, and that many neurons previously identified as unisensory can perform multisensory integration (e.g., subthreshold multisensory neurons; reviewed in (Meredith et al., 2011), it would be expected that bimodal neurons provide a function that unisensory neurons do not. To test this last

hypothesis, the functional properties of bimodal and unisensory neurons were compared (Chapter IV). The above hypotheses were confirmed by the experiments presented in this thesis as described below.

As initially postulated, the laminar distribution of axon terminals from somatosensory and visual inputs corresponded with laminae that demonstrated a high proportion of multisensory neurons. Chapter II and Chapter III identified that the main sources of anatomical projections from distinct sensory modalities to the PPr arise from somatosensory area SIII and visual area PPc. Examination of the pattern of axon terminations from tracer injections, revealed that both areas preferentially targeted layers 2-3 of the PPr. Laminar recordings performed in PPr revealed that these layers contained a preponderance of multisensory neurons, thus matching the expectation that the overlap of projections from SIII and PPc would correlate with the presence of multisensory neurons. These observations are consistent with the notion that projections from SIII and PPc converge to generate the multisensory responses observed in layers 2-3 of the PPr. This is further supported by the observation that the somatosensory and visual receptive fields of the PPr (Manger et al., 2002) were essentially a superimposition of the receptive fields observed in visual area PPc (Manger et al., 2002) and somatosensory area SIII (Chapter SII). Additionally, the latency of responses in SIII and PPc were shorter than for those in PPr (Chapter IV), again consistent with the arrangement that these cortical areas generate sensory responses in the PPr. Collectively, these observations indicate that the overlap of the different cortico-cortical projections to the PPr are consistent with the generation of the multisensory responses observed in the PPr.

This arrangement of inputs and multisensory responses suggests that the laminar organization of the PPr is distinct from that of the well-examined primary unisensory areas. First,

the PPr has a reduced layer 4, representing only 8.5% of the cortical thickness as compared to primary sensory cortices in which layer 4 was found to represent up to 21% of the cortical thickness. Furthermore, the PPr does not receive input from principal thalamic nuclei (Chapter III), and thus does not receive information directly relayed from the periphery through the thalamus to the cortex. Ultimately, the preponderance of inputs carrying sensory information to the PPr arises not from thalamus, but from cortical areas that target not layer 4, but layers 2-3 (Chapter III). In fact, thalamic inputs represented only 11% of the total inputs to PPr whereas the other 89% arose from cortical sources. Collectively these results show that the laminar organization of the PPr is distinct from primary sensory cortices which receive inputs from principal thalamic nuclei that preferentially target layer 4 (and lower layer 3) and have a relatively expanded layer 4 (for review (Douglas and Martin, 2004; Thomson and Lamy, 2007)).

The heterogeneous distribution of multisensory neurons and multisensory properties both within and across layers, suggests that unisensory and multisensory signals are processed in parallel as they pass through the PPr. Corresponding to the high degree of input convergence in layers 2-3 was a high proportion of multisensory neurons in those layers. In turn, these predominantly multisensory layers projected to extrinsic cortical areas as well as locally to layer 5, which is known to connect with multisensory subcortical structures (Chapter III). In contrast, layer 6 of the PPr received the lowest amount of converging extrinsic inputs from SIII and PPc and the smallest projection from multisensory layers 2-3. Layer 6 neurons also exhibited the highest laminar proportion of unisensory neurons that, in turn, connect with other unisensory structures (Chapter III). Furthermore, the experiments in Chapter IV show that bimodal and unisensory neurons process not only multisensory, but also unisensory signals in a distinct manner. This differential distribution of unisensory and multisensory connections and functions

indicates that unisensory and multisensory signals are processed in parallel as they pass through the PPr.

As previously mentioned, it was hypothesized that bimodal and unisensory neurons would differ in their functional properties. In fact, bimodal and unisensory neurons within the PPr differed on essentially all of the functional features measured. Specifically, when compared to unisensory neurons in the PPr, bimodal neurons had a significantly higher spontaneous firing rate, greater response magnitude, greater response duration to tactile stimulation, and decreased response latency to visual stimulation (Chapter IV). Thus bimodal neurons differ from unisensory neurons within a given multisensory area. The functional differences between bimodal and unisensory neurons within the PPr are of particular import, because they distinguish bimodal from unisensory neurons in a way that does not depend on multisensory integration. Previously, the ability to perform multisensory integration has been assumed to be the difference between these neuron types. As the current studies were the first to systematically compare the functional properties of bimodal and unisensory neurons, it is unknown whether these properties represent fundamental differences between bimodal and unisensory neurons in all multisensory areas. Thus, similar comparisons should be made for both cortical and subcortical multisensory areas.

In summary, the experiments contained herein demonstrate: that for a cortical multisensory region, multisensory responses are likely to be driven by cortico-cortical connections; that the laminar organization of a multisensory cortex is distinct from that of primary sensory cortices; that multisensory and unisensory information are processed in parallel within a multisensory region; and finally, that bimodal and unisensory neurons have distinct

functional properties that were previously unexamined and unknown. Future directions for multisensory research are derived from these conclusions.

Future Directions

The present studies are the first systematic structural-functional examination of the laminar features of a multisensory cortex and also the first to compare the functional properties of bimodal and unisensory neurons. As previously discussed, most studies of unisensory processing use only unisensory stimuli, while most studies of multisensory processing focus only on the features of identified multisensory neurons. Thus, it is unknown whether the present results represent a unique laminar organization of all multisensory cortices, or whether the properties observed are specific to the ferret PPr. Additionally, while other studies have defined distinct operational modes for bimodal neurons (Perrault et al., 2003; 2005), the present study is the first to show that unisensory and bimodal neurons differ from each other in their functional properties. Therefore, a logical next step would be to repeat these experiments in other multisensory areas to show whether the observations in the present study are, applicable to all multisensory regions, and possibly represent a ubiquitous plan of multisensory cortical organization and function.

The studies described herein utilized recording electrodes with recording contacts which were vertically spaced by 200μm intervals – this allowed for the sampling of many neurons in infragranular and supragranular layers, but because of the small size of layer 4 (~85μm), responses in this layer could not be resolved. Therefore, to evaluate layer 4 function, future laminar analyses of multisensory regions, including the PPr, should utilize an electrode with recording contacts that are more closely spaced together. An electrode that exhibits a vertical

recording contact spacing of 50μm would allow the responses of layer 4 neurons to be identified at last once per penetration. In addition, Simultaneous recording of all the laminae using this higher density electrode configuration would also allow the laminar current source density (CSD) profile of sensory inputs into a multisensory cortical region to be identified. As CSD analysis is a measurement of transmembrane current flow across neurons in the different layers, it would allow for identification of the layer(s) which first receive synaptic input evoked by a sensory stimulus, as well as the time course and laminar distribution of ensuing components of the response. Combining this technique with spike sorting of neuronal recordings, to characterize individual neurons as unisensory or multisensory, would allow for a fine scale resolution of where sensory inputs first arrive in the PPr as well as an indication of where in the laminar circuitry inputs are first combined to generate bimodal neurons. Ultimately, these results are important for the identification of multisensory processing within broad areal processing schemes as well as feedforward/feedback functions among them.

Given the heterogeneous distribution of bimodal neurons within a multisensory area, and their different response characteristics compared to unisensory neurons, the present experiments have established that it is likely that these neuron types exhibit connectional and intrinsic differences. These differences can be reflected in a neuron's morphology, and recent experiments have demonstrated that juxtasomal recording of single neurons, followed by labeling of the neuron with biocytin can accurately distinguish different morphological types of neurons and their typical spiking behavior to sensory stimulation (de Kock et al., 2007; Groh et al., 2010). It would be informative to apply the same or similar (i.e. intracellular recording followed by biocytin filling) techniques to multisensory cortex to determine if bimodal and unisensory neurons are morphologically distinct classes of neurons and to additionally investigate whether

there are subclasses of bimodal neurons which also have distinct morphology. In light of the fact that bimodal neurons have distinct operational modes, as identified in this, and other studies (Perrault et al., 2003; 2005), it seems likely that the distinct operational modes of different types of bimodal neurons will be reflected in their morphology. This technique also has the additional advantage of precisely measuring the spiking response latency and magnitude of sensory responses. Thus, if unisensory and bimodal neurons are recorded from in each layer, such recordings would provide data as to which neurons fire action potentials first to a sensory stimulus. This is important because neurons must reach suprathreshold activation in order to fire spikes and elicit responses from other neurons in a local circuit. While the CSD data from the experiments above would show where synaptic inputs first arrive, this does not necessarily mean that action potentials are first produced at this site. To determine the information flow through a laminar circuit evoked by sensory stimulation, it is important not only to determine where inputs first arrive (as in the CSD analysis), but also the relative latency of specific neuron types (by lamina). This is especially important in light of the fact that the present experiments demonstrate parallel processing of unisensory and multisensory stimuli within the PPr. The laminar layout of these coexistent circuits may not be identical and are likely subserved by different cell types. Thus, results from these experiments would add to the data obtained in laminar CSD recordings and would have the additional benefit of potentially identifying distinct classes of neuron types which are sequentially activated (by sensory and multisensory stimuli) in the laminar circuitry of the PPr.

As previously mentioned in this thesis, the role of multisensory and unisensory neurons within a multisensory area in driving specific behaviors remains unknown. The present experiments have identified organizational and functional properties of neurons in a multisensory

area, but to determine how these properties contribute to behavior, a behavioral role of the ferret PPr must be identified. Recent studies of the homologous primate ventral intraparietal area (VIP) have demonstrated a technique by which aspects of the behavioral function of the ferret PPr could be elucidated. These experiments (Cooke et al., 2003; Kaas et al., 2011) utilized 500ms trains of electrical pulses in the VIP of awake animals, with increasing levels of simulation current until a movement was observed. These experiments found that the electrical stimulation produced a set of movements (eye blinking, squinting, rotation of the head, etc.) consistent with movements expressed during startle and avoidance. Similar results were obtained when a puff of air was applied to the side of the face. Therefore, a logical first step in determining the behavioral function of the ferret PPr would be to repeat similar stimulation experiments in the ferret. If similar defensive behaviors are observed, these behavioral responses could then be correlated to spiking activity in a second set of experiments. This could be accomplished by recording from a population of PPr neurons in an awake, restrained ferret while providing either: non-moving tactile stimulation to the face (such as an air-puff), visual stimulation consistent with movement towards the face (movement of the tactile stimulating arm towards the ferret's face without touching it), or combined visual-tactile stimulation (movement of the tactile stimulating arm with an air puff at the end of its travel). If these stimuli produce behavioral responses, the spiking activity of the population of unisensory and bimodal neurons in the PPr could then be correlated to the presentation of the unisensory and multisensory stimulation conditions. However, since a given behavior elicited by physical stimuli presented to an awake animal may not be dependent on PPr, a third study would be conducted to determine if a functionally intact PPr is required for the observed behavioral outcomes. This could be accomplished by placing cooling coils on the PPr, thus deactivating its neuronal activity, and repeating the sensory

stimulation experiments. If deactivation of the PPr abolishes the behavioral responses, this would be a strong indication that the PPr is directly involved. A caveat to these specific experiments (involving defensive movements) is that primates and carnivores are separated by millions of years of evolution and have both independently developed an expanded parietal cortex as discussed in Chapter III, it cannot therefore, be assumed a priori, that these seemingly similar cortical areas provide the same function in both species. Nevertheless, the electrical stimulation procedure should give an indication as to the function of the ferret PPr, whether similar to, or different than the primate VIP. Once these results are known, behavioral tests matched with electrophysiology, such as in the example above, can be devised to determine the relationship between bimodal and unisensory neuron spiking and the behavioral role of the PPr. Similarly, cooling experiments will provide a necessary control to determine whether the PPr is directly involved in whatever behavioral outcome is elicited by electrical stimulation of the PPr and by presentation of sensory stimuli. These experiments would be critical for understanding the behavioral role of the ferret PPr, and would provide a model in which the different spiking behavior of bimodal and unisensory neurons can be correlated to a behavioral outcome. As one of the major goals of neuroscience research is to explain how behavior and perception arise from neuronal activity, these experiments would provide insight into a fundamental aspect of the endeavor of scientific research.

LIST OF REFERENCES

Adrian, E. D. (1940). "Double representation of the feet in the sensory cortex of the cat." J Physiol 98: 16p.

Alais D, Newell FN, Mamassian P. 2010. Multisensory processing in review: from physiology to behaviour. Seeing Perceiving 23(1):3-38.

Albus K, Donate-Oliver F. 1977. Cells of origin of the occipito-pontine projection in the cat: functional properties and intracortical location. Exp Brain Res 28(1-2):167-174.

Allman BL, Meredith MA. 2007. Multisensory processing in "unimodal" neurons: cross-modal subthreshold auditory effects in cat extrastriate visual cortex. J Neurophysiol 98(1):545-549.

Allman BL, Bittencourt-Navarrete RE, Keniston LP, Medina AE, Wang MY, Meredith MA. 2008. Do cross-modal projections always result in multisensory integration? Cereb Cortex 18(9):2066-2076.

Allman BL, Keniston LP, Meredith MA. 2008b. Subthreshold auditory inputs to extrastriate visual neurons are responsive to parametric changes in stimulus quality: sensory-specific versus non-specific coding. Brain Res 1242:95-101.

Allman BL, Keniston LP, Meredith MA. 2009. Not just for bimodal neurons anymore: the contribution of unimodal neurons to cortical multisensory processing. Brain Topogr 21(3-4):157-167.

Alvarado JC, Vaughan JW, Stanford TR, Stein BE. 2007. Multisensory versus unisensory integration: contrasting modes in the superior colliculus. J Neurophysiol 97(5):3193-3205.

Amassian VE, Devito RV. 1954. Unit activity in reticular formation and nearby structures. J Neurophysiol 17(6):575-603.

Anastasio TJ, Patton PE. 2003. A two-stage unsupervised learning algorithm reproduces multisensory enhancement in a neural network model of the corticotectal system. J Neurosci 23(17):6713-6727.

Arikuni T, Kubota K. 1986. The organization of prefrontocaudate projections and their laminar origin in the macaque monkey: a retrograde study using HRP-gel. J Comp Neurol 244(4):492-510.

Atencio CA, Sharpee TO, Schreiner CE. 2009. Hierarchical computation in the canonical auditory cortical circuit. Proc Natl Acad Sci U S A 106(51):21894-21899.

Avanzini G, Broggi G, Franceschetti S, Spreafico R. 1980. Multisensory convergence and interaction in the pulvinar-lateralis posterior complex of the cat's thalamus. Neurosci Lett 19(1):27-32.

Avendano C, Rausell E, Perez-Aguilar D, Isorna S. 1988. Organization of the association cortical afferent connections of area 5: a retrograde tracer study in the cat. J Comp Neurol 278(1):1-33.

Avillac M, Ben Hamed S, Duhamel JR. 2007. Multisensory integration in the ventral intraparietal area of the macaque monkey. J Neurosci 27(8):1922-1932.

Bajo VM, Nodal FR, Bizley JK, King AJ. 2010. The non-lemniscal auditory cortex in ferrets: convergence of corticotectal inputs in the superior colliculus. Front Neuroanat 4:18.

Bakola S, Gamberini M, Passarelli L, Fattori P, Galletti C. 2010. Cortical connections of parietal field PEc in the macaque: linking vision and somatic sensation for the control of limb action. Cereb Cortex 20(11):2592-2604.

Baldwin, M. K., P. Wong, et al. (2011). "Superior colliculus connections with visual thalamus in gray squirrels (Sciurus carolinensis): evidence for four subdivisions within the pulvinar complex." J Comp Neurol **519**(6): 1071-1094.

Barraclough NE, Xiao D, Baker CI, Oram MW, Perrett DI. 2005. Integration of visual and auditory information by superior temporal sulcus neurons responsive to the sight of actions. J Cogn Neurosci 17(3):377-391.

Bean BP. 2007. The action potential in mammalian central neurons. Nat Rev Neurosci 8(6):451-465.

Bekkers JM. 2000. Distribution and activation of voltage-gated potassium channels in cell-attached and outside-out patches from large layer 5 cortical pyramidal neurons of the rat. J Physiol 525 Pt 3:611-620.

Bell AH, Meredith MA, Van Opstal AJ, Munoz DP. 2005. Crossmodal integration in the primate superior colliculus underlying the preparation and initiation of saccadic eye movements. J Neurophysiol 93(6):3659-3673.

Beloozerova IN, Sirota MG. 2003. Integration of motor and visual information in the parietal area 5 during locomotion. J Neurophysiol 90(2):961-971.

Benevento LA, Fallon J, Davis BJ, Rezak M. 1977. Auditory--visual interaction in single cells in the cortex of the superior temporal sulcus and the orbital frontal cortex of the macaque monkey. Exp Neurol 57(3):849-872.

Bennett BD, Callaway JC, Wilson CJ. 2000. Intrinsic membrane properties underlying spontaneous tonic firing in neostriatal cholinergic interneurons. J Neurosci 20(22):8493-8503.

Bevan MD, Wilson CJ. 1999. Mechanisms underlying spontaneous oscillation and rhythmic firing in rat subthalamic neurons. J Neurosci 19(17):7617-7628.

Bizley, J. K., F. R. Nodal, et al. (2005). "Functional organization of ferret auditory cortex." Cereb Cortex 15(10): 1637-1653.

Bizley, J. K., F. R. Nodal, et al. (2007). "Physiological and anatomical evidence for multisensory interactions in auditory cortex." Cereb Cortex 17(9): 2172-2189.

Bizley JK, Walker KM, King AJ, Schnupp JW. 2010. Neural ensemble codes for stimulus periodicity in auditory cortex. J Neurosci 30(14):5078-5091.

Brasselet R, Panzeri S, Logothetis NK, Kayser C. 2012. Neurons with stereotyped and rapid responses provide a reference frame for relative temporal coding in primate auditory cortex. J Neurosci 32(9):2998-3008.

Bremmer F, Klam F, Duhamel JR, Ben Hamed S, Graf W. 2002. Visual-vestibular interactive responses in the macaque ventral intraparietal area (VIP). Eur J Neurosci 16(8):1569-1586.

Brett-Green B, Fifkova E, Larue DT, Winer JA, Barth DS. 2003. A multisensory zone in rat parietotemporal cortex: intra- and extracellular physiology and thalamocortical connections. J Comp Neurol 460(2):223-237.

Breveglieri R, Galletti C, Monaco S, Fattori P. 2008. Visual, somatosensory, and bimodal activities in the macaque parietal area PEc. Cereb Cortex 18(4):806-816.

Brodal P, Bjaalie JG, Aas JE. 1991. Organization of cingulo-ponto-cerebellar connections in the cat. Anat Embryol (Berl) 184(3):245-254.

Bruce C, Desimone R, Gross CG. 1981. Visual properties of neurons in a polysensory area in superior temporal sulcus of the macaque. J Neurophysiol 46(2):369-384.

Brumberg JC, Pinto DJ, Simons DJ. 1999. Cortical columnar processing in the rat whisker-to-barrel system. J Neurophysiol 82(4):1808-1817.

Bucci DJ. 2009. Posterior parietal cortex: an interface between attention and learning? Neurobiol Learn Mem 91(2):114-120.

Burton, H. and E. M. Kopf (1984). "Ipsilateral cortical connections from the second and fourth somatic sensory areas in the cat." J Comp Neurol 225(4): 527-553.

Callaway EM. 2004. Feedforward, feedback and inhibitory connections in primate visual cortex. Neural Netw 17(5-6):625-632.

Calton JL, Taube JS. 2009. Where am I and how will I get there from here? A role for posterior parietal cortex in the integration of spatial information and route planning. Neurobiol Learn Mem 91(2):186-196.

Cappe C, Rouiller EM, Barone P. 2011. Cortical and Thalamic Pathways for Multisensory and Sensorimotor Interplay. In: Murray MM, Wallace MT, editors. The Neural Bases of Multisensory Processes. Boca Raton, Fl.: CRC Press. p 15-30.

Carriere BN, Royal DW, Perrault TJ, Morrison SP, Vaughan JW, Stein BE, Wallace MT. 2007. Visual deprivation alters the development of cortical multisensory integration. J Neurophysiol 98(5):2858-2867.

Carvell, G. E. and D. J. Simons (1986). "Somatotopic organization of the second somatosensory area (SII) in the cerebral cortex of the mouse." Somatosens Res 3(3): 213-237.

Cazin L, Precht W, Lannou J. 1980. Firing characteristics of neurons mediating optokinetic responses to rat's vestibular neurons. Pflugers Arch 386(3):221-230.

Chan CS, Shigemoto R, Mercer JN, Surmeier DJ. 2004. HCN2 and HCN1 channels govern the regularity of autonomous pacemaking and synaptic resetting in globus pallidus neurons. J Neurosci 24(44):9921-9932.

Chomsung RD, Wei H, Day-Brown JD, Petry HM, Bickford ME. 2010. Synaptic organization of connections between the temporal cortex and pulvinar nucleus of the tree shrew. Cereb Cortex 20(4):997-1011.

Clemo, H. R. and B. E. Stein (1983). "Organization of a fourth somatosensory area of cortex in cat." J Neurophysiol 50(4): 910-925.

Clemo HR, Allman BL, Donlan MA, Meredith MA. 2007. Sensory and multisensory representations within the cat rostral suprasylvian cortex. J Comp Neurol 503(1):110-127.

Clemo HR, Sharma GK, Allman BL, Meredith MA. 2008. Auditory projections to extrastriate visual cortex: connectional basis for multisensory processing in 'unimodal' visual neurons. Exp Brain Res 191(1):37-47.

Clemo HR, Keniston LP, Meredith MA. 2011. Structural Basis of Multisensory Processing: Convergence. In: Murray MM, Wallace MT, editors. The Neural Bases of Multisensory Processes. Boca Raton, Fl: CRC Press. p 3-14.

Clemo HR, Meredith MA. 2012. Dendritic spine density in multisensory versus primary sensory cortex. Synapse.

Cohen YE, Russ BE, Gifford GW, 3rd. 2005. Auditory processing in the posterior parietal cortex. Behav Cogn Neurosci Rev 4(3):218-231.

Cooke DF, Taylor CS, Moore T, Graziano MS. 2003. Complex movements evoked by microstimulation of the ventral intraparietal area. Proc Natl Acad Sci USA 100(10):6163-6168.

Dahl CD, Logothetis NK, Kayser C. 2009. Spatial organization of multisensory responses in temporal association cortex. J Neurosci 29(38):11924-11932.

Darian-Smith, I., J. Isbister, et al. (1966). "Somatic sensory cortical projection areas excited by tactile stimulation of the cat: a triple representation." J Physiol 182(3): 671-689.

de Kock CP, Bruno RM, Spors H, Sakmann B. 2007. Layer- and cell-type-specific suprathreshold stimulus representation in rat primary somatosensory cortex. J Physiol 581(Pt 1):139-154.

Dehner LR, Keniston LP, Clemo HR, Meredith MA. 2004. Cross-modal circuitry between auditory and somatosensory areas of the cat anterior ectosylvian sulcal cortex: a 'new' inhibitory form of multisensory convergence. Cereb Cortex 14(4):387-403.

Diederich, A. and H. Colonius (2004). "Bimodal and trimodal multisensory enhancement: effects of stimulus onset and intensity on reaction time." Percept Psychophys 66(8): 1388-1404.

Do MT, Bean BP. 2003. Subthreshold sodium currents and pacemaking of subthalamic neurons: modulation by slow inactivation. Neuron 39(1):109-120.

Douglas RJ, Martin KA. 2004. Neuronal circuits of the neocortex. Annu Rev Neurosci 27:419-451.

Driver J, Noesselt T. 2008. Multisensory interplay reveals crossmodal influences on 'sensory-specific' brain regions, neural responses, and judgments. Neuron 57(1):11-23.

Duhamel JR, Colby CL, Goldberg ME. 1998. Ventral intraparietal area of the macaque: congruent visual and somatic response properties. J Neurophysiol 79(1):126-136.

Edwards, S. B., C. L. Ginsburgh, et al. (1979). "Sources of subcortical projections to the superior colliculus in the cat." J Comp Neurol 184(2): 309-329.

Felleman DJ, Van Essen DC. 1991. Distributed hierarchical processing in the primate cerebral cortex. Cereb Cortex 1(1):1-47.

Fisher RS, Shiota C, Levine MS, Hull CD, Buchwald NA. 1984. Interhemispheric organization of corticocaudate projections in the cat: a retrograde double-labelling study. Neurosci Lett 48(3):369-373.

FitzGibbon T. 2000. Cortical projections from the suprasylvian gyrus to the reticular thalamic nucleus in the cat. Neuroscience 97(4):643-655.

Fogassi L, Gallese V, Fadiga L, Luppino G, Matelli M, Rizzolatti G. 1996. Coding of peripersonal space in inferior premotor cortex (area F4). J Neurophysiol 76(1):141-157.

Forti L, Cesana E, Mapelli J, D'Angelo E. 2006. Ionic mechanisms of autorhythmic firing in rat cerebellar Golgi cells. J Physiol 574(Pt 3):711-729.

Foxworthy WA, Keniston LP, Meredith MA. 2011. Bimodal and unisensory cortical neurons are differentially sensitive to sensory experience. Society for Neuroscience Abstract.

Foxworthy WA, Meredith MA. 2011. An examination of somatosensory area SIII in ferret cortex. Somatosens Mot Res 28(1-2):1-10.

Fuentes-Santamaria V, Alvarado JC, McHaffie JG, Stein BE. 2009. Axon morphologies and convergence patterns of projections from different sensory-specific cortices of the anterior ectosylvian sulcus onto multisensory neurons in the cat superior colliculus. Cereb Cortex 19(12):2902-2915.

Garraghty, P. E., T. P. Pons, et al. (1987). "Somatotopic organization of the third somatosensory area (SIII) in cats." Somatosens Res 4(4): 333-357.

Gawne TJ, Kjaer TW, Richmond BJ. 1996. Latency: another potential code for feature binding in striate cortex. J Neurophysiol 76(2):1356-1360.

Ghazanfar, A. A., J. X. Maier, et al. (2005). "Multisensory integration of dynamic faces and voices in rhesus monkey auditory cortex." J Neurosci 25(20): 5004-5012.

Ghazanfar AA, Schroeder CE. 2006. Is neocortex essentially multisensory? Trends Cogn Sci 10(6):278-285.

Graziano MS, Yap GS, Gross CG. 1994. Coding of visual space by premotor neurons. Science 266(5187):1054-1057.

Graziano MS, Reiss LA, Gross CG. 1999. A neuronal representation of the location of nearby sounds. Nature 397(6718):428-430.

Groh A, Meyer HS, Schmidt EF, Heintz N, Sakmann B, Krieger P. 2010. Cell-type specific properties of pyramidal neurons in neocortex underlying a layout that is modifiable depending on the cortical area. Cereb Cortex 20(4):826-836.

Haight, J. R. (1972). "The general organization of somatotopic projections to SII cerebral neocortex in the cat." Brain Res 44(2): 483-502.

Harting, J. K. and D. P. Van Lieshout (1991). "Spatial relationships of axons arising from the substantia nigra, spinal trigeminal nucleus, and pedunculopontine tegmental nucleus within the intermediate gray of the cat superior colliculus." J Comp Neurol 305(4): 543-558.

Harting, J. K., B. V. Updyke, et al. (1992). "Corticotectal projections in the cat: anterograde transport studies of twenty-five cortical areas." J Comp Neurol 324(3): 379-414.

Harting, J. K., S. Feig, et al. (1997). "Cortical somatosensory and trigeminal inputs to the cat superior colliculus: light and electron microscopic analyses." J Comp Neurol 388(2): 313-326.

Hedreen JC, DeLong MR. 1991. Organization of striatopallidal, striatonigral, and nigrostriatal projections in the macaque. J Comp Neurol 304(4):569-595.

Hikosaka K, Iwai E, Saito H, Tanaka K. 1988. Polysensory properties of neurons in the anterior bank of the caudal superior temporal sulcus of the macaque monkey. J Neurophysiol 60(5):1615-1637.

Hirsch JA, Martinez LM. 2006. Laminar processing in the visual cortical column. Curr Opin Neurobiol 16(4):377-384.

Homman-Ludiye J, Manger PR, Bourne JA. 2010. Immunohistochemical parcellation of the ferret (Mustela putorius) visual cortex reveals substantial homology with the cat (Felis catus). J Comp Neurol 518(21):4439-4462.

Horn G, Hill RM. 1966. Responsiveness to sensory stimulation of units in the superior colliculus and subjacent tectotegmental regions of the rabbit. Exp Neurol 14(2):199-223.

Horton JC, Adams DL. 2005. The cortical column: a structure without a function. Philos Trans R Soc Lond B Biol Sci 360(1456):837-862.

Hughes, H. C., P. A. Reuter-Lorenz, et al. (1994). "Visual-auditory interactions in sensorimotor processing: saccades versus manual responses." J Exp Psychol Hum Percept Perform 20(1): 131-153.

Hunt, D. L., D. A. Slutsky, et al. (2000). "The organization of somatosensory cortex in the ferret." 2000 Neuroscience Meeting Planner. SFN Abstract: 243.213.

Innocenti GM, Manger PR, Masiello I, Colin I, Tettoni L. 2002. Architecture and callosal connections of visual areas 17, 18, 19 and 21 in the ferret (Mustela putorius). Cereb Cortex 12(4):411-422.

Jackson CA, Peduzzi JD, Hickey TL. 1989. Visual cortex development in the ferret. I. Genesis and migration of visual cortical neurons. J Neurosci 9(4):1242-1253.

Jackson AC, Yao GL, Bean BP. 2004. Mechanism of spontaneous firing in dorsomedial suprachiasmatic nucleus neurons. J Neurosci 24(37):7985-7998.

Jacobs B, Schall M, Prather M, Kapler E, Driscoll L, Baca S, Jacobs J, Ford K, Wainwright M, Treml M. 2001. Regional dendritic and spine variation in human cerebral cortex: a quantitative golgi study. Cereb Cortex 11(6):558-571.

Jiang H, Lepore F, Ptito M, Guillemot JP. 1994. Sensory interactions in the anterior ectosylvian cortex of cats. Exp Brain Res 101(3):385-396.

Jiang H, Lepore F, Ptito M, Guillemot JP. 1994. Sensory modality distribution in the anterior ectosylvian cortex (AEC) of cats. Exp Brain Res 97(3):404-414.

Jiang, Z. D., D. R. Moore, et al. (1997). "Sources of subcortical projections to the superior colliculus in the ferret." Brain Res 755(2): 279-292.

Jones EG, Powell TP. 1970. An anatomical study of converging sensory pathways within the cerebral cortex of the monkey. Brain 93(4):793-820.

Jones EG. 1975. Some aspects of the organization of the thalamic reticular complex. J Comp Neurol 162(3):285-308.

Jones EG, Coulter JD, Burton H, Porter R. 1977. Cells of origin and terminal distribution of corticostriatal fibers arising in the sensory-motor cortex of monkeys. J Comp Neurol 173(1):53-80.

Jones EG. 2007a. Lateral posterior and pulvinar nuclei. The Thalamus. Cambridge: Cambridge University Press. p 1009-1075.

Jones EG. 2007b. The Ventral Nuclei. The Thalamus. Cambridge: Cambridge University Press. p 705-874.

Kaas, J. H., R. J. Nelson, et al. (1979). "Multiple representations of the body within the primary somatosensory cortex of primates." Science 204(4392): 521-523.

Kaas, J. H. (1983). "What, if anything, is SI? Organization of first somatosensory area of cortex." Physiol Rev **63**(1): 206-231.

Kaas J. 2009. The Evolution of Sensory and Motor Systems in Primates. In: Kaas J, editor. Evolutionary Neuroscience: Academic Press. p 847-865.

Kaas JH, Gharbawie OA, Stepniewska I. 2011. The organization and evolution of dorsal stream multisensory motor pathways in primates. Front Neuroanat 5:34.

Kadunce, D. C., J. W. Vaughan, et al. (1997). "Mechanisms of within- and cross-modality suppression in the superior colliculus." J Neurophysiol 78(6): 2834-2847.

Karlen, S. J. and L. Krubitzer (2007). "The functional and anatomical organization of marsupial neocortex: evidence for parallel evolution across mammals." Prog Neurobiol 82(3): 122-141.

Kayser C, Petkov CI, Augath M, Logothetis NK. 2005. Integration of touch and sound in auditory cortex. Neuron 48(2):373-384.

Kawamura K, Konno T. 1979. Various types of corticotectal neurons of cats as demonstrated by means of retrograde axonal transport of horseradish peroxidase. Exp Brain Res 35(1):161-175.

Keller EL, Crandall WF. 1983. Neuronal responses to optokinetic stimuli in pontine nuclei of behaving monkey. J Neurophysiol 49(1):169-187.

Keniston, L. (2008). "The rostral suprasylvian sulcus (rsss) of the ferret: a 'new' multisensory area." 2008 Neuroscience Meeting Planner 457.10/DD34

Keniston LP, Allman BL, Meredith MA, Clemo HR. 2009. Somatosensory and multisensory properties of the medial bank of the ferret rostral suprasylvian sulcus. Exp Brain Res 196(2):239-251.

Keniston LP, Henderson SC, Meredith MA. 2010. Neuroanatomical identification of crossmodal auditory inputs to interneurons in somatosensory cortex. Exp Brain Res 202(3):725-731.

Kirsch, J. A. W. (1977). The classification of marsupials. New York, Academic Press.

Koralek, K. A., J. Olavarria, et al. (1990). "Areal and laminar organization of corticocortical projections in the rat somatosensory cortex." J Comp Neurol 299(2): 133-150.

Krook-Magnuson E, Varga C, Lee SH, Soltesz I. 2012. New dimensions of interneuronal specialization unmasked by principal cell heterogeneity. Trends Neurosci 35(3):175-184.

Krubitzer, L. A. and M. B. Calford (1992). "Five topographically organized fields in the somatosensory cortex of the flying fox: microelectrode maps, myeloarchitecture, and cortical modules." J Comp Neurol 317(1): 1-30.

Krubitzer, L., J. Clarey, et al. (1995). "A redefinition of somatosensory areas in the lateral sulcus of macaque monkeys." J Neurosci 15(5 Pt 2): 3821-3839.

Krubitzer L. 2007. The magnificent compromise: cortical field evolution in mammals. Neuron 56(2):201-208.

Leclerc SS, Rice FL, Dykes RW, Pourmoghadam K, Gomez CM. 1993. Electrophysiological examination of the representation of the face in the suprasylvian gyrus of the ferret: a correlative study with cytoarchitecture. Somatosens Mot Res 10(2):133-159.

Leergaard TB, Lyngstad KA, Thompson JH, Taeymans S, Vos BP, De Schutter E, Bower JM, Bjaalie JG. 2000. Rat somatosensory cerebropontocerebellar pathways: spatial relationships of the somatotopic map of the primary somatosensory cortex are preserved in a three-dimensional clustered pontine map. J Comp Neurol 422(2):246-266.

Leergaard TB, Bjaalie JG. 2007. Topography of the complete corticopontine projection: from experiments to principal Maps. Front Neurosci 1(1):211-223.

Lewis JW, Van Essen DC. 2000. Corticocortical connections of visual, sensorimotor, and multimodal processing areas in the parietal lobe of the macaque monkey. J Comp Neurol 428(1):112-137.

Lim HK, Keniston LP, Shin JH, Allman BL, Meredith MA, Cios KJ. 2011. Connectional parameters determine multisensory processing in a spiking network model of multisensory convergence. Exp Brain Res 213(2-3):329-339.

Linden JF, Schreiner CE. 2003. Columnar transformations in auditory cortex? A comparison to visual and somatosensory cortices. Cereb Cortex 13(1):83-89.

Lugo-Garcia, N. and E. Kicliter (1988). "Thalamic connections of the ground squirrel superior colliculus and their topographic relations." J Hirnforsch 29(2): 187-201.

Maccaferri G, McBain CJ. 1996. The hyperpolarization-activated current (Ih) and its contribution to pacemaker activity in rat CA1 hippocampal stratum oriens-alveus interneurones. J Physiol 497 (Pt 1):119-130.

Manger PR, Masiello I, Innocenti GM. 2002. Areal organization of the posterior parietal cortex of the ferret (Mustela putorius). Cereb Cortex 12(12):1280-1297.

Manger PR, Nakamura H, Valentiniene S, Innocenti GM. 2004. Visual areas in the lateral temporal cortex of the ferret (Mustela putorius). Cereb Cortex 14(6):676-689.

Manger, P. R., G. Engler, et al. (2005). "The anterior ectosylvian visual area of the ferret: a homologue for an enigmatic visual cortical area of the cat?" Eur J Neurosci **22**(3): 706-714.

Manger PR, Engler G, Moll CK, Engel AK. 2008. Location, architecture, and retinotopy of the anteromedial lateral suprasylvian visual area (AMLS) of the ferret (Mustela putorius). Vis Neurosci 25(1):27-37.

Manger PR, Restrepo CE, Innocenti GM. 2010. The superior colliculus of the ferret: cortical afferents and efferent connections to dorsal thalamus. Brain Res 1353:74-85.

Markus Z, Eordegh G, Paroczy Z, Benedek G, Nagy A. 2008. Modality distribution of sensory neurons in the feline caudate nucleus and the substantia nigra. Acta Biol Hung 59(3):269-279.

Martinez LM, Wang Q, Reid RC, Pillai C, Alonso JM, Sommer FT, Hirsch JA. 2005. Receptive field structure varies with layer in the primary visual cortex. Nat Neurosci 8(3):372-379.

Matsuzaki R, Kyuhou S, Matsuura-Nakao K, Gemba H. 2004. Thalamo-cortical projections to the posterior parietal cortex in the monkey. Neurosci Lett 355(1-2):113-116.

McCormick DA, Pape HC. 1990. Properties of a hyperpolarization-activated cation current and its role in rhythmic oscillation in thalamic relay neurones. J Physiol 431:291-318.

McGeorge AJ, Faull RL. 1989. The organization of the projection from the cerebral cortex to the striatum in the rat. Neuroscience 29(3):503-537.

McHaffie JG, Kruger L, Clemo HR, Stein BE. 1988. Corticothalamic and corticotectal somatosensory projections from the anterior ectosylvian sulcus (SIV cortex) in neonatal cats: an anatomical demonstration with HRP and 3H-leucine. J Comp Neurol 274(1):115-126.

McLaughlin DF, Sonty RV, Juliano SL. 1998. Organization of the forepaw representation in ferret somatosensory cortex. Somatosens Mot Res 15(4):253-268.

Meredith MA, Stein BE. 1983. Interactions among converging sensory inputs in the superior colliculus. Science 221(4608):389-391.

Meredith MA, Stein BE. 1985. Descending efferents from the superior colliculus relay integrated multisensory information. Science 227(4687):657-659.

Meredith, M. A. and B. E. Stein (1986). "Spatial factors determine the activity of multisensory neurons in cat superior colliculus." Brain Res 365(2): 350-354.

Meredith MA, Stein BE. 1986. Visual, auditory, and somatosensory convergence on cells in superior colliculus results in multisensory integration. J Neurophysiol 56(3):640-662.

Meredith, M. A., J. W. Nemitz, et al. (1987). "Determinants of multisensory integration in superior colliculus neurons. I. Temporal factors." J Neurosci **7**(10): 3215-3229.

Meredith MA, Clemo HR. 1989. Auditory cortical projection from the anterior ectosylvian sulcus (Field AES) to the superior colliculus in the cat: an anatomical and electrophysiological study. J Comp Neurol 289(4):687-707.

Meredith, M. A. and B. E. Stein (1996). "Spatial determinants of multisensory integration in cat superior colliculus neurons." J Neurophysiol 75(5): 1843-1857.

Meredith MA, Keniston LR, Dehner LR, Clemo HR. 2006. Crossmodal projections from somatosensory area SIV to the auditory field of the anterior ectosylvian sulcus (FAES) in Cat: further evidence for subthreshold forms of multisensory processing. Exp Brain Res 172(4):472-484.

Meredith MA, Allman BL. 2009. Subthreshold multisensory processing in cat auditory cortex. Neuroreport 20(2):126-131.

Meredith MA, Allman BL, Keniston LP, Clemo HR. 2011a. Are Bimodal Neurons the Same throughout the Brain? In: Murray MM, Wallace MT, editors. The Neural Bases of Multisensory Processes. Boca Raton, FL: CRC Press. p 51-64.

Meredith MA, Kryklywy J, McMillan AJ, Malhotra S, Lum-Tai R, Lomber SG. 2011b. Crossmodal reorganization in the early deaf switches sensory, but not behavioral roles of auditory cortex. Proc Natl Acad Sci U S A 108(21):8856-8861.

Meredith MA, Fiore TM, Foxworthy WA. 2011. Convergent multiple sensory connectivity of ferret rostral posterior parietal cortex. Society for Neuroscience. Washington, DC.

Morgan ML, Deangelis GC, Angelaki DE. 2008. Multisensory integration in macaque visual cortex depends on cue reliability. Neuron 59(4):662-673.

Monteiro GA, Clemo HR, Meredith MA. 2003. Anterior ectosylvian cortical projections to the rostral suprasylvian multisensory zone in cat. Neuroreport 14(17):2139-2145.

Montero VM. 1980. Patterns of connections from the striate cortex to cortical visual areas in superior temporal sulcus of macaque and middle temporal gyrus of owl monkey. J Comp Neurol 189(1):45-59.

Mori, A., T. Fuwa, et al. (1996). "The ipsilateral and contralateral connections of the fifth somatosensory area (SV) in the cat cerebral cortex." Neuroreport **7**(14): 2385-2387.

Nagy A, Eordegh G, Paroczy Z, Markus Z, Benedek G. 2006. Multisensory integration in the basal ganglia. Eur J Neurosci 24(3):917-924.

Nassi JJ, Callaway EM. 2009. Parallel processing strategies of the primate visual system. Nat Rev Neurosci 10(5):360-372.

Nelken I, Chechik G, Mrsic-Flogel TD, King AJ, Schnupp JW. 2005. Encoding stimulus information by spike numbers and mean response time in primary auditory cortex. J Comput Neurosci 19(2):199-221.

Nelson, R. J., M. Sur, et al. (1980). "Representations of the body surface in postcentral parietal cortex of Macaca fascicularis." J Comp Neurol 192(4): 611-643.

Nitz D. 2009. Parietal cortex, navigation, and the construction of arbitrary reference frames for spatial information. Neurobiol Learn Mem 91(2):179-185.

Nozawa, G., P. A. Reuter-Lorenz, et al. (1994). "Parallel and serial processes in the human oculomotor system: bimodal integration and express saccades." Biol Cybern 72(1): 19-34.

Oka H. 1980. Organization of the cortico-caudate projections. A horseradish peroxidase study in the cat. Exp Brain Res 40(2):203-208.

Panzeri S, Diamond ME. 2010. Information Carried by Population Spike Times in the Whisker Sensory Cortex can be Decoded Without Knowledge of Stimulus Time. Front Synaptic Neurosci 2:17.

Perez-Samartin AL, Martinez-Millan L, Donate-Oliver F. 1995. Morphology of visual cortical neurons projecting to the pons. A study with intracellular injection of lucifer yellow in the cat. Arch Ital Biol 133(1):17-30.

Perrault TJ, Jr., Vaughan JW, Stein BE, Wallace MT. 2003. Neuron-specific response characteristics predict the magnitude of multisensory integration. J Neurophysiol 90(6):4022-4026.

Perrault TJ, Jr., Vaughan JW, Stein BE, Wallace MT. 2005. Superior colliculus neurons use distinct operational modes in the integration of multisensory stimuli. J Neurophysiol 93(5):2575-2586.

Raman IM, Bean BP. 1997. Resurgent sodium current and action potential formation in dissociated cerebellar Purkinje neurons. J Neurosci 17(12):4517-4526.

Raman IM, Gustafson AE, Padgett D. 2000. Ionic currents and spontaneous firing in neurons isolated from the cerebellar nuclei. J Neurosci 20(24):9004-9016.

Reale, R. A. and T. J. Imig (1980). "Tonotopic organization in auditory cortex of the cat." J Comp Neurol 192(2): 265-291.

Reep RL, Chandler HC, King V, Corwin JV. 1994. Rat posterior parietal cortex: topography of corticocortical and thalamic connections. Exp Brain Res 100(1):67-84.

Reep RL, Corwin JV. 2009. Posterior parietal cortex as part of a neural network for directed attention in rats. Neurobiol Learn Mem 91(2):104-113.

Reiner A, Jiao Y, Del Mar N, Laverghetta AV, Lei WL. 2003. Differential morphology of pyramidal tract-type and intratelencephalically projecting-type corticostriatal neurons and their intrastriatal terminals in rats. J Comp Neurol 457(4):420-440.

Remedios R, Logothetis NK, Kayser C. 2010. Unimodal responses prevail within the multisensory claustrum. J Neurosci 30(39):12902-12907.

Remple MS, Reed JL, Stepniewska I, Lyon DC, Kaas JH. 2007. The organization of frontoparietal cortex in the tree shrew (Tupaia belangeri): II. Connectional evidence for a frontal-posterior parietal network. J Comp Neurol 501(1):121-149.

Rice FL, Gomez CM, Leclerc SS, Dykes RW, Moon JS, Pourmoghadam K. 1993. Cytoarchitecture of the ferret suprasylvian gyrus correlated with areas containing multiunit responses elicited by stimulation of the face. Somatosens Mot Res 10(2):161-188.

Rockland KS, Andresen J, Cowie RJ, Robinson DL. 1999. Single axon analysis of pulvinocortical connections to several visual areas in the macaque. J Comp Neurol 406(2):221-250.

Roda JM, Reinoso-Suarez F. 1983. Topographical organization of the thalamic projections to the cortex of the anterior ectosylvian sulcus in the cat. Exp Brain Res 49(1):131-139.

Romanski LM, Giguere M, Bates JF, Goldman-Rakic PS. 1997. Topographic organization of medial pulvinar connections with the prefrontal cortex in the rhesus monkey. J Comp Neurol 379(3):313-332.

Romanski LM. 2007. Representation and integration of auditory and visual stimuli in the primate ventral lateral prefrontal cortex. Cereb Cortex 17 Suppl 1:61-69.

Rosa MG. 1999. Topographic organisation of extrastriate areas in the flying fox: implications for the evolution of mammalian visual cortex. J Comp Neurol 411(3):503-523.

Rosell A, Gimenez-Amaya JM. 1999. Anatomical re-evaluation of the corticostriatal projections to the caudate nucleus: a retrograde labeling study in the cat. Neurosci Res 34(4):257-269.

Russ BE, Kim AM, Abrahamsen KL, Kiringoda R, Cohen YE. 2006. Responses of neurons in the lateral intraparietal area to central visual cues. Exp Brain Res 174(4):712-727.

Sabes PN. 2011. Sensory integration for reaching: models of optimality in the context of behavior and the underlying neural circuits. Prog Brain Res 191:195-209.

Saint-Cyr JA, Ungerleider LG, Desimone R. 1990. Organization of visual cortical inputs to the striatum and subsequent outputs to the pallido-nigral complex in the monkey. J Comp Neurol 298(2):129-156.

Save E, Poucet B. 2009. Role of the parietal cortex in long-term representation of spatial information in the rat. Neurobiol Learn Mem 91(2):172-178.

Schlack A, Sterbing-D'Angelo SJ, Hartung K, Hoffmann KP, Bremmer F. 2005. Multisensory space representations in the macaque ventral intraparietal area. J Neurosci 25(18):4616-4625.

Schreiner CE, Read HL, Sutter ML. 2000. Modular organization of frequency integration in primary auditory cortex. Annu Rev Neurosci 23:501-529.

Schroeder CE, Foxe JJ. 2002. The timing and laminar profile of converging inputs to multisensory areas of the macaque neocortex. Brain Res Cogn Brain Res 14(1):187-198.

Schubert D, Kotter R, Staiger JF. 2007. Mapping functional connectivity in barrel-related columns reveals layer- and cell type-specific microcircuits. Brain Struct Funct 212(2):107-119.

Sherman SM, Guillery RW. 2011. Distinct functions for direct and transthalamic corticocortical connections. J Neurophysiol 106(3):1068-1077.

Shriki O, Kohn A, Shamir M. 2012. Fast coding of orientation in primary visual cortex. PLoS Comput Biol 8(6):e1002536.

Slutsky, D. A., P. R. Manger, et al. (2000). "Multiple somatosensory areas in the anterior parietal cortex of the California ground squirrel (Spermophilus beecheyii)." J Comp Neurol 416(4): 521-539.

Stanford TR, Quessy S, Stein BE. 2005. Evaluating the operations underlying multisensory integration in the cat superior colliculus. J Neurosci 25(28):6499-6508.

Stanford, T. R. and B. E. Stein (2007). "Superadditivity in multisensory integration: putting the computation in context." Neuroreport 18(8): 787-792.

Stein BE, Spencer RF, Edwards SB. 1983. Corticotectal and corticothalamic efferent projections of SIV somatosensory cortex in cat. J Neurophysiol 50(4):896-909.

Stein, B. E., W. S. Huneycutt, et al. (1988). "Neurons and behavior: the same rules of multisensory integration apply." Brain Res 448(2): 355-358.

Stein, B. E., M. A. Meredith, et al. (1989). "Behavioral indices of multisensory integration: Orientation to visual cues is affected by auditory stimuli." J Cognitive Neuroscience.

Stein BE, Meredith MA. 1993. The merging of the senses. Cambridge, Mass.: MIT Press.

Stein BE, Wallace MT. 1996. Comparisons of cross-modality integration in midbrain and cortex. Prog Brain Res 112:289-299.

Stein BE, Stanford TR. 2008. Multisensory integration: current issues from the perspective of the single neuron. Nat Rev Neurosci 9(4):255-266.

Stevenson, R. A., M. Bushmakin, et al. (2012). "Inverse effectiveness and multisensory interactions in visual event-related potentials with audiovisual speech." Brain Topogr 25(3): 308-326.

Stevenson, R. A. and T. W. James (2009). "Audiovisual integration in human superior temporal sulcus: Inverse effectiveness and the neural processing of speech and object recognition." Neuroimage 44(3): 1210-1223.

Storm JF. 2000. K(+) channels and their distribution in large cortical pyramidal neurones. J Physiol 525 Pt 3:565-566.

Stuart G, Spruston N, Häusser M. 2007. Dendrites. Oxford ; New York: Oxford University Press.

Sugihara T, Diltz MD, Averbeck BB, Romanski LM. 2006. Integration of auditory and visual communication information in the primate ventrolateral prefrontal cortex. J Neurosci 26(43):11138-11147.

Sugino K, Hempel CM, Miller MN, Hattox AM, Shapiro P, Wu C, Huang ZJ, Nelson SB. 2006. Molecular taxonomy of major neuronal classes in the adult mouse forebrain. Nat Neurosci 9(1):99-107.

Sumby, W. H. and I. Polack (1954). "Visual contribution to speech intelligibility in noise." J. Acoust. Soc. Am. 26: 212-215.

Sur M, Wall JT, Kaas JH. 1981. Modular segregation of functional cell classes within the postcentral somatosensory cortex of monkeys. Science 212(4498):1059-1061.

Taddese A, Bean BP. 2002. Subthreshold sodium current from rapidly inactivating sodium channels drives spontaneous firing of tuberomammillary neurons. Neuron 33(4):587-600.

Takahashi T. 1985. The organization of the lateral thalamus of the hooded rat. J Comp Neurol 231(3):281-309.

Tanaka D, Jr. 1987. Differential laminar distribution of corticostriatal neurons in the prefrontal and pericruciate gyri of the dog. J Neurosci 7(12):4095-4106.

Taylor, A. M., G. Jeffery, et al. (1986). "Subcortical afferent and efferent connections of the superior colliculus in the rat and comparisons between albino and pigmented strains." Exp Brain Res 62(1): 131-142.

Thomson AM, Lamy C. 2007. Functional maps of neocortical local circuitry. Front Neurosci 1(1):19-42.

Torigoe Y, Blanks RH, Precht W. 1986. Anatomical studies on the nucleus reticularis tegmenti pontis in the pigmented rat. I. Cytoarchitecture, topography, and cerebral cortical afferents. J Comp Neurol 243(1):71-87.

Van Essen DC. 2005. Corticocortical and thalamocortical information flow in the primate visual system. Prog Brain Res 149:173-185.

Van der Gucht, E., F. Vandesande, et al. (2001). "Neurofilament protein: a selective marker for the architectonic parcellation of the visual cortex in adult cat brain." J Comp Neurol 441(4): 345-368.

Van Horn SC, Sherman SM. 2004. Differences in projection patterns between large and small corticothalamic terminals. J Comp Neurol 475(3):406-415.

VanRullen R, Guyonneau R, Thorpe SJ. 2005. Spike times make sense. Trends Neurosci 28(1):1-4.

Veening JG, Cornelissen FM, Lieven PA. 1980. The topical organization of the afferents to the caudatoputamen of the rat. A horseradish peroxidase study. Neuroscience 5(7):1253-1268.

Veenman CL, Reiner A, Honig MG. 1992. Biotinylated dextran amine as an anterograde tracer for single- and double-labeling studies. J Neurosci Methods 41(3):239-254.

Wallace MT, Meredith MA, Stein BE. 1992. Integration of multiple sensory modalities in cat cortex. Exp Brain Res 91(3):484-488.

Wallace, M. T., M. A. Meredith, et al. (1993). "Converging influences from visual, auditory, and somatosensory cortices onto output neurons of the superior colliculus." J Neurophysiol 69(6): 1797-1809.

Wallace MT, Wilkinson LK, Stein BE. 1996. Representation and integration of multiple sensory inputs in primate superior colliculus. J Neurophysiol 76(2):1246-1266.

Wallace MT, Ramachandran R, Stein BE. 2004. A revised view of sensory cortical parcellation. Proc Natl Acad Sci U S A 101(7):2167-2172.

Wallace, M. T. and B. E. Stein (1997). "Development of multisensory neurons and multisensory integration in cat superior colliculus." J Neurosci 17(7): 2429-2444.

Wilson CJ. 1987. Morphology and synaptic connections of crossed corticostriatal neurons in the rat. J Comp Neurol 263(4):567-580.

Woolsey, C. N. (1943). ""Second" somatic receiving areas in the cerebral cortex of cat, dog and monkey." Fed Proc **2**(55).

Xu X, Callaway EM. 2009. Laminar specificity of functional input to distinct types of inhibitory cortical neurons. J Neurosci 29(1):70-85.

Yeterian EH, Pandya DN. 1989. Thalamic connections of the cortex of the superior temporal sulcus in the rhesus monkey. J Comp Neurol 282(1):80-97.

Zeki S, Shipp S. 1988. The functional logic of cortical connections. Nature 335(6188):311-317.

Zhang ZW, Deschenes M. 1997. Intracortical axonal projections of lamina VI cells of the primary somatosensory cortex in the rat: a single-cell labeling study. J Neurosci 17(16):6365-6379.

Zhang ZW, Deschenes M. 1998. Projections to layer VI of the posteromedial barrel field in the rat: a reappraisal of the role of corticothalamic pathways. Cereb Cortex 8(5):428-436.

Zikopoulos B, Barbas H. 2007. Circuits formultisensory integration and attentional modulation through the prefrontal cortex and the thalamic reticular nucleus in primates. Rev Neurosci 18(6):417-438.

VITA

William Alex Foxworthy was born on November 10, 1983, in Haymarket, Virginia and is an American citizen. He graduated from Stonewall Jackson High School, Manassas, Virginia in 2001. He received his Bachelor of Science in Psychology from Virginia Commonwealth University in 2006.

PERSONAL INFORMATION

Name:	William Alex Foxworthy
Institution Name:	Virginia Commonwealth University School of Medicine
Address:	1101 E. Marshall St., Sanger Hall Rm. 12-067
City, State, Zip:	Richmond, Virginia 23298-0709
Business Phone:	804 828-9533
Business Fax:	804 828-9477
Business Email:	foxworthwa@vcu.edu

EDUCATION

GRADUATE

2008-2012 Virginia Commonwealth University, Richmond, VA; Ph.D. in Neuroscience, Thesis title: "Unique Features of Organization and Neuronal Properties in a Multisensory Cortex" M. Alex Meredith, Ph.D., Thesis Advisor.

UNDERGRADUATE

2004-06 Virginia Commonwealth University, Richmond, VA, BS in Pschology
Magna Cum Laude, August 2006

SPECIAL AWARDS AND HONORS

2010 Invited to speak at VCU Computer Science Seminar Series

MEMBERSHIP IN SCIENTIFIC OR PROFESSIONAL SOCIETIES

2008 Society for Neuroscience
2010 Phi Kappa Phi Honor Society
2006 Psi Chi Honor Society

TEACHING

2010	Dental Gross Anatomy- Basic Organization of the Nervous System
2010	Psychology 101 – Behavioral Neuroscience
2005-2006	Supplementary Instructor for Psychology 101 - *Awarded* "Years Best SI Instructor"

SERVICE ACTIVITIES

SERVICE TO THE UNIVERSITY

2011-12	Officer - Central Virginia Chapter for Society for Neuroscience
2010-2011	Mentor for undergraduate student Tim Fiore -Student won undergraduate research fellowship award
2010	Created New University Sports Club
2008	Recreational Sports Advisory Committee

PUBLICATIONS

PAPERS PUBLISHED IN PEER REVIEWED JOURNALS

1. Foxworthy WA and Meredith MA. An examination of somatosensory area SIII in ferret cortex, Somatosensory and Motor Research, 28:1-10, 2011 PMCID: PMC3195941

2. Foxworthy WA, Clemo HR and Meredith MA. Laminar and Connectional Organization of a Multisensory Cortex. (Submitted)

3. Foxworthy WA, Allman BL, Keniston LP and Meredith MA. Bimodal and Unisensory Neurons Exhibit Distinct Functional Properties. (Submitted).

PUBLISHED ABSTRACTS OR PROCEEDINGS

MA Meredith, T Fiore, WA Foxworthy. Convergent multiple sensory connectivity of ferret rostral posterior parietal (PPr) cortex. Soc Neurosci Abstr 41:481.01, 2011.

WA Foxworthy, L Keniston, MA Meredith. Bimodal and unisensory cortical neurons are differentially sensitive to sensory experience. Soc Neurosci Abstr 41:481.03, 2011.

WA Foxworthy, TM Fiore, LP Keniston, BL Allman and MA Meredith. Connectional Basis for Multisensory Properties of the Rostral Posterior Parietal Cortex of the Ferret. Central VA Society for Neuroscience 2010

BL Allman, LP Keniston, WA Foxworthy, and MA Meredith. Multisensory properties of the rostral portion of the posterior parietal cortex of the ferret. Central VA Society for Neuroscience 2009

COMMUNITY ACTIVITIES

2010 Maggie Walker Governor's School – Spikerbox Electrophysiology Lab

2010 Brain Day –Coordinated Maggie Walker Eletrophysiology Displays

2011 Brain Day – Spikerbox Electrophysiology